International Scientific-Theoretical and Production Journal

ADVANCES IN ELECTROMETALLURGY

3, 2004

Quarterly

English translation of the quarterly «Sovremennaya Elektrometallurgiya» journal published in Russian since January 1985

Founders: *E.O. Paton Electric Welding Institute of the NAS of Ukraine*
International Association «Welding»

Publisher: *International Association «Welding»*

Editorial and advertising offices are located at PWI:
International Association «Welding»,
E.O. Paton Electric
Welding Institute
of the NAS of Ukraine,
11, Bozhenko str., 03680,
Kyiv, Ukraine
Tel.: (38044) 227 67 57,
269 26 23,
Fax: (38044) 268 04 86
E-mail: journal@paton.kiev.ua
http://www.nas.gov.ua/pwj

Subscriptions:
$184, 4 issue per year,
postage and packaging included.
Back issue available

CONTENTS

70 years at advanced positions of technical progress 2

ELECTROSLAG TECHNOLOGY

Paton B.E., Medovar L.B. and Saenko V.Ya. About some "old–new" problems of ESR 6

Troyansky A.A., Ryabtsev A.D. and **Galyan N.N.** Application of electroslag technology for producing iron aluminides 9

Eryomin E.N. and **Zherebtsov S.N.** Centrifugal electroslag casting of flange billets using inoculating modifying 13

ELECTRON BEAM PROCESSES

Paton B.E., Trigub N.P., Zhuk G.V., Akhonin S.V. and **Berezos V.A.** Producing hollow titanium ingots using EBCHM 16

Zhuk G.V., Kalinyuk A.N. and **Trigub N.P.** Production of titanium ingots-slabs using method of EBCHM 20

Gavrilyuk O.Ya., Nesynov V.I., Komarov N.S., Rudenko Yu.V., Lebedev B.B. and **Podoltsev A.D.** Controller of anode current of electron beam guns with a preheated cathode 23

PLASMA-ARC TECHNOLOGY

Zhadkevich M.L., Shapovalov V.A., Melnik G.A., Prikhodko M.S., Zhdanovsky A.A. and **Zhirov D.M.** Engineering method of calculation of main power parameters of plasma ladles-furnaces 31

VACUUM-INDUCTION MELTING

Zhadkevich M.L., Shejko I.V., Teslevich S.M., Shapovalov V.A., Konstantinov V.S. and **Stepanenko V.V.** Investigation of composition of gas atmosphere in induction melting of spongy titanium in a sectional mould 34

GENERAL PROBLEMS OF METALLURGY

Bulyk I.I., Panasyuk V.V., Trostyanchin A.M., Grigorenko G.M., Kostin V.A., Taranova T.G. and **Grigorenko S.G.** X-ray and metallographic examinations of phase transformations during Solid-HDDR in ferromagnetic alloy of didymium–iron–boron system 38

ELECTROMETALLURGY OF STEEL AND FERROALLOYS

Chepurnoj A.D., Razinkin B.I., Tsertsek A.B., Kovalyov A.G. and **Leontiev A.A.** Investigation of steel degassing in electric arc melting and circulation vacuum degassing 42

Kostyakov V.N., Najdek V.L., Poletaev E.B., Grigorenko G.M., Bystrov Yu.A. and **Medved S.N.** Specifics of metals reduction by carbon from oxide materials in liquid-phase reduction melting 45

ENERGY AND RESOURCE SAVING

Lakomsky V.I. and **Grigorenko G.M.** Specifics of thermoanthracite heating in AC electric field 48

INFORMATION

Jubilee of International Center of Electron Beam Technologies of the E.O. Paton Electric Welding Institute of the NAS of Ukraine 51

70 YEARS AT ADVANCED POSITIONS OF TECHNICAL PROGRESS

The Electric Welding Institute was founded by Evgeny O. Paton in 1934 as a constituent part of the All-Ukrainian Academy of Sciences at the facilities of Electric Welding Laboratory at the Chair of Engineering Constructions and Electric Welding Committee. The establishment and all future activity of the Paton Welding Institute are connected with the name of this outstanding engineer and scientist. He defined the main scientific trends of the Institute in the field of technology of welding and welded structures, which are actual at present.

Evgeny O. Paton could foresee the huge prospects in the development of technology of electric welding of metals, the creation N.N. Benardos and N.G. Slavyanov, the talented Russian inventors. The convincing confirmation of this scientific prediction is the indisputable fact that welding today is the leading technological process of a permanent joining of metallic and non-metallic materials under conditions and media, including space and World Ocean. This is a great contribution of the Institute staff for 70 years of its activity.

At the first stage, the Institute specialists proved a feasibility of manufacture of welded structures, being not inferior by their strength and reliability to riveted structures, but even superior to them by some characteristics. This served a basis for mass application of welding in future. At the same years a scientific conception about the arc welding as a metallurgical process was substantiated and the investigations on arc welding automation were conducted under the supervision of E.O. Paton. By 1940 the development was completed and implementation of high-efficient submerged arc welding was started at factories of the country.

The automatic submerged arc welding played an important role during the Great Patriotic War. Directly in the shops of the tank plant in the Urals the Institute associates developed and implemented the technology of automatic welding of armour steel that allowed them to organize the line production of welded bodies of tank T-34 and to mechanize welding of other types of military machinery. Under the shop conditions the Institute staff did not interrupt the research works.

Pre-war and war stages in the Institute activity are the periods of establishment of a scientific school, which authority was confirmed convincingly by giving the name of Paton Evgeny Oskarovich to the Institute in 1945.

In the years of postwar restoration of national economy the efforts of the Institute staff were directed to widening the fields of application of high-efficient automatic and mechanized submerged arc welding instead of manual welding, to the optimization of welded structures and their industrial manufacture. The Institute staff was the first in the world who realized the automatic welding of sheet structures directly in site conditions.

The participation of specialists-welders was widened in the development of weldable structural steels in collaboration with metallurgists for their application in critical welded structures and constructions. The works of this period influenced positively the rates of postwar restoration of industry, the progress in advanced manufacture of building metal structures, manufacture of highly-reliable welded products of heavy, transport, chemical and power industries.

The solution of main problem, such as the increase in productivity and level of mechanization of welding jobs, required the continuous widening of investigations in the Institute to search for new methods and procedures of mechanized welding to increase the rational fields of application of submerged arc welding. The search for feasibility of submerged arc welding of joints, located in different spatial positions, was finalized by the development under the supervision of E.O. Paton of the method of a forced weld formation, which made a good start to the mechanization of arc welding of joints in vertical plane.

On August 12, 1953 the domestic and world science suffered a terrible bereavement: E.O. Paton died at the age of 84. He was the person who added a glorious page to history of the national science and technology. His pupils and successors, all the staff of the Institute continued with dignity the life-work started by his founder. Since 1953 and until now his son, academician Paton Boris Evgenievich, is the director of the Institute.

One of the most remarkable achievements of the Institute of the beginning of the 1950s was the development of the new technology of fusion welding of thick metal, i.e. electroslag welding, which changed radically the manufacture of heavy frameworks, boilers, hydraulic units and other unique welded-rolled, welded-cast structures. Its application allowed producing high-quality welded joints within the wide range of thicknesses.

Later, in collaboration with TsNIITMASh and other organizations, a method of CO_2 welding with thin wire was developed and found the wide spreading in industry and providing the noticeable growth in the level of mechanization of welding jobs. The further development of gas electric welding with con-

sumable electrode was the development of the process and equipment for pulsed-arc welding, welding in mixtures of active and inert gases. In this connection, the importance of works on the creation of semi-automatic machines, which forced out gradually the low-efficient rod electrode welding, where it was possible and rational, should be especially noted.

At the end of the 1950s the investigations in the field of electron beam welding started their rapid development. The efforts of scientists were directed to the study of physical-metallurgical processes in action of powerful (up to 100 kW) sharply-focused beam of electrons on thick-sheet (150–200 mm) structural materials. The especially important problem, solved successfully by the Institute, was the development of technology of closing the circumferential welds which prevented the root defects in the form of cavities, pores and discontinuities.

The further stage in the development of beam technology was its application for the purposes of welding and cutting using laser. Systematic investigations in the field of pulsed and continuous laser welding are carried out at the Institute. Over the recent years the hybrid heat sources such as laser-arc and laser-plasma have been developed by the specialists of the Institute.

At all the stages of the Institute activity a special attention was paid to the study of physical, chemical and metals science peculiarities of welding metals. Laboratories of the Institute were equipped by the research equipment for these purposes.

Investigations in all main trends of pressure welding –– flash-butt welding and resistance welding, spot, friction and diffusion welding, were carried out at the Institute.

Physical and technological features of new technological processes of flash-butt welding were studied, systems of automatic control and diagnostics of quality of welded joints were developed. On the basis of the new technologies the manufacture of several generations of specialized and universal machines for flash-butt welding of widely used components, made from low-alloy and high-strength steels and having up to 200,000 mm^2 cross-section area and also from alloys of aluminium, titanium, chromium and copper, have been developed and implemented in industry. Machines for welding rails of different classes in the field and stationary conditions, machines for welding pipes of diameter from 150 up to 1420 mm in construction of main pipelines, installations for welding elements of aerospace engineering structures have found the most wide spreading. Equipment for rail flash-butt welding is exported to many countries of the world.

Using the explosion energy, the new methods of welding, cutting, cladding and treatment of welded joints were created. Explosion welding and cutting can be realized in the field conditions, where the use of cumbersome welding equipment is difficult.

Over many years the Institute carries out investigations in the field of space welding. In 1969 on the board of spaceship «Soyuz-6» V.N. Kubasov, the pilot-cosmonaut, performed for the first time in the world the experiment on electron beam, plasma and consumable electrode welding using unit «Vulkan», designed and manufactured at the Paton Institute. Thus, the start was made for the space technology having a great importance in the program of exploration of space. In 1984 a very important experiment, prepared by the Paton Institute, was performed on the board of orbital station in the open space. Cosmonauts S. Savitskaya and V. Dzhanibekov performed for the first time in open space the processes of welding, brazing, cutting and coating deposition using an electron beam versatile hand tool (VHT). The period from 1985 till 2000 is characterized by the growth in volume of jobs made in space. The works were continued on coating deposition and welding of metals, integrated experiments on deployment of 12 m truss structure, accompanied by welding and brazing of its separate sub-assemblies using VHT, were made, two 15 m truss structures, being the load-carrying base for multiple-use solar batteries of technological module, docked to the orbital station «Mir», were deployed.

In parallel, such complicated problem was also solved at the Institute as mechanization of arc welding under water which became of a great importance in exploration of a near-coast shelf of the World Ocean. Specialists of the Institute have created the equipment for the mechanized arc welding and cutting by a special flux-cored wire at the depths down to 60 m and they are carrying out successfully now the research works on welding application at large depths.

Basic importance was given to the systematic Institute studies in the field of physical-metallurgical peculiarities of welding different metals and alloys by fusion: processes of weld metal crystallization were studied, nature of its structural and chemical inhomogeneity was established, mechanism of pores and cracks formation was studied and measures for their prevention were found. Results of these studies are actually a serious base for the creation and improvement of different types of welding and surfacing consumables.

Intensive progress in modern engineering is accompanied by a constant widening of grades of structural metals and alloys for welded structures. As a result of study of processes proceeding in weld pool, the new welding consumables ---- electrodes, flux-cored wires, fluxes and gas mixtures, have been developed.

Due to increasing volumes of application of plastics as structural material, the investigations on their welding and, first of all, on welding plastic pipes have been started, including those on adhesion bonding.

Experimental-theoretical studies and scientific developments in the field of strength of welded joints and structures represent traditional trends in subjects of the Institute, which were started by E.O. Paton. Today, these studies have a comprehensive nature and advanced laboratory-test equipment is used for their conductance, the unique full-scale experiments and computer modeling are performed. This allows researchers to develop new effective methods of improving reliability of critical engineering constructions at static and cyclic loads, and also to establish the cal-

culation-design principles of assurance of preset service properties of the welded joints. The problem of creation of reliable welded structures covers also the aspects of selection of materials, rational design solutions, technology of manufacture and erection, reduction in metal content, which are solved successfully by the Institute in collaboration with many branch organizations and enterprises. The intensive works are carried out over the recent years for improving the reliability and life of welded structures, and also for the development of effective methods of their diagnostics.

The works of the Institute are not limited by the investigations in the field of metallic materials. The Institute associates showed also an interest to the problems of welding polymeric materials and products. During recently, one more direction has appeared ---- electric welding of soft live tissues. Results of these investigations have found their application in practice of surgery operations.

Since the beginning of the 1950s, the search works and experimental developments were started at the Institute by the initiative of Prof. Boris E. Paton for finding the feasibility of use of welding heat sources for producing metals and alloys of super quality and reliability, on the basis of which the main second trend in the Institute activity was formed, namely the special electrometallurgy. Efforts and achievements of the staff in this new field provided a remarkable progress in the development of the national quality metallurgy.

The new electrometallurgical processes include first of all the electroslag remelting of consumable electrode into a water-cooled mould. Fundamental studies of principle of the electroslag process, its physical-chemical, metallurgical and electrotechnical features ensured the advanced positions of the Institute in the development and application of the electroslag technology (cladding, casting, hot-topping, etc.).

Over the recent years a complex of research works has been fulfilled at the Institute, which served a basis for the development of the new generation of electroslag technologies based on producing ingots and billets directly from the molten metal without remelting of consumable electrodes. These technologies are patented in Ukraine and abroad and realized in industry. In particular, a unique complex on production of bimetal rolling rolls of the world level has been created at the Novokramatorsk machine-building plant.

Two more metallurgical technologies have been created at the Institute: plasma-arc and electron beam. Development of technologies and techniques of these remelting processes was carried out in parallel with fundamental studies of physical-metallurgical peculiarities of refining in a controllable atmosphere or vacuum and processes of crystallization of steels, complex-alloyed alloys, non-ferrous and refractory metals.

Plasma-arc remelting has opened wide opportunities for the production of the new class of structural steels ---- high-nitrogen steels, owing to the comprehensive investigations of gas–metal systems. And the creation of powerful metallurgical plasmatrons allowed the Institute to enter the big metallurgy. New designs of installations of ladle–furnace type of up to 100 t capacity have been developed. The purity of metal, provided in these installations, is not inferior to the electroslag metal by the quality.

Owing to the joint efforts of scientists of the Institute, branch research institutions and manufacturers, the electron beam equipment has been created, and the technology of electron beam melting in vacuum became an indispensable process for producing superquality materials in metallurgy and machine-building. Works in this direction are concentrated now at the Research-Engineering Center «Titan», established at the Paton Institute, which fulfills orders both for enterprises of Ukraine and also for foreign companies.

Investigations of the process of evaporation of metallic and non-metallic materials in vacuum and their subsequent condensation as the basis of a vapour-phase metallurgy gave an opportunity to produce coatings for different materials, including heat-resistant, refractory and composite materials, made it possible to regulate the composition, structure and properties of the deposited layers. Thickness of deposited coatings, depending on purpose of their application, is regulated from tens of micrometers up to several millimeters.

At the beginning of the 1980s a new research trend was formed, namely the integrated investigations for creation of new and improvement of existing technological processes of thermal spraying of protective and wear-resistant coatings. At present, the Institute is developing almost all the advanced processes of deposition of protective and strengthening coatings. Technology and equipment for plasma-arc spraying of wear-resistant coatings, and also equipment for detonation spraying, which can operate using different working gases (acetylene, propane, hydrogen) have been developed.

At all the stages of the Institute activity the development of equipment for mechanization of processes of welding and hardfacing to replace the manual labour of the welder was one of its main tasks. The main principles of design of welding machines, laid by E.O. Paton, are being developed by the staff of Design Office of the Paton Institute taking into account the new tendencies in the progress of welding and metallurgical industries.

A great attention in the Institute is paid to the creation and wide application of automatic monitoring and control of technological processes of welding, special electrometallurgy and spraying using the advanced electronic computational engineering. These developments were based on fundamental studies of definite technological processes as objects of control. The first investigations in this field were started by Prof. B.Evgeny Paton as far back as during the Great Patriotic War and are being developed successfully now by his direct supervision.

A great contribution to the creative achievements of the Institute staff was made by those divisions and scientists dealing with mathematical investigations, developing new methods of modern physical and chemical investigations, creating information systems, databases and expert systems, dealing with pre-

diction and systematic analysis of economical aspects in the progress of welding science and technology.

Owing to the combination of purposeful fundamental theoretical studies with engineering-applied developments, close creative collaboration with industrial enterprises in realization of technological innovations, the Institute for the 70 passed years of its activity was transformed into the largest research center in the field of welding and allied technologies in the country and in the world.

Today, the Institute is the scientific-technical complex, which incorporates the experimental design-technological bureau, three pilot plants, a number of engineering centers. All its subdivisions have in total a staff of about 3500 persons, 1700 among them are working at the Institute proper. The scientific potential of the Institute amounts 300 scientists, among them 8 academicians and 6 correspondent-members, 72 Dr. of Techn. Sci. and more than 200 Cand. of Techn. Sci.

The activity of the Institute and self-financing subdivisions is strictly coordinated and oriented completely for the joint solution of problems in main scientific directions.

Active and direct participation of the Institute scientists in a practical realization of their developments increases their importance as workers of the academic science in the conductance of fundamental studies and search developments in the field of welding and allied processes, and also special electrometallurgy, having an interindustry importance. During 70 passed years the Institute has proved the vitality of orientation to the purposeful fundamental investigations. On the credit side of the Institute scientists there are unique results in knowledge of physics of arc discharge and low-temperature plasma, properties of powerful sharply-focused electron beams, nature of melting, evaporation, crystallization and condensation of metals, physical-chemical and thermophysical processes of welding and refining remelting, strength and reliability of welded joints and structures.

Results of these works were confirmed by licenses and patents. Institute sold more than 150 licenses to the USA, Germany, Japan, Russia, Sweden, France, China and others. About 2600 patents of Ukraine, Russia and foreign countries and also by more than 6500 author's certificates were obtained.

Over the years of the Institute activity more than 60 outstanding developments, made and implemented in the national economy by the Institute specialists in collaboration with industrial workers, were awarded by Lenin, State prizes and also the prizes of names of the famous scientists of Ukraine.

Realization of challenging scientific developments and innovation projects of the Institute is also realized by Technological Park, organized at the Paton Institute, including above 30 research institutions, enterprises, engineering centers and pilot plants, specialized in the field of welding and allied technologies. Among them, such well-known manufacturers of welding equipment as KZESO and SELMA.

One of main trends in the Institute activity is the education and training of scientific and engineering staff. There are post-graduate coarses and the specialized council on approval of theses for defence in the field of welding, special electrometallurgy and automatic control of technological processes.

Education of engineering staff is carried out together with National Technical University of Ukraine «Kiev Polytechnic Institute». Scientists of the Institute deliver review courses to the students and supervise the purposeful preparation of masters. Scientific-industrial and diploma practical works are made in research departments and laboratories of the Institute.

Education of engineers-physicists and mathematicians for their work in the field of welding and special metallurgy is realized at the Chair of Physical Metallurgy and Materials Science of Kiev Division of Moscow Physical-Technical University organized on the base of the Paton Institute.

Professional-technical training and retraining of specialists of welding industry is performed at the Educational Center of the Institute. System of education in the center is very flexible. Structure of educational programs envisages both grouped and also individual education and training of audience of courses. Training is realized in accordance with National and European standards with issue of appropriate certificates.

Center of certification of products of welding industry, which was accredited as a body of certification, named SEPROZ, has been created on the base of the Institute, having a unique scientific and staff potential, well-equipped test laboratories. At present the Center carries out work on improvement of certification system in accordance with International rates and rules.

Institute has wide international relations with leading centers of welding in Europe, the USA, Asia. It is the member of International Institute of Welding and European Welding Federation. Interstate Scientific Council on welding and related technologies of CIS countries, International Association WELDING and International objedineniye INTERM are functioning at the Institute facility.

Results of investigations of the Institute scientists are continuously published in journals «Avtomaticheskaya Svarka», «Sovremennaya Metallurgiya», «Tekhnicheskaya Diagnostika i Nerazrushayushchy Kontrol», «Svarshchik», manuscripts, handbooks and other books are issued. In addition, the Institute publishes «The Paton Welding Journal» and «Advances in Electrometallurgy» in English.

Institute organizes different conferences and seminars, national and international exhibitions.

A glorious way was passed by the Institute during 70 years. Today, the Institute is the union of like-minded persons, multiplying the success of Paton scientific school having a world recognition. The Institute is growing and progressing, its structure and management system are updated and all this is directed to the further development of welding and allied processes, and also to the solution of basic problems of economy of the industrial production.

ABOUT SOME «OLD–NEW» PROBLEMS OF ESR

B.E. PATON, L.B. MEDOVAR and **V.Ya. SAENKO**
E.O. Paton Electric Welding Institute, NASU, Kiev, Ukraine

Old and new problems in production of large ingots for large forgings used in heavy and power engineering sectors are considered. New capabilities of the advanced ESR and ESW and their modifications are shown, ensuring improvement of metallurgical quality of large-tonnage ingots and forged-welded billets of alloyed steels and alloys applied in production of superlarge rotors of gas and steam turbines of power plants.

Keywords: *electroslag remelting, large forging ingots, alloyed steels and alloys, nickel superalloys, electroslag welding, ESW with application of filler lumpy materials, electroslag cladding, ESC with liquid metal, ESR by double-circuit diagram, ESW with liquid metal*

The return to the old, from a direct viewpoint of time, everlasting problems is characteristic of many fields of science and technology. In particular, the increased interest to the large forging ingot of electroslag remelting for needs of machine building is observed again over the recent years.

Heavy and power machine building is developing by enlargement of products, their separate assemblies and parts whose mass is measured by tens and thousands of tons. Moreover, with increase in their dimensions and mass the level of requirements to the quality of parts and ready products, and also to the technical-economical characteristics of their production are increased simultaneously, depending, first of all, on the accepted process flow diagram, including method of welding in case of forged-welded and cast-welded products.

At the past 15th International Conference of smiths «IFM-2003», held on 26–29 October, 2003 in Kobe, Japan, several papers were presented which proved the effectiveness of ESR application for producing large ingots for forgings of rotors and discs of powerful steam and gas turbines [1–3].

The paper, presented by Saarschmiede, Germany, the known supplier of turbine forgings, describes the experience of production of rotors of steam turbine high- and medium-pressure cylinders made from 1 % CrMoV and 2 % CrMoWV steels (these steels are similar to steels of 25Kh1M1FA and EI415 grades), designed for operation at vapour temperature up to 585 °C, and low-pressure cylinders made from steel of (23–27) % NiCrMoV type (analogues to 25KhN3MFA and 26KhN3MFA steels). The important advantage of this work is a combined rotor of 2 % CrMoWV steel, which combines stages of high, medium and low pressure owing to their treatment for different structures (martensite, bainite). A superpure steel is used widely at the Saarschmiede Company that makes it possible to increase also the temperature of working medium in gas turbines at the stages of low pressure of steam turbines. Superpure steel means steel with a content of Cu, Si, Mn < < 0.03 % each, As < 0.007 %, Sb < 0.0007 %, Sn < < 0.0035 %. Actual content of phosphorus is at the level of 0.007 %, sulphur ---- of less than 0.005 %. This low content of harmful impurities in metal is the necessary condition to satisfy requirements specified to service characteristics, in particular to a long-term strength. The ESR ingots of up to 165 t mass are used for manufacture of large rotors.

It is noted in the paper, presented by Japan Casting and Forging Corp., that when melting large ingots from high-chromium steel with boron it is necessary to determine the ratio between B_2O_3 in slag and boron in metal in ESR or electroslag hot topping of a large ingot after casting by a syphon method. A special slag is poured into a lined head of this ingot and graphite and consumable electrodes are immersed. Using this technology, ingots of mass from 62 up to 106 t are produced by casting.

It is outlined in paper, prepared by Japanese specialists of Daido Steel and Mitsubishi Heavy Industries, that at addition of low content of elements-deoxidizers the vacuum electroslag remelting of electrode produced by a vacuum induction melting could provide a preset content of boron and nitrogen in a Co-containing steel for blades and bolts of steam turbine rotors operating at 650 °C. The superpure steel contains, %: 10Cr, 0.7Mo, 1.7W, 0.23V, 0.08(Nb + + Ta), 3.3Co, 0.07B, 0.022N.

Paper of A. Mitchell, the known specialist from Canada [3], describes methods of ESR, VAR, ES hot-topping and ESW as technologies of manufacture of rotors and shafts from steels and alloys prone to segregation. It is shown that to produce large-tonnage high-quality ingots from NiCrMoV and CrMoV steels a proper selection of technology of their melting, providing the superpure metal, application of moulds, optimum by geometric parameters, in pouring and also proper technology in their forging are important. Other approaches are required in melting large ingots from Ni-base alloys, in particular from Inconel 718 alloy, to provide high-quality metal because of the susceptibility of these alloys to segregation and formation of defects of «freckles» type, which are not removed in heat treatment.

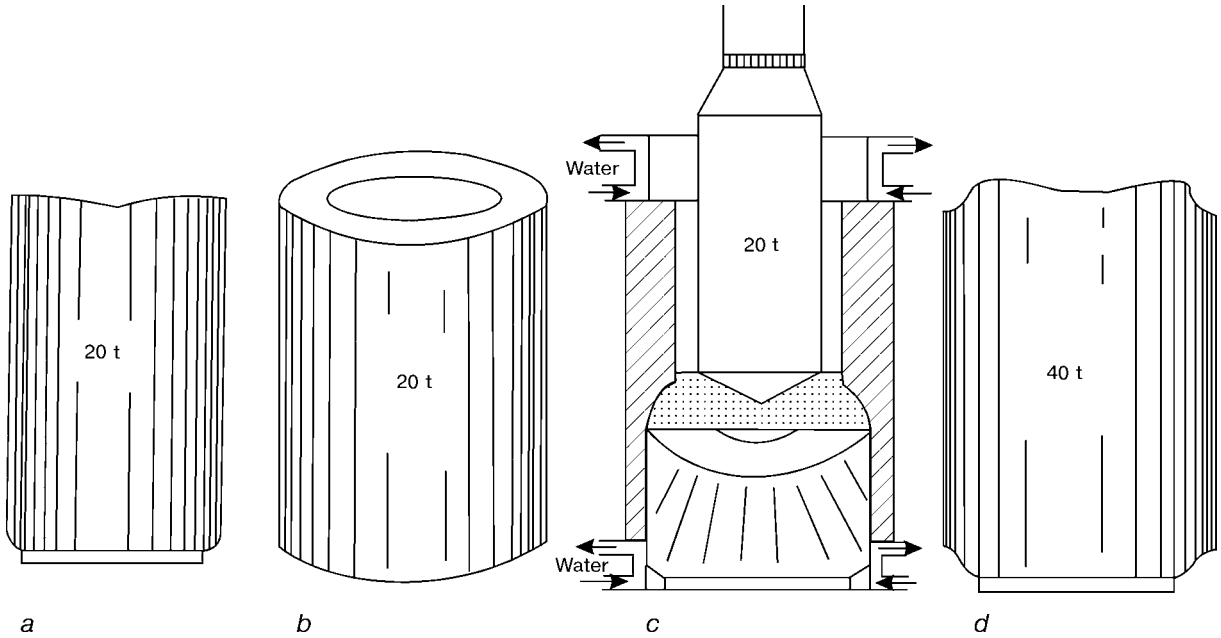

Figure 1. Scheme of enlargement of ingots by ESR in consumable moulds: *a* — ingot of 20 t mass; *b* — consumable mould; *c* — ESR in consumable mould; *d* — enlarged ingot of 40 t mass

It was noted that the application of remelting processes does not also solve all the problems of production of large ingots from Ni-based alloys with increase in their diameter: in case of VAR — by more than 1000 mm, and for existing diagrams of ESR — by more than 700 mm. As an alternative, A. Mitchell describes the method of enlargement of ingots on the basis of ESW and ESR of powder materials using a non-consumable electrode, which were developed in different years at the E.O. Paton Electric Welding Institute [4–6].

It should be outlined that the problem of producing the quality large forging ingot becomes periodically acute. The attempts to solve or to avoid the problem of suppression of structural defects of a liquation origin were made many times. It was known long ago even without a clear nature of formation of these defects that they are more distinct at larger ingot section and mass and, consequently, the larger size of a two-phase zone in the solidifying ingot, the longer time of its solidification.

The main drawback of canonical diagrams of ESR and VAR is the rigid relation between the electrical (heat) condition and rate of metal melting that stipulates a comparatively large volume of a metal pool and unfavourable its shape from the point of view of crystallization conditions.

One of the possible solutions of the problem of producing defect-free large-tonnage ESR ingots from nickel superalloys is the application of a new process of ESR of consumable electrode in a current-carrying mould using a double-circuit diagram (ESR DC), developed at the Paton Institute [7]. Using ESR DC, any preset efficiency of the process and shape of metal pool can be obtained independently of the ingot diameter. If the metal pool depth in its central part is equal usually at the canonical diagram of the ESR or VAR to the value of the ingot radius, then the metal pool in ESR DC can be much smaller and have almost a shallow shape. An important advantage of the ESR DC process is the proper formation of the ingot surface.

It is quite evident that the mentioned problem can be also solved by producing a large ingot of the required size from smaller ingots, free from defects, by their joining into a single block. These approaches were realized by using the electroslag welding process.

As far back as the beginning of the 1970s the method of ESR in a consumable mould was developed at the Paton Institute for enlargement of forging ingots without deterioration of their quality [4]. The so-called consumable mould is made by piercing and expansion of ingot or a cast hollow ingot is used. Then, an electrode of metal whose chemical composition is similar to the metal of the consumable mould is remelted in this mould. Ingot mass in this case can be 1.5–3 times increased (Figure 1) without increase in power of the electroslag furnace transformer. In case if the consumable electrode and mould are manufactured from different grades of steels and alloys, the method described allows producing bimetal billets which, when necessary, can be used in the production of bimetal shaped rolled metal or bimetal tubes.

The modifications of the mentioned process in the West were named MHKW from the names of companies of its realization (Midvale Heppenstal / Klockner-Werke) [8]. The central zone of a conventional ingot, subjected mostly to defects, is removed using a forge press. Then the hole is filled with a proper material by ESR. By the beginning of the 1980s of the last century about 30 ingots of up to 210 t mass were produced by this process at the factories in Osnabruck, Germany. In some cases the defects in the transition zone between the parent metal and a core melted were observed. They were caused by shrinkage phenomena, aggravated by a rigid ther-

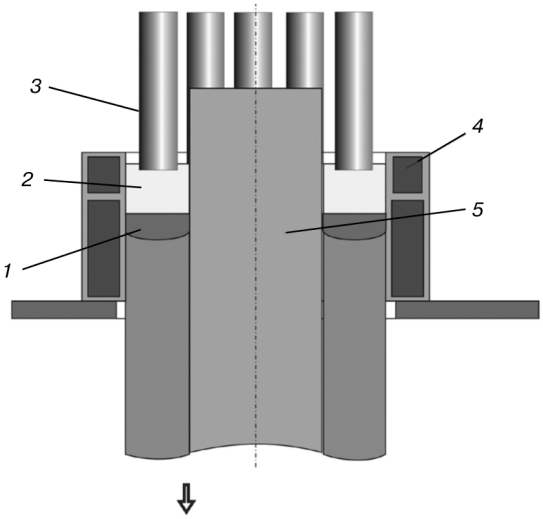

Figure 2. Scheme of enlargement of ingots by ESCe method in movable short mould: *1* — metal pool; *2* — slag pool; *3* — consumable electrodes; *4* ---- mould; *5* — ingot

modefomational cycle, observed in filling an axial zone. Due to this the process MHKW did not find the wide application for production of heavy-loaded rotors.

The more favourable thermodeformational conditions can be provided at a circumferential electroslag cladding of metal on a central axial ingot. In this case the metal pool of the metal being clad has a minimum volume, and the two-phase zone of a solid-liquid state has a minimum length that avoids the formation of crystalline defects.

The process flow diagram, developed at the Paton Institute, for the enlargement of heavy forging ingots using the method of a circumstantial electroslag cladding (ESCe) includes the placing of a central ingot into a short mould, embracing it at a preset gap, limitation of the gap at the bottom by a circular bottom plate with a primer which are included into a forming part of the mould. The ingot is formed in the ESCe process at a relative opposite movement of ingot and mould by a partial melting of a central ingot and melting of one or several consumable electrodes. Diameter of this ingot is larger than that of an initial central ingot by a value equal to a doubled preset gap (Figure 2).

Ingot, melted preliminary by the above-mentioned technology, can be used as initial ingot. Lumpy filler materials or molten metal in combination with consumable (or non-consumable) electrodes, or without them in case of use of the current-carrying mould can be used for ESCe.

The idea of producing quality forged-welded product from two or more ingots (forgings) of a comparatively small size with a guaranteed absence of structural defects of a liquation origin is rather challenging and can be realized today on the basis of application of methods of electroslag welding, for example, using a bifilar diagram (ESWb).

Several modifications of ESWb methods were realized under industrial conditions, including ESW

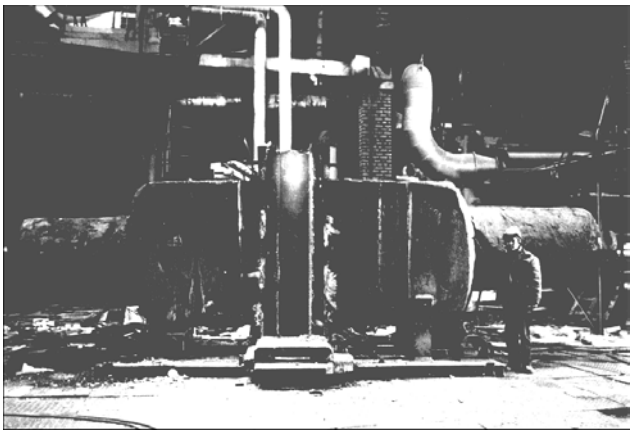

Figure 3. Forged-welded billet of a working roll, made from steel 50KhN, 103 t mass, enlarged by ESW LFM method for mill LP04500

LFM (electroslag welding with two stationary electrodes using feeding of lumpy filler materials in the form of shot or cuts into a welding gap) (Figure 3). Technology of electroslag welding using a liquid metal (ESW LM) instead of lumpy filler materials, developed now at the Paton Institute, widens greatly the ESW capabilities and provides high-quality welded joints, made from steels and alloys of almost any chemical composition, with uniform physical-mechanical properties [9, 10].

Thus, the challenging ideas, put in due time in the creation of the electroslag technology and many its modifications (ESR in consumable mould, ESWb, ESW LFM, ESC LM and others) did not lose their importance today. The tasks for improving quality and service characteristics of metal of large forging ingots and welded billets can be solved successfully on their basis: the old tasks ---- for alloy high-strength steels, and also new ones ---- for nickel superalloys.

1. Kolpishon, E.Yu. (2004) Problem of production of large ingot for large critical forgings. *Elektrometallurgiya*, **3**, 43–47.
2. Kolpishon, E.Yu., Utochkin, Yu.I. (2004) Production of large critical products for power engineering industry. *Ibid*., **5**, 43–46.
3. Mitchell, A. (2003) The prospects for large forgings of segregation-sensitive alloys. In: *Proc. of IFM-2003*, Oct. 26–29, 2003, Kobe, Japan.
4. Medovar, B.I., Emelianenko, Yu.G., Kozlitin, D.A. et al. (1974) Some peculiarities of ESR of metal in consumable moulds. In: *Refining remeltings.* Kiev: Naukova Dumka.
5. Paton, B.E., Medovar, B.I., Andreev, V.P. et al. (1978) New methods of welding of super-large section billets ---- the fixed electrode electroslag welding with lumpy material additions (ESW LFM) In: *Problems of electroslag technology*. Kiev: Naukova Dumka.
6. Medovar, B.I., Saenko, V.Ya., Nagaevsky, I.D. et al. (1984) *Electroslag technology in mechanical engineering*. Kyiv: Tekhnika.
7. Medovar, B.I., Medovar, L.B., Tsykulenko, A.K. et al. (1999) On problem of electroslag melting of large-capacity billets of high-alloy steels and alloys. *Problemy Spets. Elektrometallurgii*, **2**, 26–30.
8. Kunelt, G., Makhner, P. (1983) Current methods of production of large forging ingots. In: *Electroslag remelting*. Issue 7.
9. Medovar, B.I., Medovar, L.B., Saenko, V.Ya. et. al. (1999) Electroslag process using the liquid metal as a new way in electroslag technology development. *Problemy Spets. Elektrometallurgii*, **3**, 3–9.
10. Paton, B.E., Medovar, L.B., Saenko, V.Ya. (2003) New opportunities of electroslag technology in machine building. *Metallurgiya Mashinostroeniya*, **1**, 2–5.

APPLICATION OF ELECTROSLAG TECHNOLOGY FOR PRODUCING IRON ALUMINIDES

A.A. TROYANSKY, A.D. RYABTSEV and **N.N. GALYAN**
Donetsk National Technical University, Donetsk, Ukraine

The feasibility of producing ingots of iron aluminides Fe_3Al and FeAl using a chamber electroslag remelting of steel--aluminium composite consumable electrodes under calcium-containing fluxes in controllable atmosphere is shown. Quality and homogeneity of the produced material were confirmed by chemical and metallographic analyses.

Keywords: *chamber electroslag remelting, iron aluminides, technology, calcium-containing flux*

The creation of new equipment, operating under the conditions of high temperatures, aggressive media, erosion flows, is impossible without use of new materials, such as intermetallics and, in particular, iron aluminides. Intermetallics are chemical compounds of metals occupying an intermediate position between the metals and ceramics both by the type of a chemical bond and also by properties. Some of intermetallic compounds have chemical bonds of a metallic type, other ones ---- of a covalence type. Long-range order provides the stronger interatomic bond. Intermetallics have the better workability than ceramics. In parallel with a definite ductility they preserve their structure and strength at high temperatures and are characterized by good anticorrosion and antifriction properties, thus being much superior to ordinary metals.

Iron aluminides are a new class of extralight challenging structural materials designed for operation at 630–680 °C temperatures, exceeding operating temperatures of service of titanium superalloys (< 600 °C). Content of aluminium in compound Fe_3Al is within 14–17 wt.% ranges and that in FeAl compound is 25–32 wt.%. Aluminides are lighter than some superalloys (density of industrial Ni-base alloys is 8.3–8.9 g / cm^3, density of Fe_3Al is 6.72 g / cm^3, density of FeAl is 5.56 g / cm^3) and do not need almost the protection from oxidation at operating temperatures.

Alloys on Fe_3Al base are used in automotive industry as substitutes for stainless steel in the exhausting system [1], as a material for discs of regenerators of automobile gas turbine systems [2] and are promising for space engineering and manufacture of separate assemblies and discs of gas turbines operating at 630–680 °C temperatures [3]. Alloys on FeAl base can be used in systems of catalytic complete burning of exhaust gases, in elements for resistive heating, they are also promising as composite materials for space engineering [4].

Production of iron aluminides as structural material of appropriate level of properties for the conditions of high-temperature service does not require a large amount of deficit alloying elements. At the same time, it is still limited by the absence of relatively simple and inexpensive technologies, complicated by a great difference in temperatures of melting, evaporation and densities of aluminium and iron. Due to the high vapour pressure of aluminium it is difficult to melt these alloys in vacuum units.

The methods of producing alloys on iron aluminides base by hot and cold pressing of powders [5, 6], including those with a mechanical alloying [7] and also by arc and plasma spraying [8] and others, are known. Technology of their production is multistage and complicated that makes the product more expansive and its application less effective.

There is also information in literature about producing iron aluminides using methods of special electrometallurgy. Thus, in work [9] a method was suggested and tested for production of iron aluminide by two-stage diagram: melting of consumable electrodes of Fe_3Al composition from steel scrap and commercially pure aluminium in vacuum-induction furnace and producing ingots with 16 wt.% Al and 0.014–0.5 wt.% C content from them using the method of classical electroslag remelting. After heating to 1000 °C and 1 h soaking in furnace the ingots were subjected to plastic deformation. Here, a good workability of ingots with carbon content of more than 0.14 wt.% was observed, while the ingots with carbon content of less than 0.06 wt.% had cracks during deformation. Authors explain the improvement of mechanical properties of iron aluminides with [C] $\geq$ $\geq$ 0.14 % by a uniform distribution of Fe_3AlC inclusions and dissolved carbon in ingots.

The present work is devoted to the study of feasibility of producing ingots of iron aluminides by the methods of electroslag remelting of composite consumable electrodes using traditional flux ANF-6 in open unit and flux of CaF_2–Ca system in a chamber furnace (CESR).

The base of consumable electrode was steel 50 rolled rods of 45 mm diameter. Aluminium bars of 34×25 mm section (Figure 1, *a* and *b*) or rods of 70 and 27.4 mm^2 section (Figure 1, *c* and *d*) were fastened to them by bolts and steel wire for aluminium adding to ingot in stoichiometric ratio. Mass share of aluminium part in electrodes was 17 % (to produce

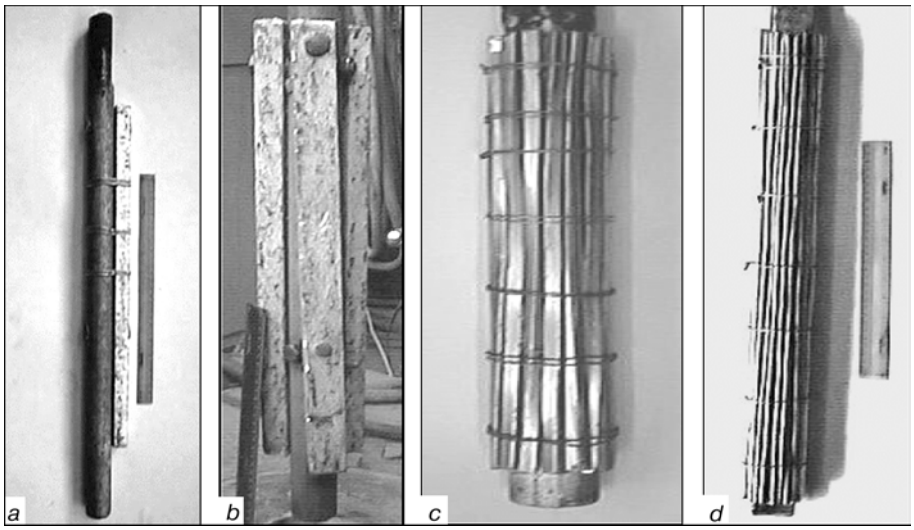

Figure 1. Iron–aluminium composite consumable electrodes: *a*, *c* — 17 % mass share of aluminium part; *b*, *d* ---- the same, 32 %

intermetallic Fe_3Al, containing 25 at.% Al) and 32 % (to produce intermetallic FeAl, containing 50 at.% Al).

Electroslag remelting of electrodes was performed in installation A-550, modified into a chamber ESR furnace, in air and in controllable argon atmosphere, into water-cooled moulds of 100 and 130 mm diameter. Technology of «solid» start on metal chips was used in both cases for slag pool setting.

In CESR the furnace chamber was pre-evacuated and then filled with argon by maintaining its excessive pressure 10^4 Pa during melting. Flux for this variant was prepared from calcium fluoride of OSCh5-2 (base) grade and metal calcium (4.0–7.4 wt.%).

Two ingots were melted by a traditional monofilar diagram using flux ANF-6. Both ingots had a smooth surface. However, the ingot with a design content of 25 at.% Al had transverse cracks, while that with a design content of 50 at.% Al fractured itself in air. This is, probably, associated with changes in slag composition during melting due to active oxidation of aluminium, that is proved by an intensive evolution of white smoke from the mould and by a possible metal saturation with carbon [10] from thermosplitting graphite placed on the slag surface for its protection.

The results obtained showed that the use of a canonical ESR diagram for the production of iron aluminides without special measures of protection of electrodes and melting spacing is not rational. Definite prospects in this direction are opened by CESR combining the feasiblity of protection of electrodes and melting space by inert gas and use of metal-containing fluxes providing highly-deoxidized actively-refining medium [11].

To produce ingots of intermetallics Fe_3Al and FeAl from steel–aluminium composite consumable electrodes, the CESR was used in argon atmosphere using a Ca-containing flux. The melted ingots of 100 mm diameter were cooled in mould during 30 min, and then the chamber was removed and ingots withdrawn. Ingots had a smooth surface (Figure 2, *a* and *b*) from which the slag «cap» and skull were removing easily.

Ingots were cut along the longitudinal axis, and then one half was used for chemical analysis, and transverse templets were manufactured from a middle part of the second half for macro- and microstructural analysis after their preliminary grinding and etching in 10 % water solution of HCl (for macrostructure) and in 10 % water solution of HNO_3 (for microstructure). Sections were examined in optical microscope

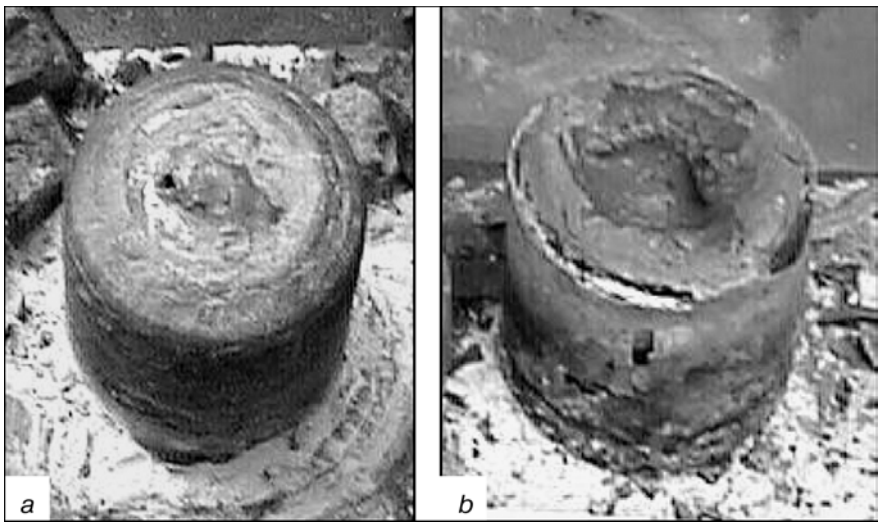

Figure 2. CESR ingots of iron aluminides: *a* — Fe_3Al ingot; *b* ---- FeAl ingot

Table 1

Points of sampling in ingot (Figure 3)	Aluminium content, %	
	Ingot Fe_3Al	Ingot FeAl
1	14.3	29.2
2	13.69	29.7
3	14.35	–
4	14.7	–

Table 2

Ingot	Microhardness, *HRC* (kgf / mm^2)	
	Ingot matrix	Inclusions of the second phase
Fe_3Al	33–34 (320–327)	570 (51)
FeAl	50 (551)	–

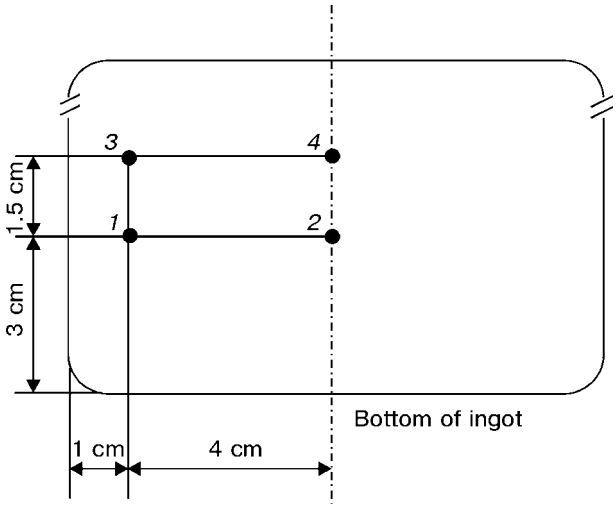

Figure 3. Scheme of sampling from CESR ingot

Figure 4. Macrostructure of CESR Fe_3Al ingot

Neophot-2 and JEOL scanning microscope JSM-T3000, determining here also a local chemical heterogeneity using X-ray spectral analysis.

Samples were photographed by a digital camera QV-100 and numerical file was analyzed using a program package ACD. Microhardness was measured by a meter PMT-3 (15 measurements per one point) by indentation of a diamond pyramid at different loads. Chemical analysis of chips from different points of the ingot (Figure 3) was made by a titrimetric complexonometric (complexon III) method.

Results of chemical analysis of CESR ingots (Table 1) indicate their insufficient homogeneity. Macrostructure (Figure 4) is dense without visible defects and has a directivity typical of the ESR ingots. Mean values of microhardness are presented statistically in Table 2. The given values of microhardness have a good correlation with earlier published data [12].

It was established by the microstructural analysis that ingot Fe_3Al produced by the CESR method has a two-phase structure which consists of a matrix and second phase in the form of rounded branched inclusions, their thickness is 50 μm on average. Inclusions are arranged uniformly throughout the ingot (Figure 5, *a*). The second phase was identified as perovskite Fe_3AlC. Ingot FeAl has a single-phase dendritic structure (Figure 5, *b*).

Microstructures, revealed by the scanning electron microscopy, are presented in Figure 6. The observed composition contrast occurs during scanning of objects by an electron probe with a local changes in chemical composition at changing the coefficients of the secondary emission and reflection of electrons. With increase in atom number of the element the reflection coefficient of electrons is growing. Therefore, the places, enriched by the heavier elements, reflect the higher amount of electrons and they are light on the photo.

Dark areas (Figure 6, *a*) correspond to inclusions of the second phase Fe_3AlC, enriched by the lighter element (carbon). In ingot FeAl, containing about 29 wt.% Al, the inclusions of the second phase are not observed (Figure 6, *b*) that can prove the transition of carbon mainly into a dissolved state.

Metal examination for a local chemical heterogeneity in a characteristic radiation Al-*k* and Fe-*k* indicates a uniform distribution of aluminium and iron in the ingot (Figure 7).

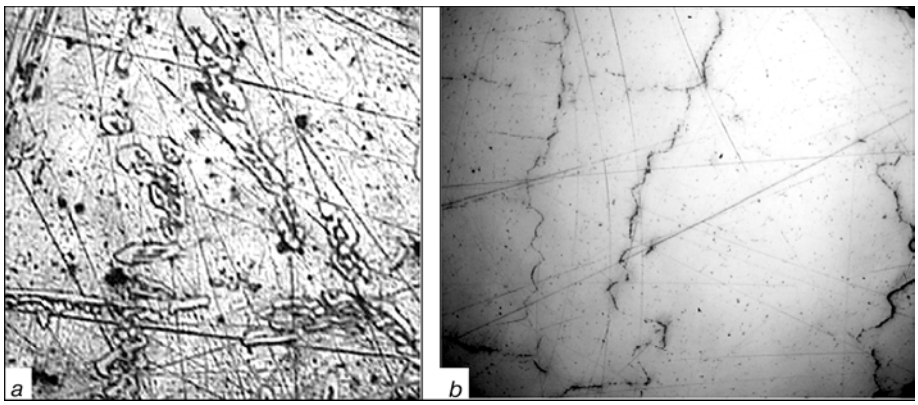

Figure 5. Macrostructure of CESR ingots: *a* — Fe_3Al ingot (×250); *b* — FeAl ingot (×150)

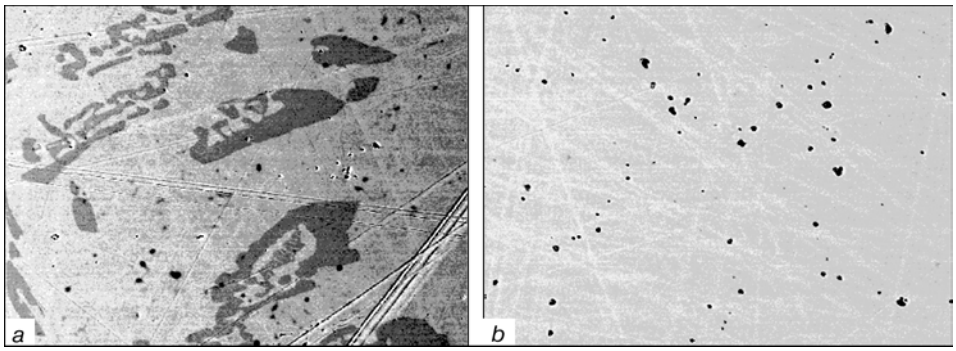

Figure 6. Microstructure of CESR ingots, obtained by scanning electron microscopy: *a* ---- Fe_3Al ingot; *b* — FeAl ingot (×500)

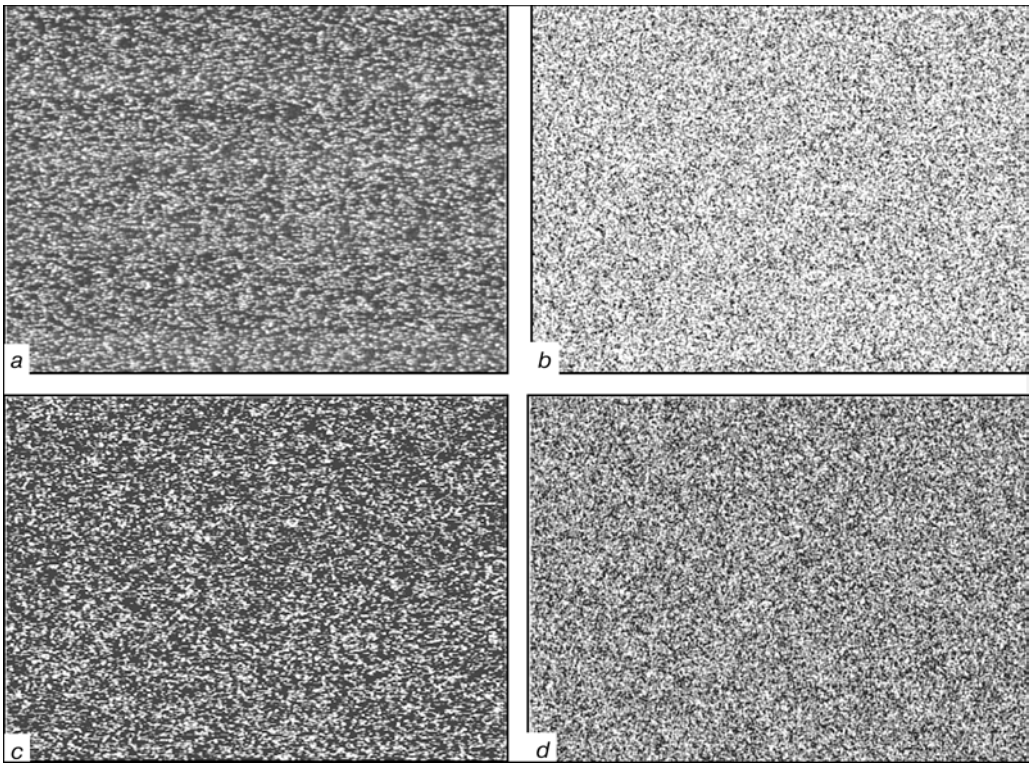

Figure 7. Distribution of aluminium and iron in CESR ingots: *a*, *b* ---- sample of Fe_3Al ingot in characteristic radiation Al-*k* and Fe-*k*, respectively; *c*, *d* — sample of FeAl ingot in characteristic radiation of Al-*k* and Fe-*k*, respectively (×1500)

The high-temperature resistance of experimental metal to oxidation was determined on samples cut out from middle parts of ingots Fe_3Al and FeAl. Samples of 1 g mass were suspended on a nichrome wire to a tensometer and placed into Tamman furnace heated to 800 °C temperature. After 2 h of holding in furnace a share of increment in mass of samples was 0.35 and 0.25 %, respectively. This indicates a high resistance of experimental metal under high-temperature conditions.

Thus, the given results of investigations prove the feasibility of producing ingots of intermetallics of Fe–Al system in chamber electroslag furnaces.

1. Irvin, R.R. (1989) Intermetallics offer potential for down-to-earth uses. In: *Metalwork News*.
2. Sikka, V.K., Viswanathan, S., McKamey, C.G. (1993) Development and commercialization status of Fe_3Al-based alloys. In: *Poc. of Int. Symp. on Structural Intermetallics, Champion*, Sept. 26–30, 1993.
3. (1995) *Superalloys II: Heat-resistant materials for aerospace and industrial power plants*. Book 2. Moscow: Metallurgiya.
4. Deevi, S.C., Sastry, D.H., Sikka, V.K. (2002) Alloy development and industrial processing of iron aluminide sheets. In: *Proc. of 3rd Int. Symp. on Structural Intermetallics*, Wyoming, April 28–May, 2002.
5. Kimugaya, M. *Method of manufacturing of combustion engine inlet and exhaust valves made of aluminide*. Appl. 438832 Japan. Publ. 31.01.92.
6. Rawers, J.S. (1994) Tensile fracture iron–iron aluminide foil composites. *Scr. Met. et Mater.*, 30(**6**), 701–706.
7. Bonetti, E., Scipione, G., Enzo, S. et al. (1994) Solid state reactivity thermal stability and structural properties of Fe–Al nanostructured intermetallic compounds. In: *Abstr. of 2nd Int. Conf. on Nanostructured Materials*, Stuttgart, Oct. 3–7, 1994.
8. Lawrynowicz, D.E., Lavernia, E.J. (1994) Spray atomization and deposition of fiber reinforced intermetallic matrix composites. *Scr. Met. et Mater.*, 31(**9**), 1277–1281.
9. Baligidad, R.G., Prakash, U., Radhakrishna, A. et al. (1996) Effect of hot working on room temperature mechanical properties and stress-rupture behavior of ESR processed Fe–16 wt.% Al intermetallic alloys. *ISIJ Int.*, 36(**9**), 1215–1221.
10. Bobro, Yu.G. (1964) *Aluminium cast irons*. Kharkov: KhGU.
11. Ryabtsev, A.D., Troyansky, A.A., Tarlov, O.V. et al. (2000) Study of possibility of manufacturing of titanium–aluminium alloy by inert atmosphere electroslag remelting method with «active» calcium-containing fluxes. *Problemy Spets. Elektrometallurgii*, **1**, 75–78.
12. Baligidad, R.G., Prakash, U., Ramakrishna, V.R. et al. (1996) Effect of carbon content on mechanical properties of electroslag remelted Fe_3Al-based intermetallic alloys. *ISIJ Int.*, 36(**12**), 1453–1458.

CENTRIFUGAL ELECTROSLAG CASTING OF FLANGE BILLETS USING INOCULATING MODIFYING

E.N. ERYOMIN and **S.N. ZHEREBTSOV**
Omsk State Technical University and Omsk Plant of Special Production, Ltd., Omsk, Russia

Method of producing high-quality billets of flange type using the centrifugal electroslag casting with metal modifying by dispersed particles of titanium carbonitride is described. Results of comparative analysis of cast metal are given and advantages of the method are shown.

Keywords: *centrifugal electroslag casting, modifying, structure, mechanical properties, flange billets*

At the present time the products in the form of ring-shaped billets of a flange type are widely used at the enterprises of gas and petroleum refining industry for joining different pipelines. These products are produced by GOST 12820–80, GOST 12821–80 from 20, 09G2S, 10G2, 2Kh13, 08Kh18N10T grade steels and others and operate at high pressures and under severe climatic conditions, at abrupt drops of temperatures of transporting media and, therefore, they are critical components supervised by the GOSGORTEKHNADZOR of Russian Federation.

These products can be manufactured using different technological processes. Forging, stamping, casting by traditional methods (open methods of melting) with a post mechanical treatment of billets are most widely used. These standard technologies have both advantages and drawbacks.

Advantages of the traditional technology of casting are the high accuracy of billets with minimum tolerances for machining and a high factor of metal utilization. Its drawbacks refer to a poor quality of metal and difficulty in producing dense billets, because the molten metal during melting and pouring is saturated with gases, non-metallic inclusions, harmful impurities and prone to structural and chemical inhomogeneity. Therefore, the cast billets for manufacture of critical components are not used in principle.

Products, made by forging, have the higher metal quality, though they can inherent the defects of cast billets and ingots used in this case. The important drawbacks of this technology are the high cost of billets, stipulated by the use of a large number of intermediate operations (forging of ingots for billets, their cutting, piercing and expansion), a low factor of metal utilization and the need in expensive forging and rolling equipment. Thus, the hot working in manufacture of flange billets is a forced procedure which is used due to a poor quality of casting.

The challenging trend in the solution of this problem is the replacement of forged billet by high quality castings with minimum tolerances for machining. As these components have central through holes, then it is rational to use a promising technology for their manufacture: a centrifugal electroslag casting which is free from many above-mentioned drawbacks owing to its technological features [1].

The principle of the technology consists in electroslag remelting of electrode in a melting unit, providing accumulation of molten metal and slag in required amounts and its subsequent pouring into a rotating mould. Consumable electrodes of any shape and cross-section can be used as remelting metal. It is this technology that was used for manufacture of critical flange billets.

Remelting of the consumable electrode was performed under the flux, representing a mixture of calcium fluoride, electric corundum, magnesite and silica. Such flux provides the molten metal refining in a melting unit from sulphur and phosphorus, protection from a harmful effect of surrounding medium, and is characterized also by a significant fluidity at high rate of cooling [2].

Method of electroslag casting is simple and efficient. Equipment for the realization of this technology includes serial installations of A-550U or EShP-0.25 types, a skull melting unit of a special design, a centrifugal machine with a vertical axis of rotation and a casting mould.

Accuracy of the produced casting is defined a casting mould. Therefore, a composite metal chill mould,

Figure 1. General view of dismantled metal chill mould with casting in a skull

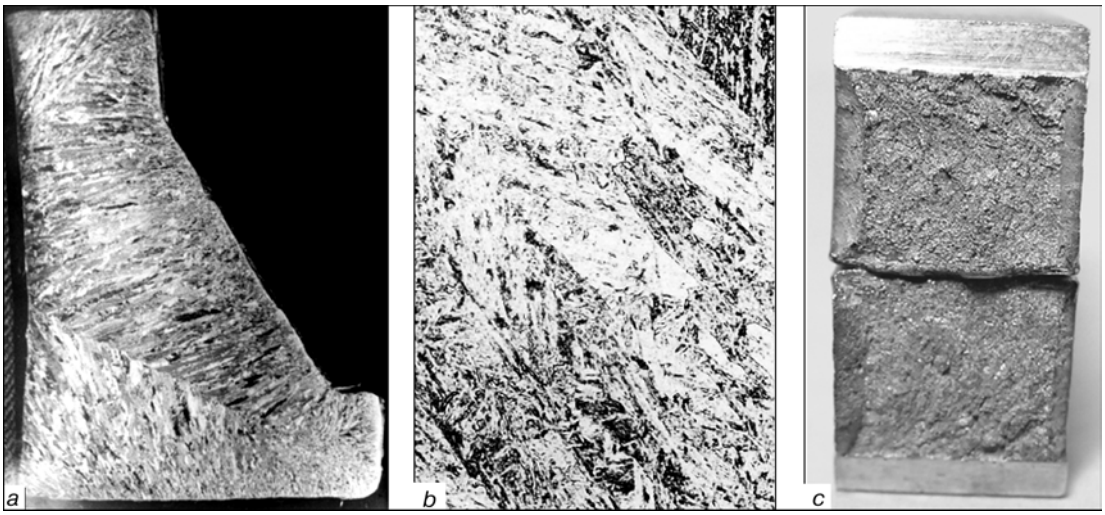

Figure 2. Structure of cast non-modified steel 2Kh13: *a* — macrostructure; *b* — microstructure (×200); *c* — fracture relief

manufactured using a method of a lathe machining of ring-shaped billets, each of them repeats a part of an external configuration of the piece being cast, was used. During pouring out of a slag-metal jet into a mould its separation is occurred under the action of centrifugal forces. Slag prevents the casting sticking to the cast mould walls, thus spreading by a thin and uniform layer over its surface. A larger part of the slag is forced out inside and upward the casting where it is a hot top and does not allow formation of cavities. With a general reduction in temperature of metal and slag, a skull, separated from billet only after its withdrawal from the mould, is formed. As an example, the Figure 1 shows a general view of a dismantled metal chill mould with a casting.

The important advantage of this technology is the feasibility of billet metal hardening owing to its modifying. The modifier was selected in accordance with a procedure described in work [3]. It was established that an integrated modifying with synthetic ultradispersed particles of titanium carbonitride in the amount of 0.3–0.5 % of the melt mass is most effective. The modifier was produced by mixing the powdered components with a subsequent cold pressing into tablets of 25–30 mm diameter and 8–15 mm thickness. Sizes of tablets were selected from the condition of their dissolution in a molten metal being modified during 20–30 s. The modifier was added at 1650 °C temperature for 2 min before the pouring out that provided the uniform distribution of dispersed particles-inoculators in the entire volume of the molten metal in the melting unit. Metal pouring into a metal casting chill mould was made at 1600 °C temperature.

Billets of flanges, produced by the centrifugal electroslag casting with a modifying (CESCM), satisfy all specified requirements to the products: this is a geometric accuracy of casting and also high properties of the metal. Thus, the tolerance for machining as to the external surface is 2.0–2.5 mm, in height ---- up to 4 mm, as to the internal diameter ---- 8–15 mm. Here, the metal utilization factor is 0.6–0.8. This reduces significantly the metal content of the product and power consumption for its manufacture.

The electroslag modified metal is differed from metal, produced by an open melting, by a fine-grain structure, high chemical homogeneity, absence of foreign oxide inclusions, air bubbles, pores, cavities, cracks, low content of harmful impurities of sulphur and phosphorus, uniform density of metal in the entire volume and, consequently, also by the isotropy of

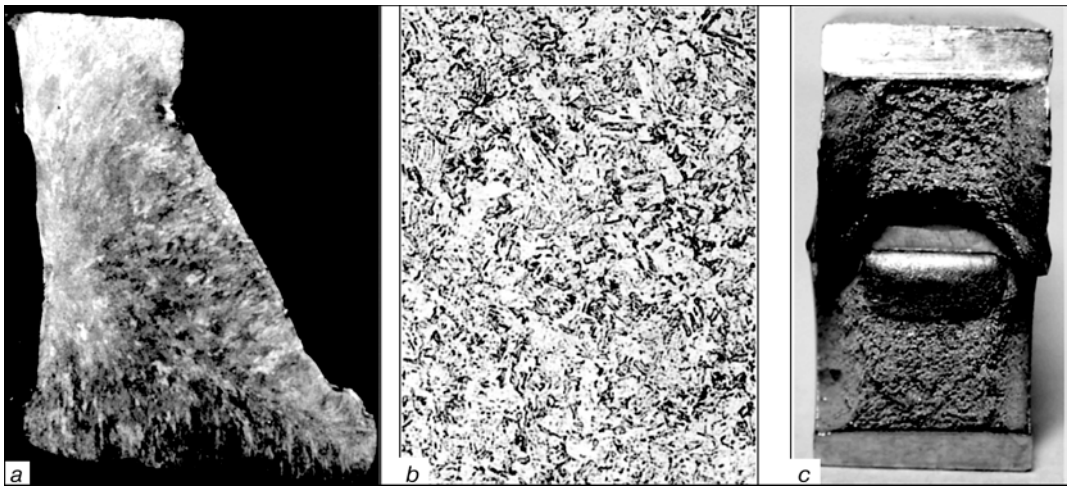

Figure 3. Structure of cast modified steel 2Kh13: *a* — macrostructure; *b* — microstructure (×200); *c* ---- fracture relief

Steel grade	Heat treatment conditions	σ_t, MPa	σ_y, MPa	δ, %	ψ, %	KCU^{+20} MJ / m^2
09G2S	Normalizing at 930 °C, air	505	332	34	62	1.34
09G2S (induction melting)		481	324	21	49	0.76
09G2A (CESCM)		512	343	29	61	1.25
2Kh13	Quenching at 1959 °C, oil, tempering at 660 °C, air	808	636	21.3	68.5	1.42
2Kh13 (induction melting)		784	615	15.4	50.2	0.68
2Kh13 (CESCM)		816	622	20.4	64.6	1.39
08Kh18N10T	Austenization at 1050 °C, air	546	278	55.2	67.5	2.62
08Kh18N10T (induction melting)		514	249	44.3	50.1	1.64
08Kh18N10T (CESCM)		598	324	52.6	61.2	2.13

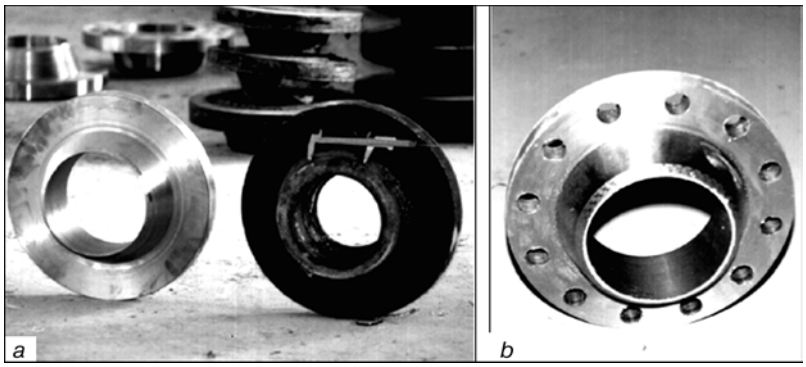

Figure 4. General view of casting, cleaned from skull, and flange D_n 200, produced from it, after preliminary (*a*) and final machining (*b*)

physical-mechanical properties in all the directions. Thus, for example, the analysis of structure of castings produced from 2Kh13 steel proves that non-modified metal has a directed transcrystalline structure with long primary axes of dendrites. Metallographic analysis showed that coarsening of martensite structure is occurred in this case accompanied by a significant increase in hardness with a intercrystalline form of metal fracture (Figure 2).

Adding of 0.4 % of modifier into metal leads to a noticeable change in structure and properties of the cast metal. Zones of transcrystallization in ring-shaped castings are eliminated, sizes of dendrites are abruptly decreased, acquiring a favourable shape in the entire volume of the metal solidified. Structure of castings is characterized by the presence of ferrite-martensite matrix with compact carbides arranged mostly in micrograins, and fracture of impact samples has mainly a transcrystalline nature (Figure 3).

In this case the level of mechanical properties of castings is not almost differed from properties of a forged billet. Results of mechanical tests of some grades of steels used for the manufacture of flanges are given in the Table.

The comparative analysis shows a significant advantage of the electroslag metal over the metal of the open induction melting and small differences as to the properties of the forged metal. Ultrasonic testing and magnetic flaw detection showed a dense cast structure, absence of microcracks and any defects. After mechanical treatment these flanges have passed successfully hydraulic tests for air tightness under 44 MPa pressure. As an example, Figure 4 shows a general view of casting and ready flange D_n 200 at pressure of working medium P_n 10 MPa. As a whole, the properties of electroslag metal satisfy the requirements of TS26-0157-24–69 that makes it possible to use the cast electroslag castings instead of forgings. In addition, this technology provides high flexibility in the production of different types and dimensions of the flange billets.

Using technology, developed at «Omsk Plant of Special Production, Ltd.», the production of cast flanges from D_n 50 to D_n 500 at working medium pressure from P_n 0.1 to P_n 20.0 MPa and made from steels of 20, 09G2S, 17GS, 10G2, 2Kh13, 08Kh18N10T, Kh17N13M3T and Kh23N18 grades has been mastered.

1. Medovar, B.I., Shevtsov, V.L., Marinsky, G.S. (1983) *Centrifugal electroslag casting*. Kiev: Znanie.
2. Medovar, B.I., Tsykulenko, A.K., Shevtsov, V.L. (1986) *Metallurgy of electroslag process.* Kiev: Naukova Dumka.
3. Eryomin, E.N. (1998) Principles of complex modifying of cast electroslag metal. In: *Analysis and synthesis of mechanical systems.* Omsk: OGTU.

PRODUCING HOLLOW TITANIUM INGOTS USING EBCHM

B.E. PATON, N.P. TRIGUB, G.V. ZHUK, S.V. AKHONIN and **V.A. BEREZOS**
E.O. Paton Electric Welding Institute, NASU, Kiev, Ukraine

Technology of production of thick-walled hollow large-diameter ingots using the method of electron beam cold hearth melting (EBCHM) was developed. Using a mathematical model the optimum melting conditions were selected. Quality of produced ingots was examined.

Keywords: *hollow ingot, electron beam melting, cold hearth, mathematical modeling, titanium alloys, large-diameter pipes*

Tubular billets from titanium alloys are produced traditionally either by mechanical treatment of rolled rods or by press piercing of cylindrical ingots melted using vacuum-arc remelting (VAR) and passed preliminary mechanical treatment [1]. In this case the plastic working is labour-consuming and requires maintenance of a large park of forge-press equipment. Mechanical treatment of both VAR ingot and also of tubular billet leads to significant losses in metal (up to 15 %).

Recently, a number of successful attempts was made for the production of titanium pipes from ingots of electron beam melting [2, 3]. Ingots are melted out both into a closed-bottom mould using electromagnetic stirring and also using a cold hearth (EBCHM). Quality of the pipes produced from EBCHM metal satisfies the requirements of standards [2, 3]. At the same time, the tubular billets are produced by the methods of drilling and piercing of rolled rods.

The radically new approach in the production of a tubular billet from the point of view of material saving and reduction in technological operations, is the producing hollow ingots using a method of EBCHM. The use of this technology in production of titanium ingots allows not only almost complete separation of the processes of melting and crystallization and, thus, the control of the formation of hollow ingot structure, but also removal of non-metallic inclusions and such harmful interstitial impurity, as hydrogen, from titanium. The traditional VAR technology does not guarantee the complete removal of these inclusions. EBCHM allows overheating of melt surface to the higher temperatures than those in VAR and gives opportunity to hold metal in a molten state for any necessary time [4, 5].

Analysis of results of experimental melts showed that during the time of molten metal holding in a cold hearth the heavy inclusions of carbides of tungsten and molybdenum are precipitated on the bottom and accumulated in a skull, while the lighter refractory inclusions of titanium nitride and particles of α-titanium, saturated with nitrogen, are dissolved in the process of molten metal holding in cold hearth under the conditions of heating the molten metal surface by electron beams [6].

To optimize the technology of producing hollow titanium ingots, the experimental melts in the electron beam cold hearth installation of the UE-182M type were performed at the E.O. Paton Electric Welding Institute of the NAS of Ukraine. An open-bottom mould with a central mandrel was used as a forming unit. The process of producing hollow ingots was realized as follows.

The initial billet was loaded into furnace and it was evacuated. After reaching the operating pressure of 10^{-3} Pa in melting chambers and 10^{-2} Pa in electron beam heater the electric units of supply and of the electron beam heater were connected in a certain sequence. The billet being remelted was fed into a zone of action of electron beams by a horizontal feeding mechanism. With increase in filament current of cathodes the power of electron beams was increased and the billet was heated. After heating the billet was melted into a copper water-cooled cold hearth where molten metal was accumulated and refined from harmful impurities, gases and non-metallic inclusions. After definite accumulation the molten metal was poured out from the cold hearth by portions along a pouring lip into a forming mould composed of an external shell and inner mandrel made from a water-cooled copper where a hollow ingot was formed. With an ingot solidification it was withdrawing gradually from the mould by a withdrawal mechanism rod.

During melting the electron beams were moved over an upper edge of the ingot formed and a zone of molten metal contact with a working surface of mandrel and mould, thus compensating the heat dissipation to the mould and mandrel that influences favourably the structure of the ingot produced. The beam scanning over a free surface of the molten metal pro-

vides simultaneously a preset temperature condition in a metal pool. This type of ingot heating prevents the formation of a shrinkage cavity in its upper part, promotes spreading of metal entered and formation of the quality lateral surface. The process is continued until a complete melting of the initial billet and producing hollow ingot of a required length. Power and rate of melting are maintained constant.

To study the laws of titanium refining from hydrogen in EBCHM of hollow ingots, a mathematical model of hydrogen desorption in melting of solid ingots using this method was used [7]. In this case, the mathematical model was corrected for the presence of mandrel which forms an inner surface of the ingot. The mathematical model, constructed on the material balance of hydrogen in three zones of metal refining (consumable billet edge being melted, and also molten metal pool in cold hearth and mould), establishes the dependence of refining effectiveness on technological parameters of melting and kinetic constants of hydrogen in titanium.

Processing of results of experimental melts of a non-alloyed titanium made it possible to obtain numerical values of a coefficient of mass transfer of hydrogen in molten titanium β_H and constants of rate of surface reaction of hydrogen molecule formation from ions k_2^H in titanium:

$$\beta_H = 3.1 \cdot 10^{-3} \text{ m / s}; \quad k_2^H = 6.0 \cdot 10^{-2} \text{ m / (\%·s)}. \qquad (1)$$

Calculations made from mathematical model for the hollow ingot allowed us to establish dependence of titanium refining effectiveness on hydrogen in EBCHM at different rates of melting v (Figure 1).

Analysis of relationships obtained showed that the refining degree is growing monotonically with decrease in melting rate. This is stipulated by the increase in time of molten metal holding in vacuum. It was found that the metal refining in melting of hollow ingots is governed by the same laws as in producing of solid ingots.

Thus, it was stated that the required level of hydrogen content in EBCHM of hollow ingots is provided within the wide range of values of technological parameters, and the technological process should be optimized from the point of view of formation of a necessary structure of hollow ingot and cost of its production.

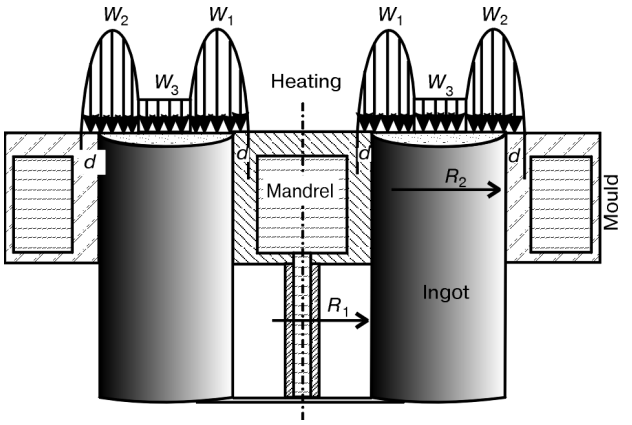

Figure 2. Model of process of hollow ingot formation in EBCHM

To define the optimum thermophysical conditions of ingot formation, the calculations were made in the scope of the mathematical model of heat processes in a cylindrical ingot [8], adapted for the case of a hollow ingot (Figure 2). In the model used the molten metal is poured into a mould by portions, and the ingot is withdrawn from it periodically. The ingot surface is heated by three electron beams, moreover, power W_3 of one of them is distributed uniformly in a central zone ($R_2 < r < R_1$), while power of two other beams W_1 and W_2 is concentrated in periphery zones. The following technological parameters are controllable in the mathematical model: power of beams W_1, W_2 and W_3, periodicity of pouring τ, height of portion h poured into mould, value of deflection d of peripheral beam from the center to the mould wall.

The process of heat transfer is described by equations of heat conductivity in a cylindrical system of coordinates (r, o, z) for the case of an axial symmetry. Axis oz of system of coordinates coincides with an ingot axis (symmetry axis), while axis or coincides with a radial direction. Beginning of coordinates was preset on the ingot bottom.

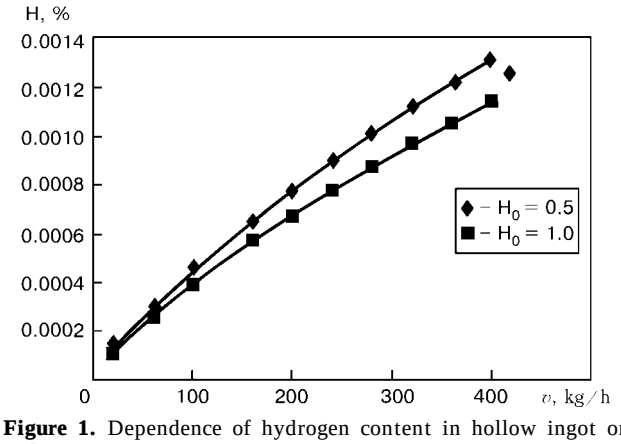

Figure 1. Dependence of hydrogen content in hollow ingot on melting rate

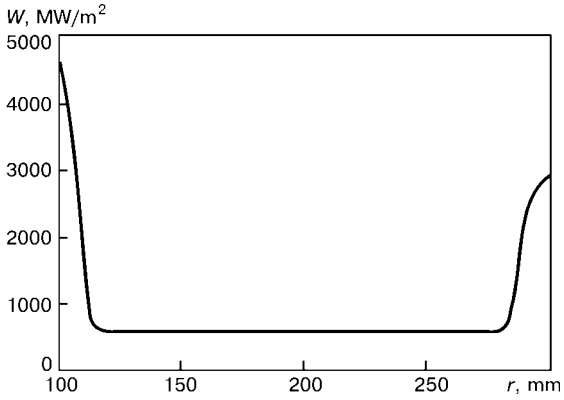

Figure 3. Distribution of specific power in ingot edge surface

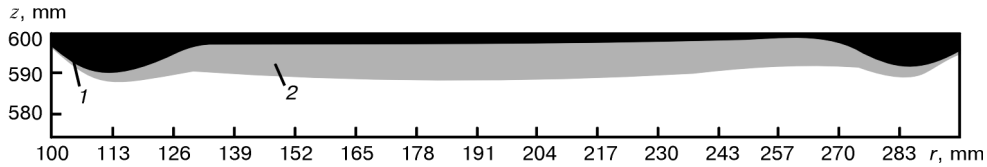

Figure 4. Temperature field in titanium hollow ingot of 600 mm outside and 200 mm inner diameter: *1* — $T > 1898$ K (molten pool); *2* ---- $T = 1868$–1898 K (solid-liquid region)

Equation of heat conductivity in this case takes a form

$$c\rho \frac{\partial T}{\partial t} = \frac{1}{r}\frac{\partial}{\partial r}\left(r\lambda(T)\frac{\partial T}{\partial r}\right) + \frac{\partial}{\partial z}\left(\lambda(T)\frac{\partial T}{\partial z}\right), \quad (2)$$

$$R_2 < r < R_1; \quad 0 < z < s(t); \quad t > 0,$$

where c is the specific heat content; ρ is the density; λ is the coefficient of heat conductivity; R_1 and R_2 are the external and internal radii of ingot; $s(t)$ is the current height of ingot. Here, a boundary condition on the ingot internal surface is the heat exchange with the mandrel wall. The heat exchange of ingot with the mould is realized by different laws depending on the ratio of ingot surface temperature and some critical temperature T_{cr} (at which the ingot surface is removed from the mould wall).

At $T < T_{cr}$ it is the following by the Stefan–Boltzmann law:

$$\lambda(T)\frac{\partial T}{\partial r}\Big|_{r=R_2} = \varepsilon\sigma\,(T^4 - T_{av}^4), \quad (3)$$

where ε is the emissivity factor; σ is the Stefan–Boltzmann constant; T_{av} is the temperature of mould wall.

At $T > T_{cr}$ it is the following by the Newton–Richman law:

$$\lambda(T)\frac{\partial T}{\partial r}\Big|_{r=R_2} = \alpha(T - T_{av}), \quad (4)$$

where α is the coefficient of heat transfer between the ingot and mould.

The rate of melting was taken equal to 100 kg / h, periodicity of pouring molten metal portions ---- to 3 min. As a result of calculations the distribution of power of electron beams in the mould (Figure 3) providing a shallow molten pool over the entire surface of the ingot (Figure 4) was selected as optimum. Such distribution of power provides the uniform spreading of poured portions of molten metal and almost plane front of solidification, thus promoting the formation of a homogeneous structure from equiaxial grains in the ingot.

Using the designed condition of electron beam heating of hollow ingot in the mould, the experimental hollow ingots of titanium alloy VT1-0, having 600 mm outside diameter, 200 mm inner diameter and 2 m length, were melted in the UE-182M type electron beam installation (Figure 5). The external surface of ingots was melted by the electron beam [9].

To reveal flaws in hollow titanium ingots in the form of non-metallic inclusions, and also pores and discontinuities, the method of ultrasonic flaw detection (UFD) was used. Examinations were performed by echo-pulsed method at a contact variant of control using the UD-11UA device. The test frequency of UFD was 2.5 and 5 MHz that provided a maximum «signal–noise» ratio.

Examination of hollow ingots was made by a successive scanning of the lateral surface along the cylinder generatrix (parallel to longitudinal axis). Pitch between lines of scanning was 10–20 mm. Radiation axis corresponded to the cylinder radius. All the lateral surface of the hollow ingot was subjected to scanning that provided the examination of the entire its volume. Numerous reflections of a low amplitude

Figure 5. Appearance of hollow ingot of 600 mm outside and 200 mm inner diameter after surface melting

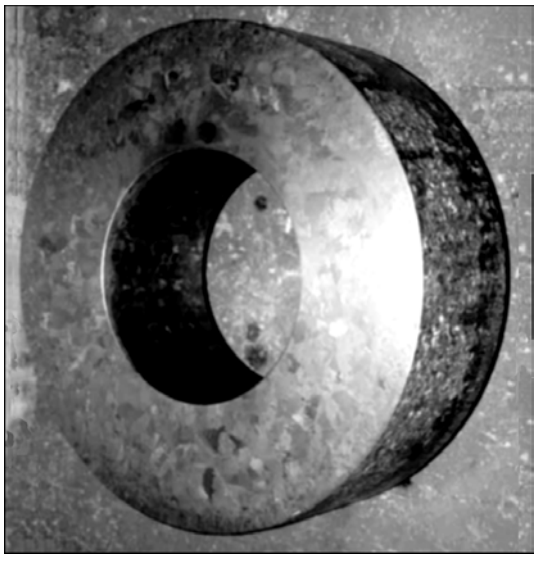

Figure 6. Fragment of hollow ingot after etching

were observed that is typical of the cast metal and is a result for the signal reflection from the boundaries of grains. Analysis did not reveal reflections which could be interpreted as coarse non-metallic inclusions, pores, shrinkage cavities.

Thus, the UFD showed that there are no discontinuities, non-metallic inclusions of more than 1 mm size, and also dense clusters of finer inclusions in the hollow titanium ingots examined. These results were confirmed by visual inspection of an etched fragment of the hollow ingot (Figure 6). Structure of ingot is homogeneous, consisting of equiaxial grains of 10–30 μm size.

Thus, a thick-walled hollow large-diameter titanium ingot was produced for the first time in the world's practice using the EBCHM technology developed at the E.O. Paton Electric Welding Institute. The application of this technology of production of hollow titanium ingots and electron beam melting of their surface makes it possible to decrease significantly the metal consumption and to reduce the number of technological operations.

1. Anoshkin, N.F., Ermanyuk, M.Z., Agarkov, G.D. et al. (1979) *Semi-finished products of aluminium alloys*. Moscow: Metallurgiya.
2. Buryak, T.N., Vakhrusheva, V.S., Ladokhin, S.V. et al. (2001) Production of titanium tubes from electron beam melting billets using the waste. *Problemy Spets. Elektrometallurgii*, **3**, 24–29.
3. Kalinyuk, A.N., Kozlovets, O.N., Akhonin, S.V. (2002) Manufacture of semi-finished products from titanium ingots produced by the EBCHM method. *Advances in Electrometallurgy*, **2**, 21–24.
4. Paton, B.E., Trigub, N.P., Zamkov, V.N. et al. (2000) Development of electron beam melting technology of titanium. *Problemy Spets. Elektrometallurgii*, **2**, 34–40.
5. Paton, B.E., Trigub, N.P., Akhonin, S.V. (2003) Prospective technologies of electron beam melting of titanium. *Titan*, **2**, 20–25.
6. Akhonin, S.V. (2001) Mathematical modeling of process of dissolution process of TiN inclusions in titanium melt during EBR. *Problemy Spets. Elektrometallurgii*, **1**, 20–24.
7. Akhonin, S.V., Trigub, N.P., Kalinyuk, A.N. et al. (1995) Mathematical modeling of metal refining processes from gases during electron beam remelting in cold hearth. *Ibid.*, **2**, 36–42.
8. Zhuk, G.V., Akhonina, L.V., Trigub, N.P. (1998) Mathematical modeling of process of Ti–6Al–4V titanium alloy solidification in EBCHM. *Ibid*., **2**, 21–25.
9. Pikulin, A.N., Zhuk, G.V., Trigub, N.P. et al. (2003) Electron beam surface melting of titanium ingots. *Advances in Electrometallurgy*, **4**, 16–18.

PRODUCTION OF TITANIUM INGOTS-SLABS USING METHOD OF EBCHM

G.V. ZHUK, A.N. KALINYUK and **N.P. TRIGUB**
E.O. Paton Electric Welding Institute, NASU, Kiev, Ukraine

Technology of production of ingots-slabs of titanium alloy VT6 using the method of electron beam cold hearth melting (EBCHM) was developed. Dependence of structure and properties of ingots metal on melting c onditions was investigated. The ways are shown for preventing the anisotropy of properties of titanium alloy rolled metal.

Keywords: *ingot-slab, electron beam melting, titanium alloys, ingot structure, mechanical properties, anisotropy*

One of the drawbacks of semiproducts, produced from titanium alloys, is the anisotropy of their mechanical properties. Thus, according to data of work [1] the difference in tensile strength of metal of samples, which were cut along and across the rolling, is about 20 %. Undoubtedly, the anisotropy of properties of titanium alloys after rolling depends greatly on structure of initial ingots, as the rolling of slabs is realized along the longest side of the ingot, i.e. in the direction of growth of crystallites. Thus, the initial cast structure of slabs has a great influence on the anisotropy of properties of plates and sheets from titanium alloys. During rolling from slabs with a columnar structure the structural anisotropy is increased. If the initial ingot-slab has an equiaxial structure across the entire section, then anisotropy can appear during rolling only due to the conditions of rolling.

The important factors which influence the crystallization of titanium alloys in electron beam cold hearth melting (EBCHM) are both a total power of electron beam heating Q of ingot in the mould, and also its spreading over the ingot surface [2]. Conditions of local heat removal from the zone of ingot upper edge, heated by molten overheated metal, entered from the cold hearth, and by electron beam are different [3]. An intensive removal of heat occurs at the water-cooled mould walls, while it is decreased near the ingot axis as the ingot thickness shows great resistance to the heat flows. It is evident that it is necessary to shift the maximum of electron beam heating to the ingot periphery part to create the more uniform heat removal along the ingot radius and to increase the rate of cooling during crystallization in the ingot center.

Experimental melts were performed at the E.O. Paton Electric Welding Institute of the NAS of Ukraine to determine the effect of electron beam heating on the structure of ingot forming in an open-bottom mould. Ingots of 150×500 mm cross-section and up to 2 m length were melted from titanium alloy VT6 (Ti–6Al–4V) in the UE-121 type electron beam installation of 0.9 MW capacity (Figure 1) using EBCHM method (Figure 2). A copper water-cooled mould was used for melting. Pure components, such as titanium sponge TG-130, vanadium–aluminium master alloy VNAL, commercial pure aluminium (with allowance for losses in its evaporation), were used as a charge. During melting the following technological parameters were maintained: 0.05 Pa residual pressure in a melting chamber, 0.005 Pa in electron guns, 200 kg / h efficiency of melting.

To optimize the conditions of heating ingot surface in the mould two types of beam scanning were used:

Figure 1. General view of the UE-121 type installation for electron beam cold hearth melting

Figure 2. Appearance of ingots-slabs

scanning at 10 Hz frequency over the surface (central heating) and at 1 Hz frequency along the periphery of the ingot upper edge (periphery heating). In melting with use of the central heating the minimum power of the electron beam heating of the ingot surface in the mould was 65 kW. With decrease in power below the above-mentioned value a crust of solidified metal was formed along the ingot periphery, influencing negatively its surface quality. At the higher power of heating a developed pool of metal with a characteristic convection (swirling) was observed in the mould. Melts with use of the periphery heating were performed at electron beam power of 45 (condition 1), 52 (condition 2) and 60 kW (condition 3).

When melting using condition 1, a solid-liquid phase along the periphery and solidified metal in ingot center were formed at the ingot surface. When melting using condition 2, a liquid phase existed at the ingot periphery during all the technological cycle (pouring of due portion of metal–period between pourings), islands of a solid phase appeared in a central part of ingot before pouring (at the moment of the most intensive cooling of the ingot surface). When melting using condition 3, all the ingot surface in the mould was in a molten state, while the convective flows of molten metal, symmetrical relative to the ingot surface central axis directed parallel to the larger (500 mm) side of the mould were observed in the center of ingot. Process of melting took on average 2.5 h. At the end of melting the shrinkage cavity was removed by a gradual decrease in power of heating the ingot upper edge in the mould.

Examination of macrostructure of longitudinal and transverse templets, cut out from an ingot central part, showed that distribution of power of electron beam heating over the slab surface in the mould has a determinant effect on crystalline structure of the ingot (Figure 3). The central heating leads to the formation of a columnar structure along the entire longitudinal section of the slab. The periphery electron beam heating of slab in the mould makes it possible to decrease the heat load to a central its part, maintaining a molten pool near the mould wall, which is responsible for the ingot lateral surface condition. In this case the cooling rate in crystallization is increased greatly, volume crystallization is occurred and the ingot structure is changed. The structure of longitudinal section of slabs melted out using a periphery heating is characterized by the presence of equiaxial grains.

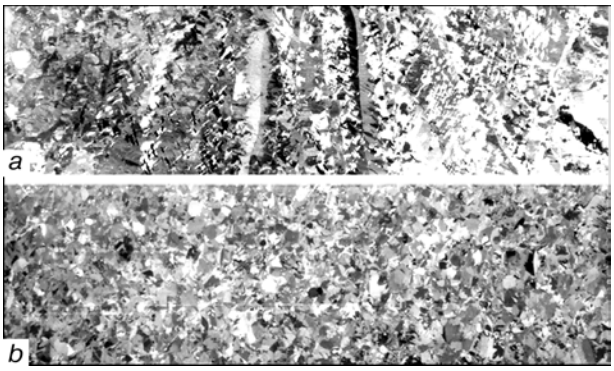

Figure 3. Structure of longitudinal section of slabs melted out under different conditions of heating in the mould: *a* — central; *b* — periphery

The slabs produced were subjected firstly to rolling in β-region (35 % working degree), and then in (α + β)-region (57 % working degree). Deformed metal was subjected to mechanical tests. Results showed (Table) that mechanical properties of the rolled titanium alloy VT6 are high enough and exceed significantly the requirements of GOST for plates and sheets [4]. At the same time the properties of rolled metal produced from slabs melted out under different conditions of electron beam heating of ingot are very different.

If the tensile strength of samples, cut out across the rolling, is almost similar at all the heating conditions and equals to 1100–1130 MPa, then the strength of longitudinal samples of rolled metal is

Mechanical properties of as-rolled 150×500 mm cross-section ingots from titanium alloy VT6

Heating condition	Along rolling					Across rolling				
	σ_t, MPa	$\sigma_{0.2}$, MPa	δ, %	ψ, %	*KCV*, J / cm^2	σ_t, MPa	$\sigma_{0.2}$, MPa	δ, %	ψ, %	*KCV*, J / cm^2
Central	968–999 / 980	887–898 / 893	12–13 / 12	27–28 / 28	29–30 / 29	1113–1127 / 1123	1058–1092 / 1072	13–14 / 13	43–46 / 45	24–30 / 27
Periphery										
1	1078–1096 / 1087	1022–1039 / 1030	10–12 / 11	19–29 / 24	25–30 / 29	1117–1131 / 1125	1068–1103 / 1080	7–8 / 7	13–28 / 18	22–28 / 26
2	1058–1079 / 1072	1011–1037 / 1024	10–12 / 11	25–27 / 26	28–30 / 29	1093–1100 / 1100	1065–1086 / 1076	9–11 / 10	16–33 / 24	21–26 / 24
3	1009–1012 / 1010	936–950 / 943	9–15 / 12	35–41 / 38	37–38 / 38	1086–1113 / 1099	1044–1061 / 1065	9–11 / 10	41–46 / 44	36–43 / 39

Note. Minimum and maximum values are given above the line, mean values are given under the line.

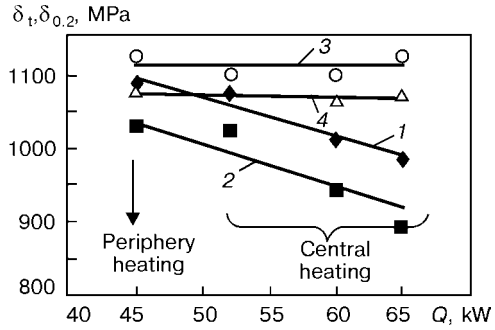

Figure 4. Dependence of mechanical properties of rolled metal produced from EBCHM slabs on power of their heating in the mould: *1, 3* — tensile strength along and across rolling, respectively; *2, 4* — yield strength along and across rolling, respectively

decreased both with increase in heating power and also at a transition from periphery to central heating, i.e. from equiaxial to columnar structure of the slab. Thus, tensile strength of plates rolled from slabs with an equiaxial structure exceeds the tensile strength of plates produced from slab with a columnar structure by more than 100 MPa on average.

The same can be said about the yield strength of the rolled metal. The yield strength of metal of plates manufactured from slabs with an equiaxial structure is by 120 MPa higher than that of plates rolled from slabs with a columnar structure.

A clear tendency is observed to the increase in anisotropy of properties of the rolled metal at increase in power of electron beam heating of metal in the mould, i.e. in transition from equiaxial to columnar structure. Anisotropy of strength properties, tensile and yield strengths of alloy VT6, is especially manifested (Figure 4). If the difference in strength along and across the rolling direction for rolled metal from slabs melted out at 65 kW power of electron beam heating of metal in the mould is 15–20 %, then the difference in strength properties does not exceed 5 % for rolled metal from slabs melted out at 45–52 kW heating (at almost equiaxial structure).

CONCLUSIONS

1. Shifting of electron beam heating to the periphery zone of ingot surface in the mould promotes the formation of isotropy structure favourable for subsequent rolling of the ingot-slab. In melting of 150×500 mm cross-section slab from Ti–6Al–4V alloy a structure consisting of equiaxial grains over the entire its section was produced.

2. Technology of production of 150×500 mm cross-section slabs from titanium alloy VT6 with use of periphery heating of ingot in the mould promotes the increase in both strength and also ductile properties of the alloy after rolling.

1. Anoshkin, N.F., Ermanyuk, M.Z., Agarkov, G.D. et al. (1979) *Semi-finished products of titanium alloys*. Moscow: Metallurgiya.
2. Zhuk, G.V. (2003) Influence of power of electron beam heating on structure and properties of titanium ingots. *Metallurgich. i Gornorudnaya Promyshlennost*, **3**, 36–38.
3. Paton, B.E., Trigub, N.P., Kozlitin, D.A. et al. (1997) *Electron beam melting*. Kiev: Naukova Dumka.
4. *GOST 23755–79.* Plates of titanium and titanium alloys. Specifications. Moscow: Standart.

CONTROLLER OF ANODE CURRENT OF ELECTRON BEAM GUNS WITH A PREHEATED CATHODE

O.Ya. GAVRILYUK[1], **V.I. NESYNOV**[1], **N.S. KOMAROV**[2], **Yu.V. RUDENKO**[2], **B.B. LEBEDEV**[2] and **A.D. PODOLTSEV**[2]
[1]International Center of Electron Beam Technologies of E.O. Paton Electric Welding Institute, NASU, Kiev, Ukraine
[2]Institute of Electrodynamics, NASU, Kiev, Ukraine

Peculiarities of application of high-frequency transistor converters as an anode current source of electron beam guns with a preheated cathode are considered. The advantage of these converters as compared with traditional mains electric supply sources is shown on the basis of analysis of electromagnetic processes.

Keywords: *electron beam technologies, high-frequency transistor converters, electric power supply sources*

Electron beam vacuum installations with use of filamentary cathode electron guns have found a wide spreading in the electron beam technology of deposition of protective coatings. In these guns the beam current is adjusted by control of tungsten cathode filament current. The simplified functional scheme of gun power supply is shown in Figure 1.

The power supply source of the installation is composed of a powerful high-voltage source of anode voltage and filament current source being under a high potential. The change in filament current leads to the increase in power dissipated in the form of heat at the cathode, increase in temperature of the latter and, respectively, to emission of electrons. The supplied electric power is equalized by the energy of emission and cathode radiation. Emission properties of tungsten are manifested at 2000–2500 K. At these temperatures many factors influence the anode current value: change in cathode resistance, change in radiation power, intensity of electric field, etc. Parametric control of anode current value is low-effective due to difficulty in accounting for many factors, that required to design the anode current controllers in the form of static systems of automatic control. To evaluate the accuracy of this system, its dynamic properties and stability, it is necessary to analyze all its links and, first of all, the cathode itself, that required to develop the electrophysical model of the preheated cathode.

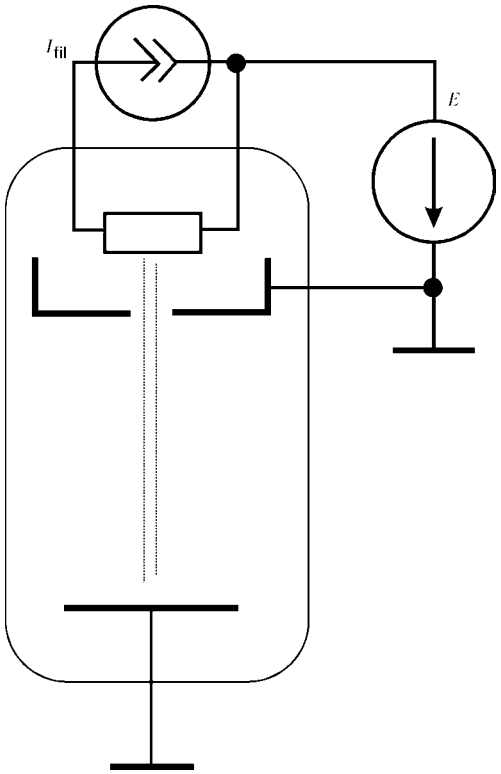

Figure 1. Functional scheme of power supply of electron gun with a filamentary (directly heated) cathode

Density of current of thermoelectron emission, according to work [1], is defined by Richardson's expression

$$J_S = AT^2 e^{-\frac{B}{T}},$$

where T is the temperature by Kelvin, and coefficients A and B are found using electrophysical constants. Specified values A and B for the tungsten cathode are as follows:

$$A = 60.2 \cdot 10^4 \text{ À / (m}^2 \cdot \text{Ê}^2\text{)}, \quad \hat{A} = 52700 \text{ Ê}.$$

In the gun considered a filamentary (directly heated) cathode is made in the form of a strip (Figure 2), whose geometric sizes are as follows: width $a = 3 \cdot 10^{-3}$ m, height $b = 6 \cdot 10^{-4}$ m, length $l = 65 \cdot 10^{-3}$ m.

We think that emission of electrons is occurred from the cathode surface parallel to anode, i.e.

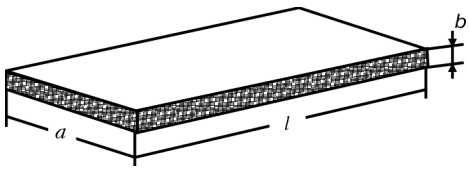

Figure 2. Geometry of strip cathode

Table 1

T, K	P'_{rad}, W	R'_c, Ohm	T, K	P'_{rad}, W	R'_c, Ohm
400	$6.24 \cdot 10^{-2}$	$10.26 \cdot 10^{-6}$	1800	44.54	$63.74 \cdot 10^{-6}$
600	$9.54 \cdot 10^{-2}$	$16.85 \cdot 10^{-6}$	2000	75.37	$72.19 \cdot 10^{-6}$
800	0.53	$24.19 \cdot 10^{-6}$	2200	119.8	$80.83 \cdot 10^{-6}$
1000	1.891	$31.74 \cdot 10^{-6}$	2400	181.2	$89.65 \cdot 10^{-6}$
1200	5.21	$39.46 \cdot 10^{-6}$	2600	263	$98.66 \cdot 10^{-6}$
1400	12.01	$47.37 \cdot 10^{-6}$	2800	368.9	$107.8 \cdot 10^{-6}$
1600	24.32	$56.46 \cdot 10^{-6}$	3000	503.5	$117.2 \cdot 10^{-6}$

$$S_e = al.$$

Anode current will be defined as

$$I_a = J_S S_e.$$

Cathode loses heat, supplied to it by radiation and electron emission. Radiation power will be written as

$$P_{rad} = \gamma w S_c,$$

where γ is the specific radiation; w is the coefficient of secondary emission; S_c is the active area of cathode.

Power, lost by the cathode as a result of electron emission, is proportional to emission current I_S:

$$P_{em} = \varphi I_S.$$

As the value of work functions of electrons φ is low, then the losses of energy for electron emission can be neglected.

Cathode resistance is defined by specific resistance ρ of its material and geometric sizes:

$$R_c = \rho \frac{l}{ab}.$$

It is necessary to account for effect of temperature on specific resistance of the cathode material. Tungsten cathode has a high specific emission at temperature of about 2500 K (temperature of tungsten melting is 3683 ± 20 K). Effect of temperature on value of specific resistance can be evaluated by the following data:

T, K	$\rho \cdot 10^8$, Ohm·m
240	5.5
900	27.9
1000	31.6
1100	35.6
1200	39.5

In work [1] the conception of a unit cathode of 1 cm^2 section and 1 cm length, made from tungsten, was introduced. For the unit cathode of a round section the dependencies of power lost due to radiation and resistance on temperature are calculated (Table 1).

Table 2

T, K	R_c, Ohm	P_{rad}, W	P_{el}, W
1000	0.0089	2.82	200.2
2000	0.02	112	450
3000	0.033	750	742

Let us find expression for cathode resistance and lost power in recalculation from the round unit cathode to the real rectangular cathode. Here, let us take areas of cross-sections of round and rectangular cathodes equal. Then, for the real cathode the resistance will have a form

$$R_c = R'_c \cdot 10^{-2} \frac{l\pi}{4ab}.$$

In recalculation of radiation power, let us take equality of area of cathode surface, i.e. equality of parameters of cross-section of round and rectangular cathodes. Then, the radiation power for real cathode will be found from expression

$$P_{rad} = P'_{rad} \cdot 10^4 \frac{2(a+b)l}{\pi}.$$

Thus, at 1000, 2000 and 3000 K temperature of cathode and 150 A filament current the values of cathode resistance, supplied electric power P_{el} and lost power by radiation are given in Table 2.

It follows from Table 2 data that the thermal equilibrium of cathode is provided at temperature $2000 < T < 3000$ that corresponds to maximum density of emission current of the tungsten cathode.

Heat capacity of cathode is determined by a specific heat capacity of its material, mass and temperature:

$$C = C_{sp} m_c \left(1 + \frac{T}{6000}\right).$$

It should be noted that the heat capacity for the case considered has an order $C = 0.3$ J / deg. This high heat capacity stipulates significant time lag of processes in the gun, defined by units of seconds.

Dynamics of changing the cathode temperature can be determined from equation

$$C \frac{\partial T}{\partial t} = P_{el} - P_{rad}.$$

In transition from derivative to increment for a small interval of time we shall obtain

$$T_{l+\Delta l} = T_l + \frac{(P_{el} - P_{rad})}{C} - \Delta t.$$

The magnetic amplifiers operating at mains frequency are used as filament current controllers in electron beam installations. One of the variants of design of high-potential filament current source is shown in Figure 3. The source includes three single-phase magnetic amplifiers (MA1–MA3), high-potential transformers (Tr1–Tr3) and output rectifiers. To reduce losses in the rectifier operating at low-ohmic load, it is desirable to use the transformer with two output half-windings. The feedback circuit consists of reference voltage source U_{ref}, anode current sensor $I_a R_ø$, error amplifier and executive circuit, controlling bias current of magnetic amplifiers.

At such design of the filament source in the system of automatic control there are two main time lag links. The first link is stipulated by a final heat capacity of the cathode, while the second link — by a limited quick-response of magnetic amplifier. At commensurable time constants of the above-mentioned time lag links the transition processes in the automatic control system in the presence of disturbances have an oscillating nature.

Modeling of processes in the anode current controller with a magnetic amplifier was performed using the following parameters:

• cathode parameters: $a = 3 \cdot 10^{-3}$ m, $b = 6 \cdot 10^{-4}$ m and $l = 65 \cdot 10^{-3}$ m — geometric parameters; $p =$ = 19100 kg / m^3 — tungsten density; $C_{sp} =$ = 134 J / (kg·deg) — specific heat capacity of tungsten; $I_{a-c} = 0.025$ m — distance between anode and cathode; $U_{a-c} = 20000$ V — anode voltage; $A =$ = 602000 A / (m^2·K^2) and $B = 52700$ K — coefficients of emission equation;

• parameters of magnetic amplifier: $\tau = 0.02$ s — period of mains voltage; $U_m = 10$ V — amplitude of voltage at the secondary semi-windings of transformer; $k_1 = 0.1$ — coefficient of transmission of error link; $\tau_m = 0.1$ s — time constant of magnetic amplifier; $R_i = 0.01$ Ohm — internal output resistance of filament supply source.

Volume of cathode V_c, active emission area S_e, cathode mass m_c and its heat capacity C_c were determined according to expressions:

$$V_c = abl; \quad S_e = al;$$

$$m_c = V_c p; \quad C_c = C_{sp} m_c.$$

Results of modeling are shown in Figure 4. Scale for electric power and radiation power was taken equal to 2 kW / cell, for reference current and anode current 1 A / cell, for cathode temperature 1000 K / cell, for filament current 200 A / cell and for cathode voltage 10 V / cell. For better visuality the zero level of filament current function is shifted upward for one cell.

The Figure shows the area of cathode preheating before the emission beginning. In this area the filament current requires a forced limitation because of a low temperature of the cathode. It follows from the graph that the anode current I_a, with an accuracy to a static error, is approaching the reference value I_{ref}. Transition processes caused by jumpy changing in reference current have a damping oscillating nature. Operation of magnetic amplifier at the region of control of output current causes voltage distortion at the input of output transformers, thus increasing pulsations of the output voltage. However, due to a high heat capacity of the cathode this change in pulsations does not influence greatly the nature of changing the cathode current and, respectively, anode current.

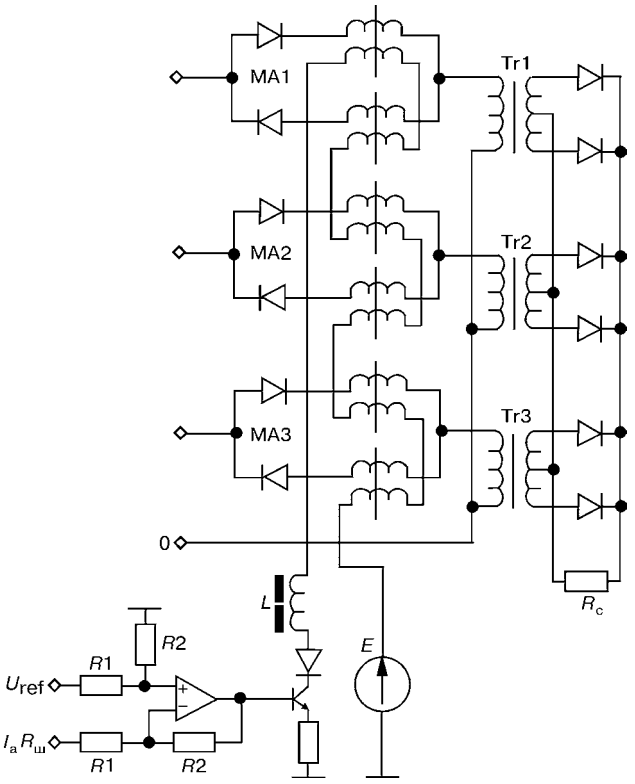

Figure 3. Functional scheme of filament current controller on the base of magnetic amplifier

Let us describe the main drawbacks of controllers of cathode filament current of the electron beam installation based on magnetic amplifiers, which operate at the industrial mains frequency: low dynamic characteristics of the controller and oscillating nature of transition processes; large dimensions of magnetic amplifiers and high-potential transformers that need

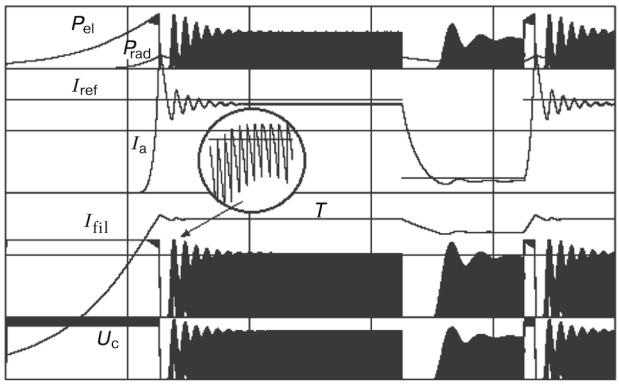

Figure 4. Time diagrams of process of filament current control by magnetic amplifier

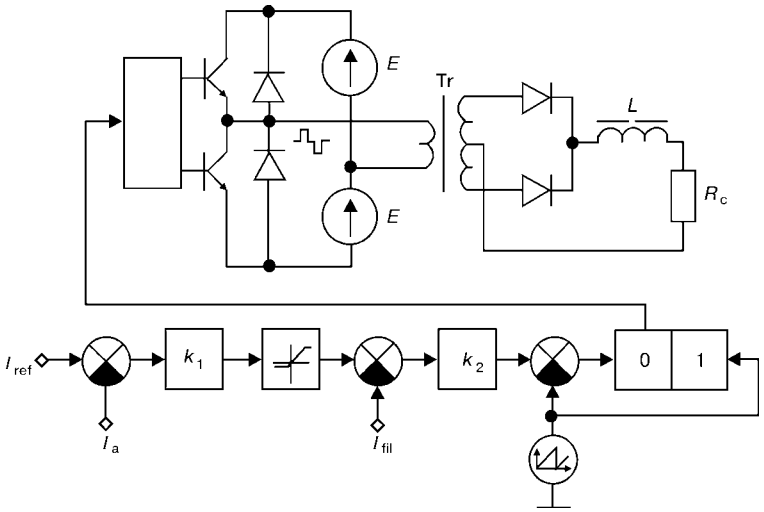

Figure 5. Functional scheme of filament current controller on the base of pulse transformer

their removal from vacuum chamber, thus leading to difficulties in energy supply to the installation and increase in losses in high-current filament circuits.

It is possible to improve the dynamic properties of the filament source by application of transistor converters with a high-frequency pulsed modulation. Scheme of such device is shown in Figure 5. The device consists of a half-bridge inverter, high-potential transformer, rectifier and output choke. Control circuit includes anode current and filament current feedback that allows anode current stabilization at the level of reference current and limitation of maximum value of filament current.

Let us consider the processes in such controller of anode current at the following parameters of pulsed controller: τ_{pulse} = 25 μ / s ---- period of a pulsed modulation; U_m = 3 V ---- amplitude of synchronizing saw-shaped voltage; E_2 = 15 V ---- amplitude of pulses at the rectifier output; k_1 = 50 and k_2 = 1 ---- coefficients of transmission of links of feedback circuit; L_{ch} = = 10 μH ---- inductance of output choke; R_s = 0.01 ---- resistance of shunt in filament source circuit.

Results of modeling are shown in Figure 6.

It follows from the Figure that time lag properties of a pulsed controller with respect to time lag of cathode are very low and system is «degenerated» into the first-order circuit. This eliminates the dips and splashes of anode current at transition processes

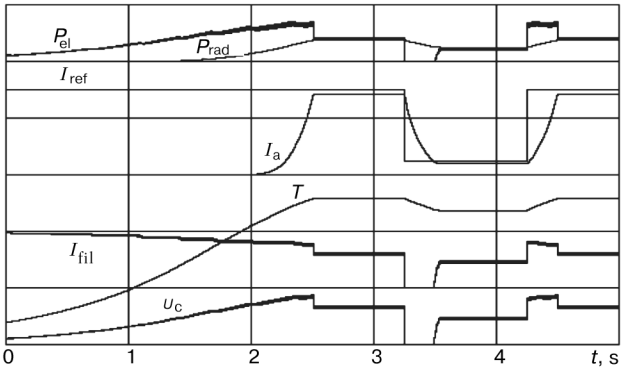

Figure 6. Time diagrams of process of filament current control by pulse transformer

caused by abrupt change in reference signal. The presence of a relatively low inductance in output circuit of filament current provides the significant reduction in filament current pulsations and, respectively, cathode voltage.

Thus, the transition for high frequency of energy conversion improves the dynamic characteristics of the current controller. Simultaneously, this transition gives possibility to decrease the mass-dimension characteristics, in particular, of high-potential transformer and output filter of supply circuits of cathode filament, that, in their combination with output rectifier into a single small-sized high-potential transformer-rectifier unit (HTRU), will make it possible to arrange the latter directly on the operational chamber of the electron beam installation. This solution will give an opportunity to simplify significantly the design of high-voltage input and to reduce the length of high-current high-potential output circuits, thus decreasing the power losses in them. In this case the HTRU should satisfy the following technical requirements:

Output current, A	150
Output voltage of DC, V	10
Voltage pulsation in active load, %	≤ 3
Amplitude of input pulses of voltage, V	300
Frequency of conversion, kHz	≥ 20
Class of isolation of voltage input–output of DC galvanic isolation, kV	25
Maximum overheating relative to surrounding medium, K	50

There is a number of specific requirements to the high-potential transformer (HPT) and its supplying inverter as units of power supply to the electron beam installation which should be taken into account in designing. In particular, these are requirements to protect inverter from breakdowns in the high-potential circuits and to limit the leakage inductance of HPT.

Let us consider the latter requirement in detail. Figure 7, *a* shows the equivalent scheme of supply source of cathode filament, and Figure 7, *b* shows diagrams of current and voltage in this scheme.

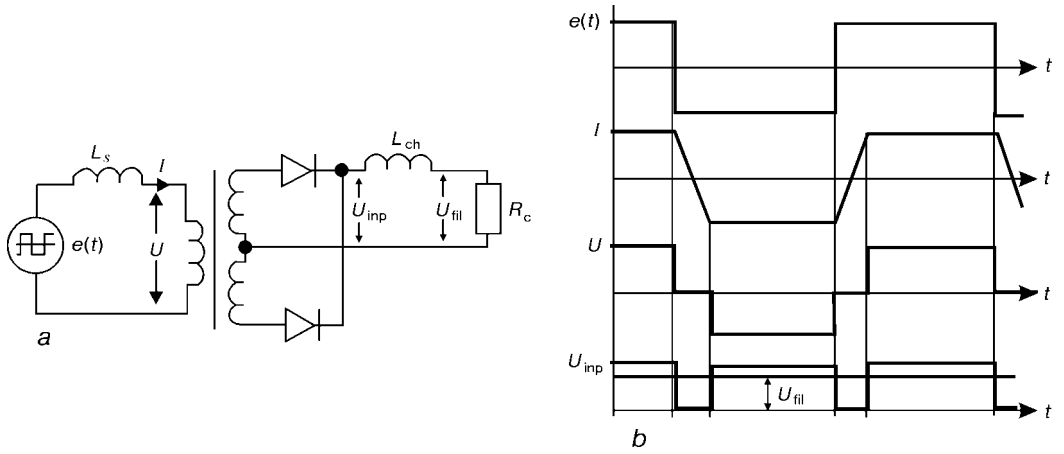

Figure 7. Equivalent circuit of pulse transformer (*a*) and time dependencies of currents and voltages (*b*)

Here, the leakage inductance L_s of transformer refer to the primary winding and active resistance of windings, current of transformer magnetizing, voltage drop at diodes and choke current pulsations are neglected.

At the intervals of equality of input current and load current, applied to primary winding, there are no changes in currents, the voltage drop at leakage inductance is equal to zero and the input voltage is applied to transformer primary winding.

With change in polarity of voltage at the transformer output the above-mentioned equality is disturbed and load current is short-circuited through both diodes of the rectifier that causes the redistribution of voltages. The input voltage is applied to leakage inductance and its rapid recharge occurs by the linearly changed current. Duration of process of recharge of leakage inductance Δt will be defined as

$$\Delta t = \frac{L_s 2 I_1}{E},$$

where E is the amplitude of voltage of pulsed generator $e(t)$; I_1 is the amplitude of load current I applied to primary winding; L_s is the leakage inductance applied to primary winding. Voltage U at load applied to primary winding has amplitude E, and its mean value for a half-period of pulses repetition t_{pulse} will have a form

$$U_1 = E\left(1 - \frac{2\Delta t}{t_{\text{pulse}}}\right). \qquad (1)$$

Using expression (1), we shall determine the active power in applied load:

$$P_1 = EI_1\left(1 - \frac{4L_s I_1}{t_{\text{pulse}}}\right).$$

From equation $\frac{dP_1}{dI_1} = 0$ we shall find that maximum power $P_{\max}$ in applied load

$$P_{\max} = \frac{E^2 t_{\text{pulse}}}{16 L_s} \qquad (2)$$

is attained at extreme value of current I_{ex} in this applied load

$$I_{\text{ex}} = \frac{E t_{\text{pulse}}}{8 L_s}.$$

Dependence of output power on load current is shown in Figure 8.

It should be noted that at the point of power extremum (2) the amplitude of input pulses and voltage at applied resistance of load are in a definite ratio

$$U_1 = E\left(1 - \frac{4\, L_s I_{\text{ex}}}{E t_{\text{pulse}}}\right) = \frac{E}{2}.$$

Consequently, to provide condition of transformation of preset power at maximum allowable value of leakage inductance it is necessary to select the transformation ratio from the condition

$$k_{\text{tr}} = \frac{n_2}{m} = \frac{U_2}{U_1} = \frac{2U_2}{E}.$$

Thus, the maximum allowable value of leakage inductance to provide the preset output power should satisfy the condition

$$L_{s_{\max}} < \frac{E^2 t_{\text{pulse}}}{16 P_1}$$

and for the case considered at E = 300 V, t_{pulse} = = 50 μs, P_1 = 1500 W should not exceed 187.5 μH.

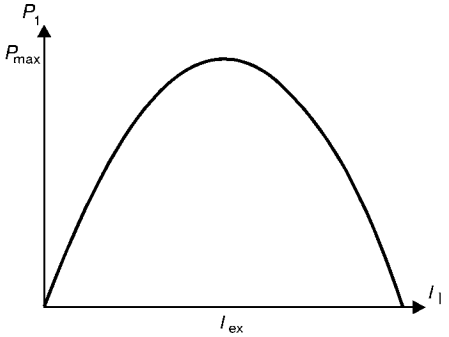

Figure 8. Dependence of output power of pulse transformer on load current

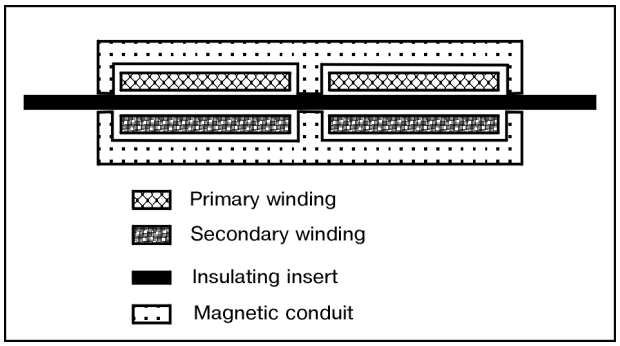

Figure 9. Design of high-potential transformer with a separated magnetic conduit

These low requirements to leakage inductance allow us to use the simpler designs of transformers for cathode filament supply as compared with known designs of HPT [2].

In addition, it is necessary to take into account a number of specific requirements specified to insulation of the device considered. This insulation should withstand not only high accelerating voltage of direct current, but also voltage of alternating current, stipulated by pulsations and overvoltages occurring in transition conditions or at breakdowns in high-voltage circuits of operational electron beam installations. When selecting the type of insulation it is necessary to take into account also the peculiarities of structure of insulation, degree of non-uniformity of electric field and method of cooling.

As a main insulation in high-voltage equipment a cast insulation on the base of solidified polymeric materials is widely used. In the present device, the application of HPT with a cast insulation is seemed to be not rational due to difficulties and high labour consumption in its manufacture, decrease in reliability in overheating. It is necessary also to take into account that at the same value of high voltage the length of air discharge gap over the surface of solid body is by several orders larger than the length of discharge gap across thickness of a solid insulation. Therefore, the dimensions of high-voltage devices with an external insulation, made in the form of combination of solid and gaseous insulation, are defined mainly at small sizes of elements by a value of discharge air gaps over the surface of a solid body of these elements.

Design of HPT with a separate magnetic core [3], shown schematically in Figure 9, is an alternative to the design with a cast insulation. This design represents a magnetic system separated into two parts using an insulating insert. Each part of the HPT magnetic system has one of windings and one of cores of magnetic conduit. In this design of HPT the insulating insert fulfills the function of main insulation both between the windings and also between cores of the magnetic conduit. A conductive layer, for example, of comparatively highly-ohmic resistive layer, electrically connected to the core and winding of a proper part of HPT, is deposited on the both sides of insert in places of contact with cores. Layers of both sides of insert form plates of capacitor, to which the high voltage of a galvanic isolation is applied. It is possible to decrease the non-uniformity of field at the capacitor edges by making a special shape, for example, of Rogovsky electrode that will provide the high reliability of insert insulation at high intensities of the electric field.

Thickness of insert δ is selected coming from the value of the highest accelerating voltage U and allowable value of intensity of uniform electric field E in the insert material:

$$\delta = \frac{U}{E}.$$

Value of intensity of apparent charge of partial discharges may serve as a criterion of quality of insulation of insert of the selected thickness [4, 5].

The drawbacks of this design of HPT are the increased value of magnetizing current due to the presence of a non-magnetic gap in the magnetic conduit and increased value of leakage inductance.

Let us make the quantitative evaluation of these factors at different values of gap. The appearance of a non-magnetic gap in the transformer core causes the decrease in magnetizing inductance. If the magnetizing current becomes commensurable with load current, applied to the primary winding, the nature of electromagnetic processes in the transformer is somewhat changed. Diagrams of currents and voltages for this case are given in Figure 10, where U_{Lm} is the voltage on magnetizing inductance; U_{Ls} is the voltage on leakage inductance; I_{rect} is the rectifier current; I_{Lm} magnetizing current; I_{Ls} is the current of primary winding.

In this case the voltage on magnetizing inductance is differed from that calculated by equation (1) due to change in magnetizing current at the interval of a pulse formation:

$$U_{Lm} = ED_L\left(1 - \frac{2\Delta t}{t_{\text{pulse}}}\right), \qquad (3)$$

where $D_L = L_m/(L_m + L_s)$ is the transfer ratio of inductive voltage divider, formed by magnetizing inductance L_m and leakage inductance L_s of transformer with a non-magnetic gap.

To define limitations for value of leakage inductance of transformer with a gap, it is necessary to use the expression (3) and to make transformations, similar to those made earlier for HPT without gap. Thus, we shall obtain the limiting allowable value of leakage inductance of transformer with a non-magnetic gap in the form

$$L_{s_{\max}} \le \frac{E^2 D_L t_{\text{pulse}}}{16P_1},$$

where D_L is the inductive divider of voltage.

Magnetizing inductance can be determined by geometric parameters of magnetic conduit with a non-magnetic gap

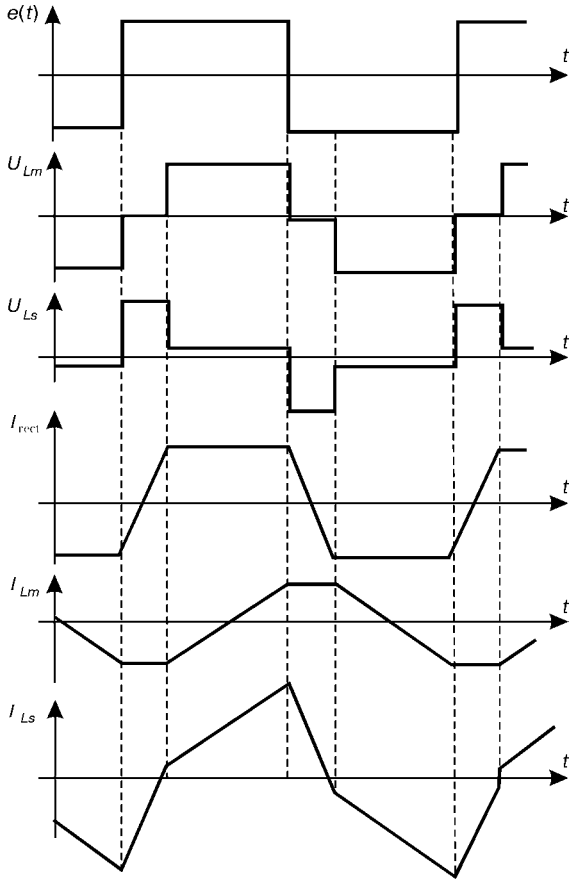

Figure 10. Time diagrams of processes in pulse transformer for case of a non-magnetic gap in transformer

$$L_m = \frac{\mu_i \mu_0 n_1^2 A_{\text{ñ}}}{l_m + \mu\delta_1}, \quad (4)$$

where μ_i is the relative initial permeability of magnetic conduit material; $\mu_0 = 4\pi \cdot 10^{-7}$ H / m is the magnetic constant; n_1 is the number of turns of primary winding; A_e, l_m, δ_1 is the effective cross-section area, mean length of line of magnetic force and line of non-magnetic gap of magnetic conduit.

The leakage inductance of this HPT design depends also on thickness of insulating insert and can be determined for windings, arranged one over another, for example, using mean geometric distances by formula

$$L_s = \frac{\mu_0 n_1^2 p_{\text{p.t}}}{2\pi s} \ln\left(\frac{g_{1.2}^2}{g_1 g_2}\right), \quad (5)$$

where $g_1 = 0.2235(h_1 + b_1)$ and $g_2 = 0.2235(h_2 + b_2)$ are the mean geometric distances of sections of windings; $g_{1.2} = h_0 + 0.5(h_1 + h_2)$ is the mean geometric distance between sections of windings; h and b are the height and width of sections of windings (index corresponds to number of winding); h_0 is the distance between neighboring edges of windings; $p_{\text{p.t}}$ is the mean perimeter of turn of windings; s is the number of cores of magnetic conduit, containing the parallel-connected winding.

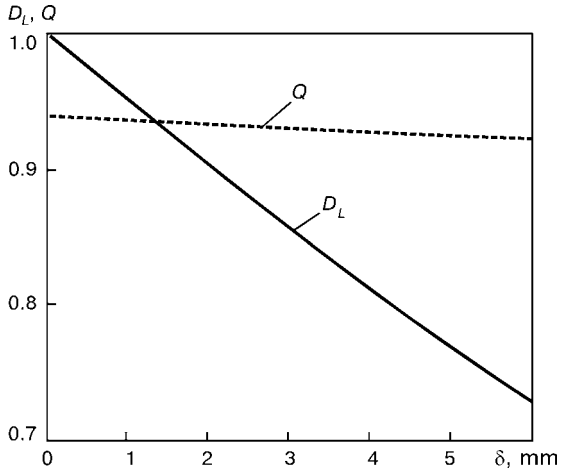

Figure 11. Dependence of coefficient of transfer ratio of inductive divider and relative pulse duration of voltage on value of non-magnetic gap

Results of calculation of transfer ratio of inductive divider of voltage and relative pulse duration Q of voltage U_{Lm} depending on the value of a non-magnetic gap for HPT with an output capacity of 1.5 kV·A, made of six sets of cores PK40×18 from ferrite of M2500NMC1, are given in Figure 11.

Using these data, let us define dependencies of limiting allowable leakage inductance $L_{s_{\max}}$, and also magnetizing inductance and leakage inductance of the transformer considered, calculated according to equations (4) and (5), on value of a non-magnetic gap (Figure 12). As is seen, the actual leakage inductance of HPT is lower than limiting allowable leakage inductance.

Assuming that intensity of electric field in dielectric of gap is 8 kV / mm, we shall select gap in magnetic cores (δ = 3 mm) on the curve $E(\delta) = U / \delta$, given in Figure 13.

Effect of gap on currents in HPT is shown in Figure 14, where amplitudes of the following values are given: I_{Ls} ---- current through leakage inductance; I_{Lm} ---- magnetizing current; I_1 ---- load current.

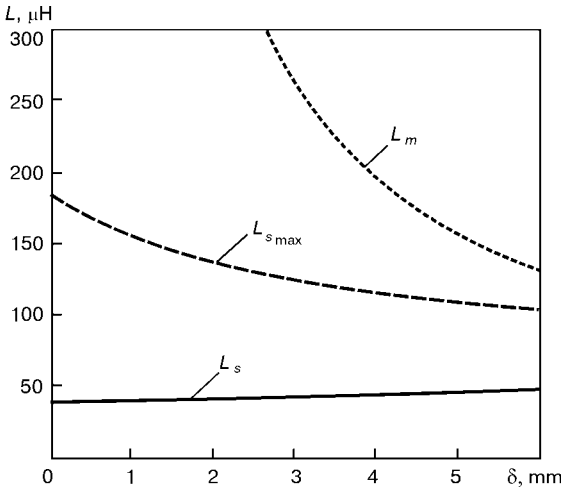

Figure 12. Dependence of limiting allowable leakage inductance, magnetizing inductance and leakage inductance on value of non-magnetic gap

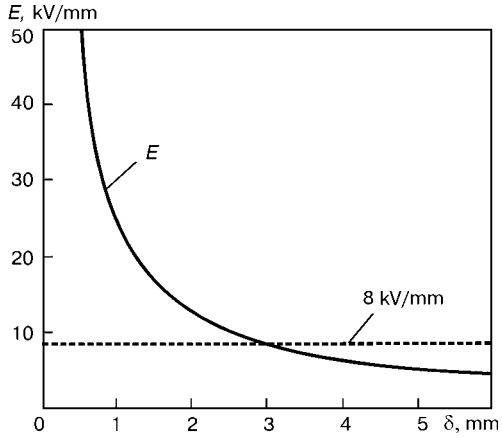

Figure 13. Dependence of electric field intensity on value of non-magnetic gap

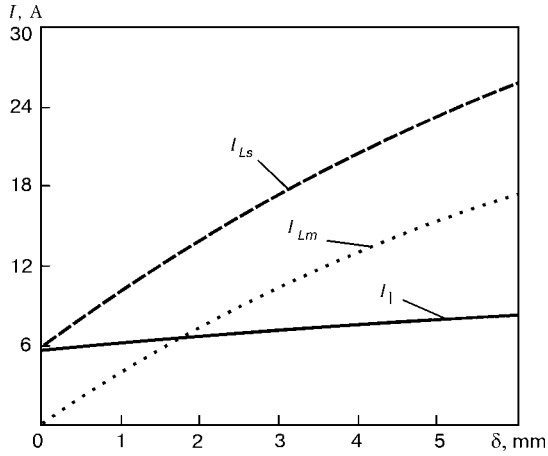

Figure 14. Dependences of currents in scheme of pulse transformer on value of non-magnetic gap

Consequently, the application of the above-described design of HPT requires the increase in the set power of the inverter and increase in amplitude of its output current.

CONCLUSIONS

1. The application of transistor converters with high-frequency pulsed modulation for design of anode current controllers for electron beam installations with a preheated cathode improves the dynamic characteristics and nature of transition processes occurring in anode current control.

2. Transition for increased frequency of conversion makes it possible to decrease greatly the mass of high-potential transformer, to arrange it on vacuum chamber and to simplify the power supply to the installation.

3. High-potential high-frequency transformer can be manufactured with an insulated insert, providing the simpler its design and conformity of electric strength of insulation between primary and secondary windings to the requirements specified.

1. Katsman, Yu.A. (1968) *High- and low-frequency electron tubes.* Moscow: Vysshaya Shkola.
2. Komarov, N., Podoltsev, A., Kusheryavaya, I. et al. (2001) High-frequency high-voltage DC isolation transformer-rectifying module for power supply of technological equipment. *EPE J.*, 11(**1**), 33–44.
3. Biebach, J., Ehrhart, P., Muller, A. et al. (2001) Compact modular power supplies for superconducting inductive storage and for capacitor charging. *IEEE Transact. on Magnetics*, 37(**1**), 353–357.
4. Ginzburg, L.D. (1978) *High-voltage transformers and chokes with epoxy insulation*. Leningrad: Energiya.
5. Babkin, V.V., Vdoviko, V.P. (2003) Introduction of tests with measuring of partial discharges for electric equipment with cast epoxy insulation. *Elektro*, **4**, 42–46.

ENGINEERING METHOD OF CALCULATION OF MAIN POWER PARAMETERS OF PLASMA LADLES-FURNACES

M.L. ZHADKEVICH, V.A. SHAPOVALOV, G.A. MELNIK, M.S. PRIKHODKO, A.A. ZHDANOVSKY and **D.M. ZHIROV**
E.O. Paton Electric Welding Institute, NASU, Kiev, Ukraine

Method of calculation of main power parameters of plasma ladles-furnaces has been developed. This procedure makes it possible to determine the power and main electric characteristics of plasma heat sources for ladles-furnaces of capacity from 30 to 100 t within the wide range of technological parameters depending on the metal melt heating rate required by the technology.

Keywords: *plasmatrons, plasma ladles-furnaces, plasma gas, metal melt, volt-ampere characteristics, active specific power, efficiency factor of plasmatrons, effective thermal parameter, power parameters*

Plasma ladle treatment of steel (PLTS), the new generation of technology of out-of-furnace treatment, in which the compensation of heat losses or preheating of slag and metal melts are realized using a low-temperature plasma in plasma ladles-furnaces, equipped with three-phase plasma heating AC complexes of 3.5–6.0 MW capacity, thus providing the rate of steel heating within 1.0–5.2 °C / min ranges.

As compared with existing analogues abroad, the plasma ladles-furnaces are advantageous by the fact that they make it possible to widen the power, technological and metallurgical capabilities of an integrated out-of-furnace treatment of steel, to reduce the specific consumption of electric power, preheating duration, wear of ladles lining, consumption of graphitized electrodes. Technology of PLTS promotes the active use of gas and slag phases, prevention of metal contamination with carbon, nitrogen and hydrogen, effective purification of metal from non-metallic impurities, improvement of quality of steel produced and ecology of the technological process.

Investigations, carried out at the E.O. Paton Electric Welding Institute, showed that it is the use of plasma heat sources and gases and slags, activated in plasma, that provides the optimum conditions of proceeding reduction-refining reactions for producing high-quality cast iron, steel and ferroalloys.

To create plasma technology and equipment which can be offered to plants for implementation, it is necessary to develop the engineering methods of calculation of power parameters, to investigate these characteristics within the wide range of technological conditions and to study the specifics of plasma melting and metals refining with gases and slags, activated in plasma.

One of main tasks, confronting developers of technology and equipment for ladle treatment, is the determination of power required for metal heating at a preset rate.

At preset mass of metal heated and rate of metal melt heating the total capacity W^{Σ} (W) of plasmatrons will be determined by formula

$$W^{\Sigma} = W_{sp} m \nu, \qquad (1)$$

where m is the metal mass in ladle, t; ν is the preset rate of metal melt heating, °C / min; W_{sp} is the active specific power, a universal parameter for calculation of power conditions of operation of ladle-furnace of a definite capacity, kW·h / (t·°C). Value of this parameter is within the 0.3–0.6 kW·h / (t·°C) ranges [1] and depends on the ladle capacity, design features of the unit, efficiency factor of plasmatrons, ladle temperature at the moment of steel pouring beginning, amount of adding alloying elements and so on. Here, it is necessary to take into account that with increase in capacity of ladles-furnaces the values of parameter W_{sp} are decreased.

It is known from the literature [2, 3] that most safe operation of plasmatrons is provided in the 300–600 mm ranges of arc lengths. At operation both in argon and also in nitrogen and their mixtures, the volt-ampere characteristics (VAC) are flat enough, and the averaged arc voltage U_a in the current ranges from 2 to 8 kA is 120–150 V for argon. For further calculation the averaged voltage of 150 V will be used.

Knowing the total capacity of plasmatrons obtained by formula (1), we shall calculate the approximate value of current I_a (A) of one plasmatron, which will be used further as reference value for calculation of region of VAC of arc discharge of plasmatron within all the range of PLTS technological conditions:

$$I_a = W^{\Sigma} / z U_a, \qquad (2)$$

where z is the number of plasmatrons.

Taking into account that the current adjustment in the ranges of 1–3 of its rated value during the accomplishment of technological operations, we shall determine the current values of one plasmatron for VAC calculated:

$$I_a^{min} \geq I_a / 3; \quad I_a^{max} \leq 3 I_a. \qquad (3)$$

Coming from above-mentioned, we shall calculate the VAC region for all the range of technological conditions taking into account the values of arc lengths in the 300–600 mm ranges according to work [2].

VAC of arc discharge of plasmatron at its operation in ladles-furnaces are steep rising, their steepness is (0.5–0.7)·10^{-2} V / A in use of argon as a plasma-forming gas and (0.7–1.0)·10^{-2} V / A in use of nitrogen or its mixture with argon as a plasma-forming gas, or in arc burning at starting period when air of increased humidity is available practically in melting space.

VAC of arcs of three-phase group of plasmatrons in use of argon as a plasma-forming gas and their burning in a steady condition are described by an empiric relationship

$$U_a^{Ar} = 1.1\ [(b\ I_a^m\ L_a) + l_e Å_c + 10], \qquad (4)$$

where b is the coefficient equal to 1.65–2; m is the exponent equal to 0.065–0.075; L_a is the arc length, cm; l_e is the electrode buried into nozzle, mm; E_c is the gradient of voltage of arc column part arranged in a nozzle channel, V / mm.

In use of nitrogen or its mixture with argon as a plasma-forming gas, and also other gases or their mixtures and in arc burning at a starting condition in atmosphere of humid air and others, the total arc voltage U_a^{total} is calculated by formula

$$U_a^{total} = U_a^{Ar}[10^2\ \{\ G\ \}]^n, \qquad (5)$$

where G is the volume share of gas in its mixture with argon; n is the exponent, in operation with use of air, nitrogen the value n is varied within 0.12–0.17, while in use of helium it is 0.05–0.08 and in hydrogen use ---- 0.32–0.35.

After calculation and plotting of VAC we shall select the optimum values of current and arc voltage at the distance L_{pl} between plasmatrons and arc length at which the safe operation of plasmatrons is guaranteed. Optimum values L_{pl} and L_a (mm) are found in the ranges

$$I_a^{k_1} < L_{pl} < I_a^{k_2}; \qquad (6)$$

$$I_a^{k_3} < L_a < I_a^{k_4}, \qquad (7)$$

where k_1 = 0.68, k_2 = 0.75, k_3 = 0.63–0.65 and k_4 = = 0.70–0.72 are the exponents.

From the set of VAC of arcs of technological conditions of service of plasma ladles-furnaces being investigated (conditions of starting and steady conditions) we shall select the ranges of current and voltage and determine the main technical characteristics of plasmatron–short circuit–power source system. The necessary conditions of stability of the mentioned system and stability of arc burning are as follows: falling external VAC of plasmatron–short circuit–power source system with a steepness which is provided by its internal resistance of not less than 0.025 Ohm; ratio of voltage of plasmatron–short circuit–power source non-closed system to arc voltage in all the range of technological conditions should be not less than 2.

To define the validity of value of a total power of plasmatrons, calculated by formula (1), let us consider a heat balance of the ladle-furnace with definite geometric sizes and design specifics of its assemblies. Heat energy generated by arcs of plasmatrons is consumed for metal melt heating and compensation of total heat losses.

Total heat losses Q^{Σ} (W) during metal melt heating in the ladle-furnace will be

$$Q^{\Sigma} = \sum_1^z Q_{pl_i} + Q_l + Q_{cov} + Q_w + Q_g, \qquad (8)$$

where $\sum_1^z Q_{pl_i}$ are the total heat losses in plasmatrons and water-cooled components of their fastening on the cover, W; Q_l is the heat energy consumed for heating ladle lining from temperature, at which metal was poured to the ladle, to operating temperature, W; Q_{cov} are the heat losses from ladle cover into environment, W; Q_w are the heat losses from ladle walls and its bottom into environment, W; Q_g are the heat losses with exhausting gases, W.

We shall calculate separate items of this equation.

Total heat losses in plasmatrons and water-cooled components of their fastening on the cover are

$$\sum_1^z Q_{pl_i} = z Q_{pl_i}, \qquad (9)$$

where Q_{pl_i} are the heat losses in plasmatron which can be presented in the form

$$Q_{pl_i} = Q_{n_i} + Q_{e_i} + Q_{c_i} + Q_{body_i}, \qquad (10)$$

where Q_{n_i}, Q_{e_i}, Q_{c_i} and Q_{body_i} are the heat losses in nozzle, electrode, cathode and body of plasmatron, respectively, W.

Heat losses in nozzle, electrode and cathode are determined by formulae:

$$Q_{n_i} = I_a q_n^*; \qquad (11)$$

$$Q_{e_i} + Q_{c_i} = I_a q_e^*, \qquad (12)$$

where q_n^* and q_e^* are the effective thermal parameters of nozzle and electrode, whose values are 12–15 and 6–8 W / A, respectively, in argon operation. In case of use of mixtures of argon with helium, nitrogen, hydrogen as plasma-forming gases or at arc burning in atmosphere of these gas mixtures $q_{n_{mix}}^*$ and $q_{e_{mix}}^*$ are determined by formulae [4, 5]:

$$q_{n_{mix}}^* = r\ \{\ G\ \} + q_n^*; \qquad (13)$$

$$q_{e_{mix}}^* = d\ \{\ G\ \} + q_e^*, \qquad (14)$$

where r, d are the coefficients depending on the kind of plasma-forming gas, W / A. In use of argon + helium mixtures r = 8–9 W / A, d = 9–10 W / A; mixtures of argon with nitrogen or air ---- r = 13–14 W / A,

d = 18–19 W / A; argon + hydrogen mixtures ---- r = = 130–150 W / A, d = 130–140 W / A.

Heat losses in body (or in caisson) and water-cooled components of plasmatron fastening on the cover depend on density of heat flow, transferred from arcs, molten metal and lining to the cooling water.

Heat losses in plasmatron body are calculated by formula

$$Q_{\text{body}_i} = q_{\text{body}} F, \tag{15}$$

where q_{body} is the density of heat flow, W / m^2; F is the area of lateral surface of body of plasmatron (or its caisson), m^2. Values q_{body}, from data of literature sources [6, 7] and our experiments, are varied in the ranges $(1.4–6.3)\cdot 10^5$ W / m^2 and depend on the degree of heat isolation of body from melting space.

After calculation of total heat losses in plasmatrons it is necessary to check the correlation of obtained results with literature and experimental data:

$$\sum_1^z Q_{\text{pl}_i} = (0.15–0.30)\ I_a U_a z. \tag{16}$$

If the data obtained are beyond the limits indicated in equation (16), then the calculation should be repeated after clarifying the calculation coefficients.

Heat energy consumed for ladle lining heating is

$$Q_l = qf, \tag{17}$$

where f is the area of contact heat exchange between molten metal and ladle lateral surface, m^2; q are the specific heat losses, W / m^2, determined as

$$q = 1.189\lambda\,(T - T_0)/(\pi a)^{0.5}, \tag{18}$$

where λ is the coefficient of heat conductivity of lining, W / (m·°C); T is the operating temperature of lining (1000–1200 °C); T_0 is the temperature of lining at which the metal is poured to the ladle (400–600 °C); a is the coefficient of temperature conductivity of lining, m^2 / h.

Heat losses from ladle cover with a non-water-cooled dome into environment can be calculated by formula

$$Q_{\text{cov}_1} = \alpha_{\text{cov}}\ F_{\text{cov}_1}\ (T_{\text{cov}_1} - T_{\text{air}}), \tag{19}$$

where α_{cov} is the coefficient of heat dissipation from cover to environment, W / (m^2·°C); F_{cov_1} is the area of cover external surface, m^2; T_{cov_1} is the temperature of cover external surface, °C; T_{air} is the temperature of air in shop, °C.

From the data of work [6] α_{cov} = (28–48) W / (m^2·°C) at T_{air} = 20 °C and T_{cov_1} = 400–500 °C.

Heat losses from ladle cover with a water-cooled dome of F_{cov_2} surface (m^2) are varied in the ranges $(3.5\cdot 10^4)$–$(1.1\cdot 10^5)$ W / m^2 and depend on the melting period [8]. On average, during melting the heat losses from water-cooled cover are taken equal to $(7.5–8.7)\cdot 10^4$ W / m^2. Then the heat losses from ladle cover with a water-cooled dome are determined by formula

$$Q_{\text{cov}_2} = (7.5–8.7)\cdot 10^4\ F_{\text{cov}_2}. \tag{20}$$

Heat losses from walls and ladle bottom into environment are calculated by formula

$$Q_w = \alpha_{\text{lad}}\ F_{\text{lad}}\ (T_{\text{lad}} - T_{\text{air}}), \tag{21}$$

where α_{lad} is the coefficient of heat dissipation from external walls of ladle into environment, W / (cm^2·°C); F_{lad} is the area of ladle external surface, m^2; T_{lad} is the temperature of ladle external surface, °C.

At T_{air} = 20 °C, T_{lad} = 100–200 °C we recommend to take α_{lad} equal to 16–23 W / (m^2·°C) for calculation.

Heat losses with exhausting gases can be determined by formula

$$Q_g = (0.09–0.10) \sum_1^z I_a U_a. \tag{22}$$

Heat energy, transferred directly to the metal melted, represents difference between heat energy, generated by arcs of plasmatrons, and total heat losses. Equation for determination of heat energy transferred to metal with allowance for real heat losses has a form

$$Q_m = W^\Sigma - Q^\Sigma, \tag{23}$$

where $W^\Sigma = \sum_1^z I_a U_a$.

Let us check the correlation of the preset rate of metal heating in ladle ν (°C / min) with a real rate ν_{real} calculated with an allowance for a real heat energy transferred to the metal:

$$\nu_{\text{real}} = Q_m / (60 m c_{\text{molt}}), \tag{24}$$

where c_{molt} is the mass heat content of metal in molten state, W·h / (kg·°C); for steel c_{molt} = = 0.255 W·h / (kg·°C).

If the obtained value of real rate is differed from preset and taken values for calculation, it is necessary to select new parameters of arc on its VAC and to repeat calculation starting from equation (9).

Calculation can be considered final if the metal heating rate, calculated by equation (24), will be equal to the preset rate or to exceed it by not more than 5 %.

1. Melnik, G.A., Zabarylo, O.S., Zhadkevich, M.L. et al. (2002) Some possibilities of steel treatment in the arc and plasma ladle-furnaces. *Advances in Electrometallurgy*, **1**, 22–26.
2. Melnik, G.A., Zabarylo, O.S., Zhdanovsky, A.A. et al. (1991) Prospects of application of plasma heat sources in units for out-of-furnace treatment of steel. Report 1. *Problemy Spets. Elektrometallurgii*, **2**, 60–66.
3. Melnik, G.A., Zabarylo, O.S., Zhdanovsky, A.A. et al. (1991) Prospects of application of plasma heat sources in units for out-of-furnace treatment of steel. Report 2. *Ibid.*, **3**, 86–92.
4. Paton, B.E., Latash, Yu.V., Zabarylo, O.S. et al. (1985) Three-phase plasma heating systems and prospects of their application. Report 1. *Ibid.*, **1**, 50–55.
5. Paton, B.E., Latash, Yu.V., Zabarylo, O.S. et al. (1985) Three-phase plasma heating systems and prospects of their application. Report 2. *Ibid.*, **2**, 53–57.
6. Smolyarenko, V.D., Kuznetsov, L.N. (1973) *Energy balance of arc steel-making furnaces*. Moscow: Energiya.
7. Nikolsky, L.E., Smolyarenko, V.D., Kuznetsov, L.N. (1981) *Heat operation of arc steel-making furnaces*. Moscow: Metallurgiya.
8. Sosonkin, O.M., Kudrin, V.A. (1985) *Water-cooled electric arc furnace dome*. Moscow: Metallurgiya.

INVESTIGATION OF COMPOSITION OF GAS ATMOSPHERE IN INDUCTION MELTING OF SPONGY TITANIUM IN A SECTIONAL MOULD

M.L. ZHADKEVICH[1], **I.V. SHEJKO**[1], **S.M. TESLEVICH**[2], **V.A. SHAPOVALOV**[1], **V.S. KONSTANTINOV**[1] and **V.V. STEPANENKO**[1]
[1]E.O. Paton Electric Welding Institute, NASU, Kiev, Ukraine
[2]Zaporozhie Titanium-Magnesium Plant, Zaporozhie, Ukraine

Composition of gas phase in the zone of spongy titanium melting in use of high-frequency electromagnetic field as a heat source was determined. It was established that hydrogen and moisture are evolved in charge melting. Content of hydrogen and moisture depends on the method of preparation of melting equipment, method of charge feeding, speed of titanium melting and content of chlorine in spongy titanium.

Keywords: *melting, hydrogen, vacuum, spongy titanium*

In spite of development of new methods of titanium melting, the vacuum-arc melting of spongy titanium, pressed into a consumable electrode, is remained priory at present [1].

One of the main problems of vacuum-arc remelting of the consumable electrode consists in a removal of residual chlorine and hydrogen from the metal. As is generally known, the hydrogen has a negative effect on ductile characteristics of the metal [2]. Optimum hydrogen content in the metal, as was stated in work [3], should not exceed 0.005 wt.%. To provide this content of hydrogen in the metal, it is necessary to keep a residual vacuum of 6–13 Pa during melting. Ingots, produced in vacuum-arc furnaces, are characterized by high mechanical properties and low content of harmful impurities.

However, the spongy titanium remelting in vacuum-arc furnaces is possible only at a minimum content of residual chlorides (0.08–0.10 wt.%). To attain these values, the spongy titanium at the stage of high-temperature vacuum distillation is subjected to holding in retorts during several dozens of hours [4]. During holding the spongy titanium block is saturated partially with oxygen, nitrogen, and harmful impurities of iron, nickel and others are diffused into the block from steel walls of the retort.

Reduction in time of a vacuum separation improves the quality characteristics of the spongy titanium and technical-economic characteristics of the process, however, the increased amount of chlorides salts is remained in the block, being not separated completely. The use of an electric arc as a heat source in remelting of spongy titanium of this quality in vacuum is difficult due to intensive evolution of easily-volatile elements from the molten metal. Vapours disturb a stable arc burning that can lead to its transfer to the wall of a copper water-cooled mould. In this case, the hazard of burning-out of copper walls of the mould and its explosion may occur.

As an alternative method, the induction remelting of gas-saturated spongy titanium in a sectional mould (IRSM) [5] was tested. This remelting is realized at excessive pressure of neutral gas in a melting chamber, i.e. under the conditions of a chemical vacuum. The excessive pressure or negligible rarefaction, maintained in a melting spacing, is stipulated by design features of a sectional mould.

It was above-mentioned that one of main problems of the spongy titanium remelting consists in the hydrogen removal at all the stages of the process. Therefore, it seems rational to study the hydrogen behaviour in induction melting of the spongy titanium, having different content of chlorides in the range from 0.08 to 0.45 wt.%.

Investigations were carried out in IRSM installation, whose general view and diagram are presented in Figures 1 and 2. This installation is supplied from a high-frequency generator of 100 kW capacity. Current frequency is 66 kHz. Preliminary rarefaction in melting space is realized by vacuum pumps RVN-20 and AVP-05.

Hydrogen content was determined using a gas analyzer TP-1120 in a set with a potentiometer KSM2. Gas sampling for the analysis was performed through a cover of a charge hopper, as the highest concentration of hydrogen is available in this zone.

Before melting beginning the walls of the melting chamber, chamber of ingot, bottom plate, mould and screw feeder were cleaned carefully from sublimates condensed during previous melts. Walls were cleaned firstly by a metallic brush, and then by a cloth wetted in a technical alcohol or benzene. A primer from commercial titanium was placed on the prepared bottom plate and fixed rigidly. Spongy titanium of 2–5 mm fraction was loaded into a charge hopper.

After charge loading the furnace was pressurized and evacuated to residual vacuum of 13–15 Pa during 30–60 min. Degassed chamber was filled up to excessive pressure of 1200 GPa, some melts were performed at different periods of spongy titanium holding in a

Figure 1. General view of induction installation for remelting spongy titanium in induction mould with a measuring unit

vacuum, and also at a repeated evacuation of the chamber after its filling with argon.

It should be noted that inleakage of atmospheric gases was checked before each furnace filling with argon. It was within the 0.266–0.665 Pa / min ranges. Melts were performed in a stagnant atmosphere of the shielding gas without its additional feeding into a melting chamber.

After furnace preparation for melting and generator preheating the high-frequency current was supplied to the inductor. At the melting beginning 70–80 % of the inductor capacity were used. The titanium primer heating is occurred under the action of the high-frequency currents. Gas sampling from the melting space was made during heating and supplied to the instruments for gas composition control. Before instrument gauge switching on, the supplying pipings were blown out with an operating gas for 5 min. The primer was preheated for 8–10 min. At the moment of the primer melting, melt forcing out from the mould walls and formation of «cupola» the TP-1120 instrument recorded the hydrogen appearance in the melting chamber. Its content varied from 0.10 to 0.25 vol.% and depended on the quality of furnace preparation for melting, preliminary rarefaction, inleakage, quality of shielding inert gas and so on.

After generator bringing to 100 % of its capacity and stabilization of melting parameters, the spongy titanium was fed to a pool cupola centre by a screw feeder. Ingot was withdrawing at a gradual pool filling. The main amount of melts was performed at 2 mm / min withdrawal rate. The first series of experimental melts was realized using spongy titanium of TG-100, TG-110, TG-120 grades with ion-chlorine content up to 0.08 wt.%.

Results of measurements of hydrogen concentration in gas phase showed that with a charge feeding to the mould its content in the chamber is increased gradually from 0.10 up to 0.55 vol.% (Figure 3). This process is most intensive during 20–25 min, then the rate of hydrogen increment was delayed, while in some cases it

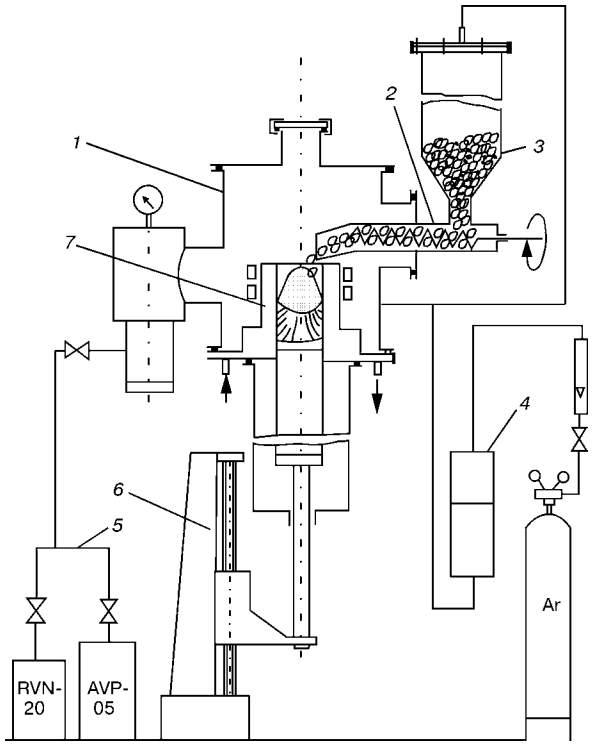

Figure 2. Diagram of laboratory installation with a sectional mould: *1* — vacuum chamber; *2* — screw batcher; *3* — charge hopper; *4* — gas supply system; *5* — system of vacuum pumps; *6* — mechanism of ingot withdrawal; *7* — mould

was interrupted. The evolution of a large amount of hydrogen from sponge of the TG-120 grade was due, in our opinion, to a large porosity of this material and, consequently, to a more developed surface of absorption of water vapours. The increase in hydrogen amount in gas phase was observed both at a discrete and also continuous feeding of the charge. In the latter case the rate of hydrogen growth was most significant.

When remelting of the gas-saturated spongy titanium of TG-TV grade with chlorine content up to 0.15 wt.%, the hydrogen concentration over the molten titanium was increased up to 1 vol.%. In case of holding the spongy titanium of the above-mentioned grade before melting in a melting chamber under conditions of vacuum during a day without subsequent depressurization of the chamber, the maximum hy-

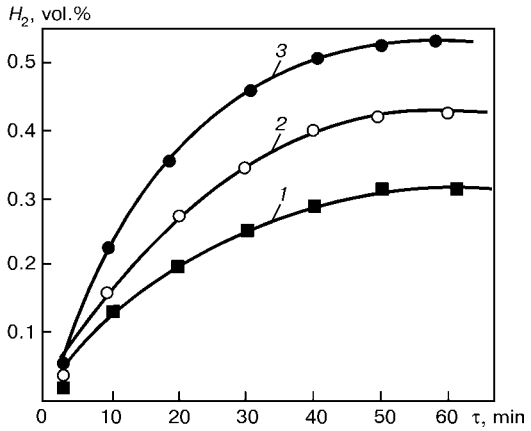

Figure 3. Change of hydrogen concentration in furnace chamber during remelting different grades of spongy titanium: *1* — TG-100; *2* — TG-110; *3* — TG-120

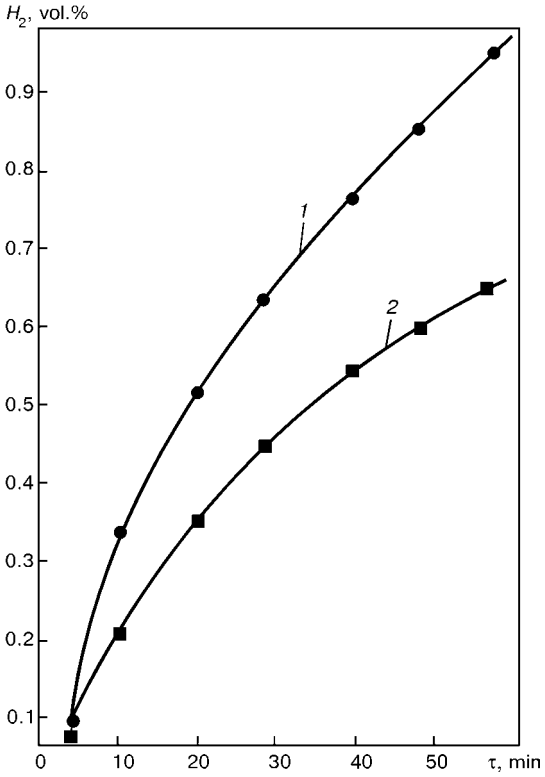

Figure 4. Change of hydrogen concentration in gas phase in the process of remelting spongy titanium of TG-TV grade using different methods of its preparation: *1* — evacuation for 1 h; *2* — holding in vacuum for 24 h

drogen concentration in a gas phase did not exceed 0.5 vol.% (Figure 4).

The rate of meting influences greatly the amount of hydrogen evolving from the charge. Thus, in remelting of titanium sponge of TG-120 grade at 2–4 mm / min rates of withdrawal the hydrogen content in a melting space at 4 mm / min rate was twice increased (Figure 5).

However, the most intensive hydrogen evolution is occurred with increase in the content of a residual chlorine in the spongy titanium. With increase in amount of chlorides from 0.08 up to 0.45 wt.%, the maximum amount of hydrogen in gas phase was varied from 0.2 to 2.0 vol.%.

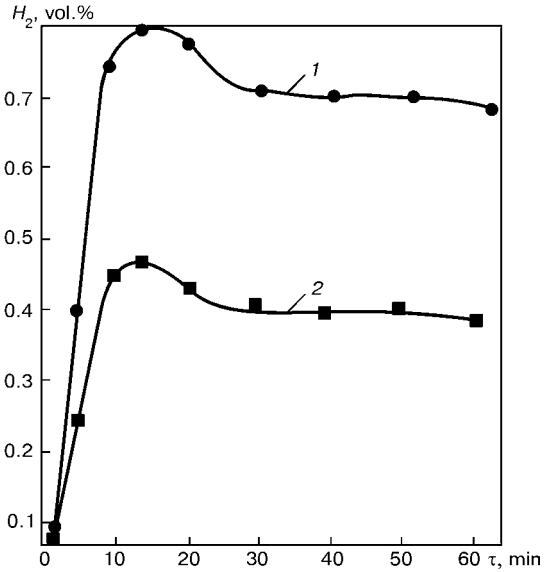

Figure 5. Change of hydrogen content in gas phase at different rates of ingot withdrawal: *1* — 4 mm / min; *2* — 2 mm / min

It should be noted in addition that intensive boiling of a metal pool with a partial splash of the molten metal occurred sometimes during melting of charge, containing a large amount of chlorides. At this extreme moment the hydrogen content in the chamber increased spontaneously up to 3.5 vol.%.

Simultaneously with a record of hydrogen content in the melting space the presence of moisture was controlled which is known to be a source of hydrogen enter into gas phase in titanium melting. Amount of moisture in the gas phase was determined using a coulomb-meter of humidity of «Bajkal-1» type. Moisture is contained in argon which fills the furnace melting space after evacuation before melting, on walls of melting chamber, in mould, primer, screw feeder and ingot chamber. Here, the moisture can be of two types: moisture, which is absorbed directly on melting chamber walls (its amount depends, probably, on material from which the chamber is manufacture and quality of its surface treatment), and moisture, which is preserved by a magnesium chloride included into composition of vapours evolving from the spongy titanium in melting and condensing on the water-cooled walls of the melting equipment (its amount depends on several factors).

It is known that magnesium chloride can combine up to six water molecules. However, this compound is instable and loses moisture in pressure reduction. This process is proceeding by reactions:

$$MgCl_2 \cdot 6H_2O \rightarrow MgCl_2 \cdot 4H_2O + H_2O;$$
$$MgCl_2 \cdot 4H_2O \rightarrow MgCl_2 \cdot 2H_2O + H_2O;$$
$$MgCl_2 \cdot 2H_2O \rightarrow MgCl_2 \cdot H_2O + H_2O.$$

The last reaction was realized under heating conditions [2].

Thus, to decrease the moisture content it is necessary to remove dust, containing chlorides, from the chamber before melting. This is performed by a cloth wetted with a benzene or technical alcohol. The measurements showed that minimum content of moisture in the shielding gas before melting is observed after walls cleaning with a cloth wetted with an alcohol. Thus, if at argon outlet from cylinder the dew point was in the –62 – –61 °C ranges, then after cleaning with a metallic brush the dew point at the argon outlet from the melting chamber was –58 – –57 °C. After cleaning with a cloth, wetted in technical alcohol, the dew point was –60 – –59 °C.

In the next series of experiments the effect of depth and time of pre-degassing on moisture content in argon before melting was investigated. The investigations showed that at 13 Pa vacuum depth the dew point after filling the chamber with argon is –60 °C. If the vacuum before chamber filling was in the 20–26 Pa ranges, then the dew point after chamber filling with argon did not increase above –40 °C.

Air inleakage from atmosphere into melting space has a great effect on moisture content in argon in furnace preparation for melting. The measurements showed that at leakages in the 0.2–0.3 Pa / min ranges

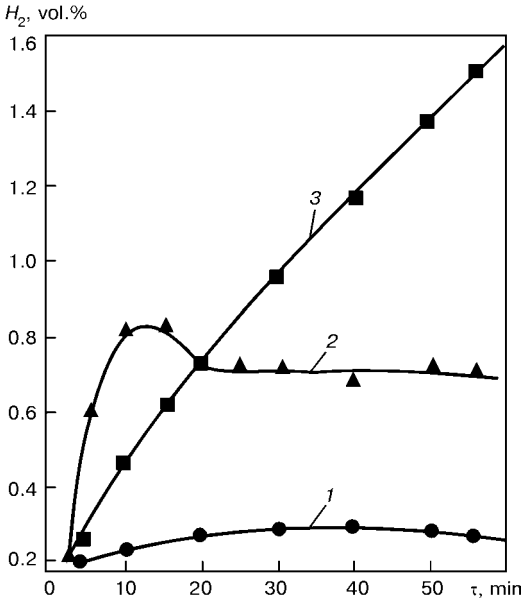

Figure 6. Change of hydrogen concentration in furnace chamber during remelting spongy titanium with different content of ion-chlorine: *1* — 0.08 wt.%; *2* — 0.15 wt.%; *3* — 0.45 wt.%

the dew point reaches –60 -- –59 °C. At 0.665 Pa / min leakage the moisture amount is increased up to 39 mg / m^3 (–50 °C dew point). Increase in moisture amount in the furnace atmosphere is, probably, associated with the fact that with increased inleakage the vacuum pumps pump out mainly the gases entered from atmosphere, but they do not «break away» the adsorbed moisture from the chamber walls with a residual magnesium chloride, being not removed during their cleaning.

A significant difference in moisture content in pure argon and argon, filled the melting chamber, was found in changing the method of its degassing. Investigations showed that a double evacuation of the melting space with an intermediate its filling with argon the difference in moisture content is 20–40 %.

The melting of spongy titanium of soft and solid grades revealed itself the different nature of moisture behaviour in the process of charge melting. In melting spongy titanium of TG-100 grade with content of chlorides up 0.06 wt.% a short-time increase in content of water vapours in gas atmosphere from 23 mg / m^3 (–50 °C dew point) up to 31 mg / m^3 (–52 °C dew point) occurred with the next its reduction to 20 mg / m^3 (–50 °C dew point) or with a approximate preserving of a constant amount of water vapours over the molten metal in the ranges up to 30 mg / m^3 (–52 °C dew point). In case of feeding the spongy titanium of TG-120 or TG-TV grades into the melting zone the moisture content in gas phase is increased up to 63 mg / m^3 (–43 °C dew point).

Increase in content of chlorides in spongy titanium up to 0.45 wt.% has led to the continuous increase in moisture content in the melting zone up to 100 mg / m^3 (–42 °C dew point) even 15 min after the beginning of spongy titanium feeding into the mould.

Due to limiting capabilities of the instrument «Bajkal-1» the further behaviour of moisture in melting

Figure 7. IRSM ingots melted out from gas-saturated spongy titanium

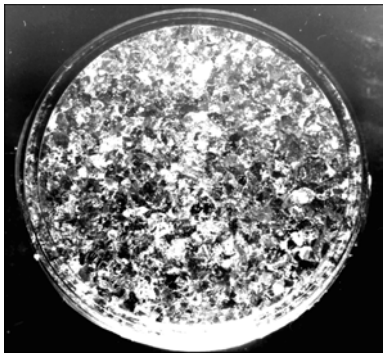

Figure 8. Macrostructure of IRSM ingot (transverse templet)

spongy titanium having a high content of chlorine was not recorded, but it is possible to state indirectly its constant increase in the melting space by the amount of hydrogen in gas phase. To decrease the amount of hydrogen and moisture in gas phase during melting, it is necessary to develop such a technology of charge preparation and its remelting which could solve this problem.

The final operations of melting the gas-saturated spongy titanium included: cooling of melted ingot, evacuation of melting space to remove hydrogen from the chamber, filling it with air, depressurization of furnace and withdrawal of ingots. Figures 7 and 8 present the general view of 70 mm diameter ingot and its macrostructure. The ingot surface has a complete penetration, there are no cracks and cold shuts. Macropores on the macrostructure templet were not observed.

1. Andreev, A.L., Anoshkin, N.F., Borzetsovskaya, K.M. et al. (1978) M*elting and casting of titanium alloys*. Moscow: Metallurgiya.
2. Livanov, V.A., Bukhanova, A.A., Kolachev, V.A. (1962) *Hydrogen in titanium*. Moscow: Metallurgizdat.
3. Dobatkin, V.I., Anoshkin, N.F., Andreev, A.L. et al. (1966) *Ingots of titanium alloys*. Moscow: Metallurgiya.
4. Garmata, V.A., Petrunko, A.N., Galitsky, N.V. et al. (1984) *Titanium*. Moscow: Metallurgiya.
5. Zhadkevich, M.L., Latash, Yu.V., Shejko, I.V. et al. (1997) On problem of capability of remelting sponge titanium with higher content of man-caused impurities. *Problemy Spets. Elektrometallurgii*, **1**, 55–60.

X-RAY AND METALLOGRAPHIC EXAMINATIONS OF PHASE TRANSFORMATIONS DURING SOLID-HDDR IN FERROMAGNETIC ALLOY OF DIDYMIUM–IRON–BORON SYSTEM*

I.I. BULYK[1], **V.V. PANASYUK**[1], **A.M. TROSTYANCHIN**[1], **G.M. GRIGORENKO**[2], **V.A. KOSTIN**[2], **T.G. TARANOVA**[2] and **S.G. GRIGORENKO**[2]

[1]G.V. Karpenko Physical-Mechanical Institute, NASU, Lvov, Ukraine
[2]E.O. Paton Electric Welding Institute, NASU, Kiev, Ukraine

Using methods of differential thermal, X-ray phase, electron-microscopic and element analysis, the peculiarities of hydrogen-initiated phase transformations such as hydrogenation, disproportionation, desorption and recombination were studied in ferromagnetic alloy under 0.1–0.5 MPa pressure in the range of temperatures from room to 920 °C. It was shown that alloy is disproportioned in hydrogen at 770 °C, while in vacuum at heating up to 900 °C the products of disproportionation are recombined into initial phase with a highly-dispersed homogeneous structure.

Keywords: *ferromagnetic alloys, hydrogen, phase transformations, HDDR-process, X-ray phase analysis, electron microscopy, microstructure*

Hydrogen, as a working medium for dispersion of ferromagnetic materials on the base of compounds of rare-earth and transition metals (and boron), is used by the leading manufacturers of permanent magnets all over the world. There are several modifications of hydrogen technology of refining, among which hydride embrittlement [1] and hydrogenation, disproportionation, desorption, recombination (HDDR-process) are most widely spread [2, 3].

The principle of hydride embrittlement or hydride dispersion is based on alloy saturation with hydrogen (hydrogenation) at room temperature under the pressure of several atmospheres. Hydrogenation is accompanied by hydrogen penetration into voids of crystalline lattice and its expansion. Stresses, occurring in this case, are so high that ingot is cracked and fractured, thus transforming into powder of particle sizes of several tens of micrometers. When this type of material treatment is used the hydrogen fulfills two functions, such as initiates cracking with the formation of powder and protects it simultaneously from contact with air oxygen, preventing oxidation and deterioration of material characteristics. Material, embrittled by this way, is refined easily to a necessary dispersity of several micrometers.

Another type of alloys treatment in hydrogen, HDDR, consists in combination of hydride formation and effect of thermal energy. There are two types of HDDR: conventional and so-called solid. The principle of conventional and Solid-HDDR consists in the fact that after alloy hydrogenation and subsequent hydride heating in hydrogen, it is decomposed (hydrogenation, disproportionation ---- HD) into several phases, among which there is a hydride of rare-earth metal. Heating of disproportionation products in vacuum gives an opportunity to desorb hydrogen and to produce again the initial structure (desorption, recombination ---- DR). However, in this case the phase has already highly-dispersed crystallite morphology.

Conventional type is differed from Solid-HDDR in the method of conductance of the first stage, i.e. HD (Figure 1) and macroscopic state of alloys after the process completion. As is seen from Figure 1, *a*, the conventional HD is realized by the alloy heating in hydrogen from room to maximum temperature. Here, the alloy is transformed in most cases into the powder. Solid-HD is realized by hydrogen supply into the chamber with alloy, heated to 600–700 °C temperature (Figure 1, *b*). Under these conditions of saturation with hydrogen the alloy preserves the mechanical integrity and has a highly-dispersed structure consisting of crystallites of sizes of several tens of micrometer. Owing to the formation of such type of morphology the ferromagnetic alloys are characterized by a high coercive force. Conditions are defined for HDDR-process, as a result of which the anisotropic alloys NdFeB with high magnetic properties are produced that makes it possible to use this method for manufacture of quality permanent magnets [4–7].

The present work, as a continuation of earlier investigations [8, 9], gives data about conditions and specifics of interaction of ferromagnetic alloys, such as didymium–iron–boron, with hydrogen, which are

*The work was fulfilled owing to financial support of Scientific-Technical Center of Ukraine.

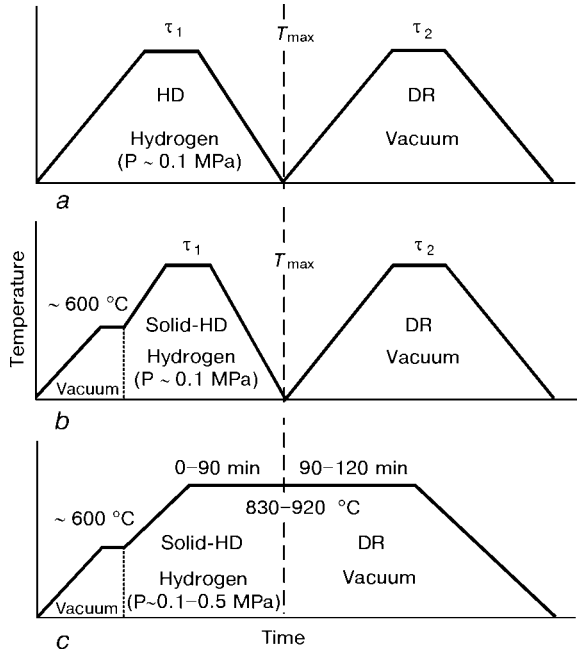

Figure 1. Schemes of HDDR (*a*) and Solid-HDDR (*b*, *c*)

used for manufacture of inexpensive permanent sintered magnets [4, 6, 10]. Presented are the results of X-ray and metallographic examinations of phase transformations in the Solid-HDDR process in industrial ferromagnetic alloy E-78 of the following composition, wt.%: 36.1Dd; 1.1B; 0.8Al; Fe ---- the rest, where Dd is the mixture of rare-earth metals: neodymium, praseodymium, lanthanum, cerium. Alloy E-78 was produced from waste of recycling uranium

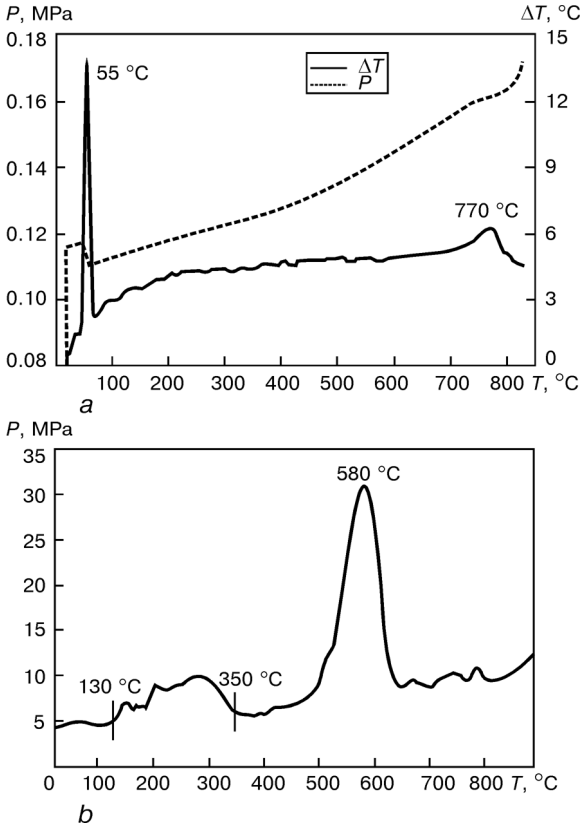

Figure 2. Thermograms (*a*) of heating alloy E-78 in hydrogen and curve of hydrogen evolution from disproportioned alloy (*b*)

ores on the basis of fluoride technology of reduction of oxides of rare-earth metals.

Experimental procedures. The alloy was melted in the induction furnace at «Ekspromag Company Ltd.» (Dneprodzerzhinsk, Ukraine). Solid-HDDR process was performed at initial pressure of hydrogen P_{H_2} = 0.1–0.5 MPa and temperature T = 830–920 °C using differential thermal analysis (DTA) in hydrogenation, disproportionation and measurement of hydrogen pressure in desorption and recombination. In

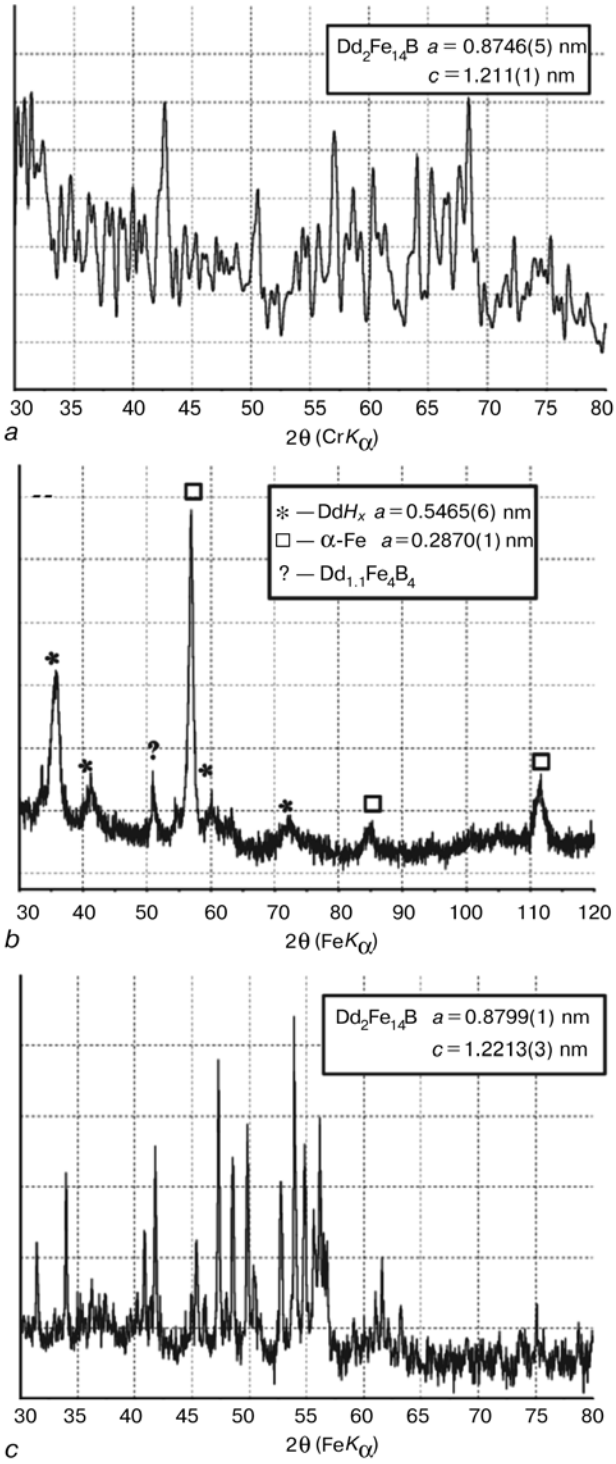

Figure 3. Diffractograms of alloy E-78: *a* — initial; *b* — Solid-disproportioned at P_{H_2} = 0.5 MPa; *c* ---- Solid-recombined after Solid-HD at P_{H_2} = 0.5 MPa

case of Solid-HD the scheme of material treatment is shown in Figure 1, *c*. To examine the microstructure after Solid-HDDR, the alloy was subjected to treatment using the same diagram, i.e. DR was made directly after HD without cooling to the room temperature. The rate of heating during HD and DR was 5 K / min. Metallographic examinations were made in JEOL. Samples were polished and etched electrolytically in agent based on chromium anhydride. Structural-phase examinations were conducted by the method of X-ray phase analysis (XPA) of powders by obtaining diffractograms in diffractometer HZG-4A using FeK_α-radiation. Diffractograms were designed using programs PowderCell.

Differential thermal and X-ray phase analyses of alloy E-78 under HDDR conditions. Using DTA by two exothermic peaks, the formation of alloy hydride at temperature 55 °C and decay (disproportionation) of initial phase at 770 °C temperature were found (Figure 2, *a*). According to XPA data, the initial alloy, in which a ferromagnetic Φ-phase ($Dd_2Fe_{14}B$) is dominated, is disproportioned after heating in hydrogen into DdH_x, α-Fe and, in our opinion, into $Dd_{1.1}Fe_4B_4$ (Figure 3, *b*).

During DR the hydrogen is evolved from products of disproportionation with a wide low-intensive peak at 130–350 °C and with an intensive peak at 580 °C (Figure 2, *b*). Φ-phase is completely restored (Figure 3, *c*). Impurity phases, existing in alloy, were not identified due to a small number of peaks.

Microstructural examinations and element analysis of composition of phases in alloy E-78 under Solid-HDDR conditions. Microstructure of initial alloy (Figure 4, *a*) is characterized by the presence of elongated grains of the ferromagnetic phase (region *1*), separated by precipitations of phase enriched by a mixture of rare-earth metals (Dd) (region *2*). Width of grains of main phase is 10–20 μm, the length is several tens of micrometers. Intergrain precipitations of a columnar type have 1–7 μm width. Phase, enriched with Dd, is brittle. Cavities remained after its crumbling were revealed in region *2a*. From the data of element analysis the content of Dd in main phase is close to its content in charge, while in phase enriched with Dd the mass ratio of Fe:Dd is approximately 1:1.

Microstructure of alloy after hydrogenation and disproportionation was subjected to changes. In region *1* (Figure 4, *b*), where Φ-phase was in initial alloy, the areas of mixture of fine-dispersed light-grey precipitations of hydride of rare-earth metals and dark disseminations of iron and iron borides were observed. Phase, enriched with Dd, is remained without changes (region *2*). Its largest part was disseminated in manufacture of microsection (region *2a*) remaining hollow

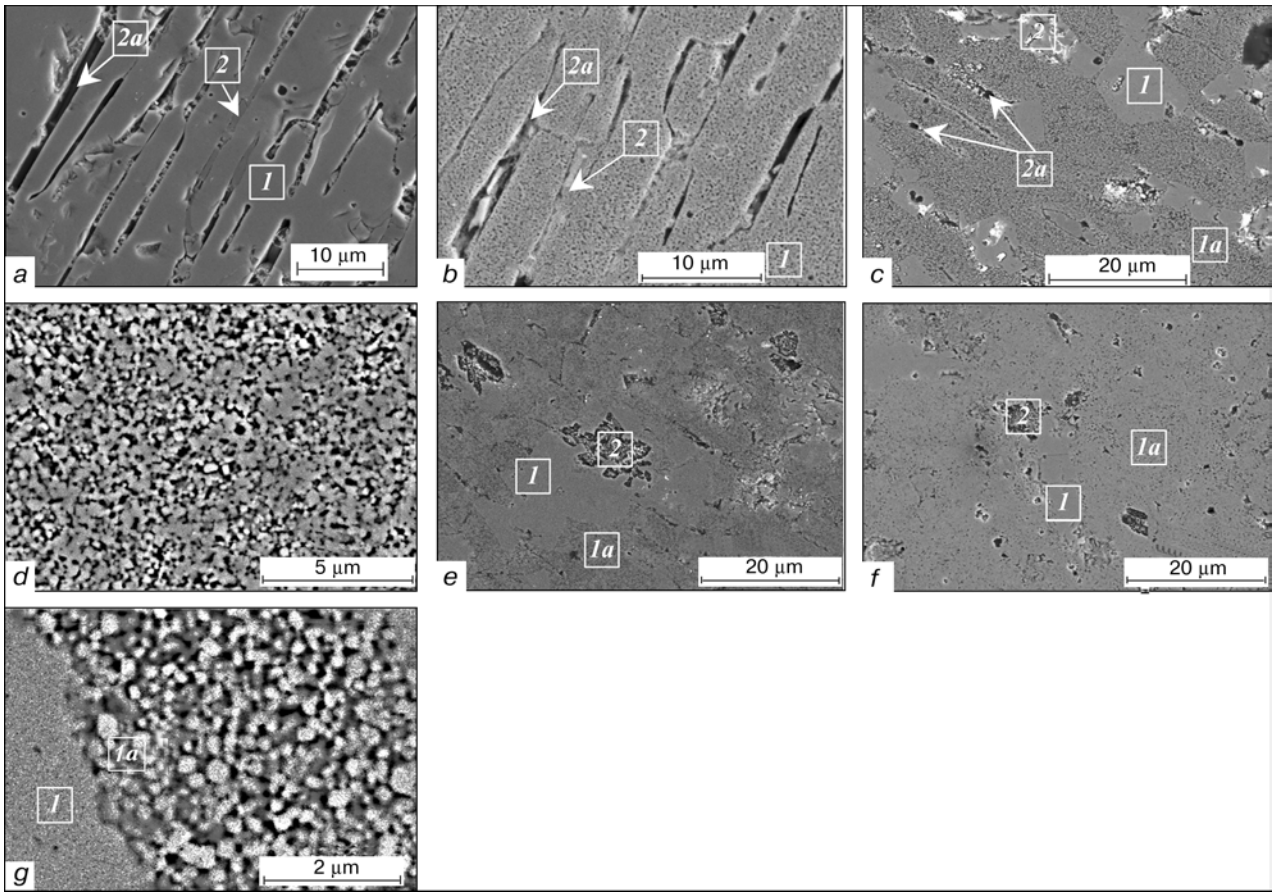

Figure 4. Microstructure of alloy E-78: *a* — as-cast alloy (×1500); *b* — Solid-disproportioned at P_{H_2} = 0.15 MPa, T_{max} = 920 °C and τ = 1 h (×2000); *c*, *d* — after Solid-HDDR at T_{max} = 870 °C, τ = 1 h during HD and τ = 2 h during DR (×1000 and ×5000, respectively); *e* — after Solid-HDDR at T_{max} = 850 °C, τ = 1.5 h during HD and DR (×1000); *f*, *g* — after three cycles of Solid-HDDR at T_{max} = = 850 °C, τ = 1 h during HD and DR (×1000 and ×10000, respectively)

cracks. Averaged concentration of elements in regions *1* and *2* remained the same as in the initial alloy.

After the complete cycle of Solid-HDDR the morphology of the material was changed greatly (Figure 4, *c* and *d*). In place of coarse grains of ferromagnetic Φ-phase the mixture of its highly-dispersed crystallites was formed (regions *1* and *1a*). Only enlarged island-like formations (region *2*) and thin thread-like traces (region *2a*), along which this phase was located in initial material, remained from the branched network of enriched Dd phase. Decrease in amount of enriched Dd phase, visible in Figure 4, *c*, was caused,in our opinion, by its transition into the highly-dispersed mixture (Figure 4, *d*).

By comparing Figure 4, *e* and *c*, it can be concluded that the change in time of parameters of Solid-HDDR influences the alloy morphology. A half an hour holding of alloy at the highest temperature of heating at the Solid-HD stage unlike 1 h holding leads to a complete transformation of branched network of enriched Dd phase into island-like coagulants and also into highly-dispersed mixture with Φ-phase. This was confirmed by the element analysis. In particular, if the content of mixture of rare-earth metals together with aluminium was ~ 30 wt.% and the rest was iron in initial alloy in the region of ferromagnetic Φ-phase, then after the complete cycle of HDDR the concentration of mixture of rare-earth metals together with aluminium was increased up to 33 wt.% in the regions *1* and *1a* (highly-dispersed mixture of Φ-phase and that enriched with Dd) (Figure 4, *e*). Similar results were also obtained on the sample shown in Figure 4, *c*, in which the concentration of mixture of rare-earth metals together with aluminium was within 33–37 wt.% ranges in regions *1* and *1a*.

In case of three-time cycle of Solid-HDDR a complete fracture of columnar structure of intergrain precipitations of phase enriched with Dd is occurred (Figure 4, *f*). Its large remnants in region *2* have a shape of islands of irregular shape of sizes from several micrometers to 15–20 μm. From data of element analysis the mass ratio of Fe:Dd in this region is approximately 1:1. The content of mixture of rare-earth metals with impurities of aluminium in regions *1* and *1a* is 34–38 wt.%, the rest was iron.

At ×10000 magnification (Figure 4, *g*) the fine-grain structure of alloy in the region of mixture of Φ-phase and phase enriched with Dd was observed. Regions *1* and *1a* in this Figure correspond to similar regions in Figure 4, *f*. Morphology of region *1* requires the further examination in microscopes with a higher resolution.

Solid-HDDR of alloy E-78 leads to dispersion of grains and its homogenization. Columnar precipitations of Dd-enriched phase are dissolved partially between highly-dispersed grains of main phase, while the remnants are transformed into coagulants of sizes up to ~ 20 μm. Increase in number of cycles of Solid-HDDR increases the alloy homogeneity.

1. Harris, I.R. (1987) The potential of hydrogen in permanent magnet production. *J. Less-Common Met*., **131**, 245–262.
2. Harris, I.R. (1992) The use of hydrogen in the production of Nd–Fe–B-type magnets and in the assessment of Nd–Fe–B-type alloys and permanent magnets. In: *Proc. of 12th Int. Workshop on Rare Earth Magnets and their Applications*, Canberra, Australia.
3. Takeshita, T., Nakayama, R. (1992) Magnetic properties and microstructures of the NdFeB magnet powder produced by hydrogen treatment. *Ibid.*
4. Hamada, N., Mishima, C., Mitarai, H. et al. (2000) Enhancement of heat resistance of Nd–Fe–B anisotropic magnet by Dy addition in HDDR process. In: *Proc. of 16th Int. Workshop on Rare Earth Magnets and their Applications*, Sendai, Japan, Sept. 2000.
5. Mishima, C., Hamada, N., Mitarai, H. et al. (2000) Magnetic properties of NdFeB anisotropic magnet powder produced by the d-HDDR method. *Ibid.*
6. Honkura, Y., Mishima, C., Hamada, N. et al. (2002) Anisotropic neo bonded magnets with high (BH)max. In: *Proc. of 17th Int. Workshop on Rare Earth Magnets and their Applications*, Newark, USA, August 2002.
7. Honkura, Y., Mishima, C. *Production method of anisotropic rare earth magnet powder*. Patent 6444052 USA. Int. Cl. H01F 1 / 055; H01F 1 / 057. Publ. 03.09.02.
8. Bulyk, I.I., Denis, R.V., Panasyuk, V.V. et al. (2001) HDDR process and hydrogen sorption properties of alloy didymium–aluminium–boron ($Dd_{12.3}Al_{1.2}Fe_{79.4}B_6$). *Fiz.-Khim. Mekhanika Materialiv*, **4**, 15–20.
9. Bulyk, I.I., Panasyuk, V.V., Trostianchyn, A.M. et al. (2004) Features of the HDDR process in R–Fe–B ferromagnetic alloys (R is a mixture of Nd, Pr, Ce, La, Dy and others). *J. Alloys and Compounds*, 370, 261–270.
10. Mishima, C., Hamada, N., Mitarai, H. et al. (2000) Magnetic properties of NdFeB anisotropic magnet powder produced by the d-HDDR method. In: *Proc. of 16th Int. Workshop on Rare Earth Magnets and their Applications*, Sendai, Japan, Sept. 2000.

INVESTIGATION OF STEEL DEGASSING IN ELECTRIC ARC MELTING AND CIRCULATION VACUUM DEGASSING

A.D. CHEPURNOJ[1], **B.I. RAZINKIN**[2], **A.B. TSERTSEK**[2], **A.G. KOVALYOV**[3] and **A.A. LEONTIEV**[3]
[1]OJSC «Mariupol Plant of Heavy Machine-Building», Mariupol, Ukraine
[2]OJSC «Leading Specialized Design-Technological Institute», Mariupol, Ukraine
[3]OJSC «Energomashspetsstal», Kramatorks, Ukraine

Effect of main technological parameters of electric arc melting and vacuum degassing on the degree of changing the content of hydrogen and nitrogen in molten steel was studied. After mathematical processing of experimental data of electric arc melts, the equations of dependence of hydrogen content in steel on the rate of carbon oxidation, duration of reduction period and also of its dependence in vacuum degassing on the metal cooling rate, duration of vacuum degassing and steel temperature were derived.

Keywords: *nitrogen, hydrogen, rate of carbon oxidation, duration of reduction period, cooling rate, vacuum degassing*

In connection with to the appearance of products of machine-building and metallurgical industries at the international markets and great competition of manufacturers over the recent decade, the actuality of improving the quality of products is growing significantly.

Requirements for content of hydrogen, oxygen, nitrogen in metal have become more strict. In Ukraine, Russia and CIS countries the melting units of metallurgical and machine-building enterprises are equipped with installations such as furnace-ladle and out-of-furnace vacuum degassing. For example, at Magnitogorsk metallurgical plant, Russia, the vacuum degassing installation is reconstructed to produce highly-ductile metal with carbon content of not more than 0.004 % for automotive industry [1, 2]; at Moldavian metallurgical plant the decision was taken in the year of 2000 about the implementation of technology of steel vacuum degassing for its high degassing from nitrogen and hydrogen to manufacture the quality cord, spring and welding wire [3]; at Nizhnedneprovsky pipe rolling plant the complex was installed for steel vacuum degassing in 100-ton ladles in manufacture of railway wheels [4]; vacuumator of Mannesman-Demag Company is available at Company «Dneprospetsstal Works» to produce quality special steels [5], installations of Danieli Company are available at the plant of heavy drilling and line pipes (Sumy) and «Machine-building plant ISTIL, Ltd.» (Donetsk) [6]. The use of vacuum degassed steel at the machine-building enterprises of Ukraine is growing.

The present work was devoted to the investigation of hydrogen and nitrogen removal from molten steel in the process of electric arc melting and vacuum degassing. To study the specifics of degassing, a series of melts using the 12KhN3MFA grade steel was performed. Steel was melted at Company «Energomashspetsstal» in electric arc furnace using additions of gaseous oxygen and iron ore for oxidation. Some works show clearly the relationship between the content of gases in metal and rate of carbon oxidation [7].

Specific feature of hydrogen behaviour during the oxidizing period of melting in electric furnace is also its transition from metal to the furnace atmosphere, except its removal by CO bubbles at the content of hydrogen in metal above the equilibrium values with the furnace gas phase. Owing to a low content ($P_{H_2O} \approx 2500$ N / m^2) of hydrogen in gas phase the metal–gas system comes quickly to the equilibrium.

Analysis of data shows that the hydrogen content in steel in electric arc furnace melting is decreased with increase in rate of carbon oxidation v_C (Figure 1). Not only v_C during oxidizing period, but also duration of the reduction period influence the final content of hydrogen in steel.

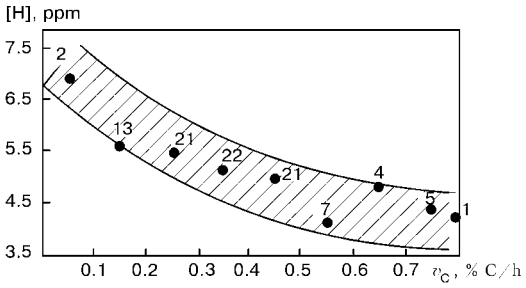

Figure 1. Dependence of total hydrogen content in ready steel on average rate of carbon cooling in electric arc melting (here and further the figures in points indicate the number of melts)

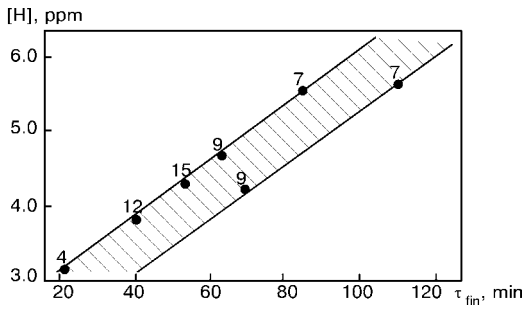

Figure 2. Effect of reduction period duration on hydrogen content in steel before its yield from furnace

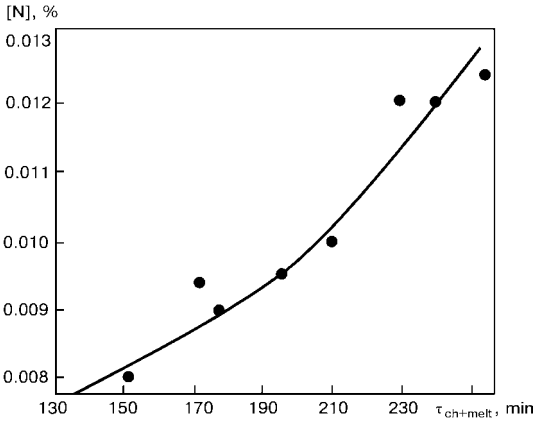

Figure 3. Effect of total duration of charging and melting on nitrogen concentration in metal during melting

Using method of multiple regression the authors obtained the equation combining the effect of intensity of carbon oxidation and duration of reduction period (period of finishing) τ_{fin} on hydrogen content in steel:

$$[H] = 5.3849 - 4.1165v_C + 0.0018\tau_{fin}, \quad r = 0.574. \qquad (1)$$

Low coefficient of correlation of equation (1) is stipulated by the effect of other factors, not taken into account, on the hydrogen content in the ready steel.

Dependence of duration of reduction period on total content of hydrogen in steel has a linear nature (Figure 2).

Mass transfer of nitrogen was also studied in experimental melts. It was established that with increase in total duration of charging and melting $\tau_{ch+melt}$ the nitrogen concentration in metal during melting is increased (Figure 3). This can be explained by the longer effect of electric arcs, thus leading to nitrogen dissociation in gas phase and transition of its atoms into metal.

With increase in carbon content in charge melting the nitrogen concentration in metal, even processed by a synthetic slag, is decreased (Figure 4). The depth of denitriding is larger with a longer bubbling of melt with floating bubbles of carbon oxide, in other words, with a longer oxidation period of melting (Figure 5).

The duration of finishing period has a different effect on nitrogen content in metal. With increase in its duration the nitrogen concentration in metal is growing (Figure 6). This is explained by the effect of electric arcs on bare metal after pouring out of oxidized slag before pouring the new slag on the preliminary oxidized metal.

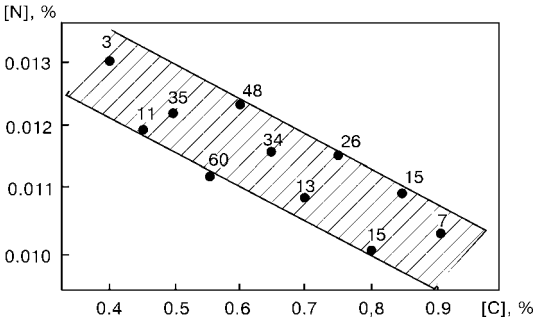

Figure 4. Dependence of nitrogen concentration in ready steel on carbon content in charge melting

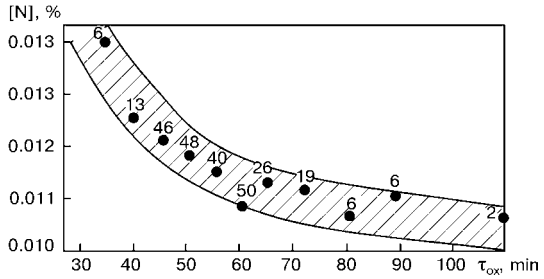

Figure 5. Variation of nitrogen concentration in ready steel depending on duration of oxidizing period

Vacuum degassing was performed in the unit of a circulation type, manufactured by German Company Rurstahl-Hereus, the electric arc steel contained from 3 to 11 ppm of hydrogen. A large scattering is explained by a simultaneous effect of many technological factors, varying from one melting to another. Circulation vacuum degassing is one of the most effective methods allowing stable degassing of metal. Processing of experimental data made it possible to establish a number of regularities of steel vacuum degassing in units of RH type.

The duration of vacuum degassing τ_{vac} influences greatly the degree of hydrogen removal (Figure 7). Increase in vacuum degassing period from 5 up to 25 min allows the hydrogen content to be decreased, on average, from 4 down to 2 ppm [1, 8]. A linear dependence of hydrogen content in steel on the rate of its cooling v_{cool} was established (Figure 8). The proper heating of the ladle lining and vacuum chamber before degassing is effective to decrease the cooling rate [5].

Regression analysis could reveal the dependence of hydrogen content in steel on rate of its cooling and duration of vacuum degassing:

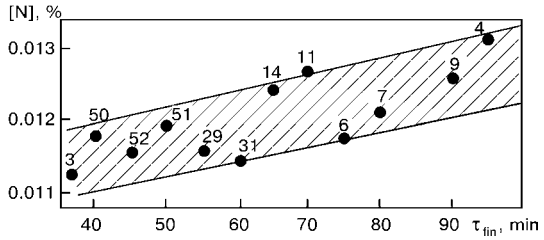

Figure 6. Effect of duration of reduction period of melting on nitrogen content in ready steel

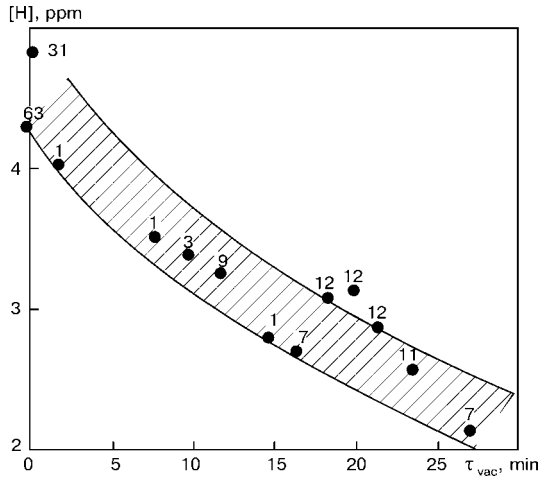

Figure 7. Variation of hydrogen content in steel depending on duration of vacuum degassing in the RH type unit (31 and 63 — number of melts, not subjected to vacuum degassing)

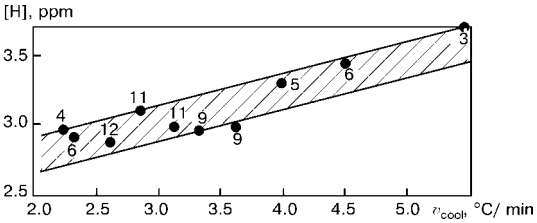

Figure 8. Dependence of hydrogen content in steel on rate of metal cooling in vacuum degassing

$$[H] = 3.2711 + 0.3848v_{cool} - 0.0499\tau_{vac}, \quad r = 0.3299. \qquad (2)$$

It follows from equation (2) that at the longer duration of vacuum degassing and lower rate of metal cooling the conditions of hydrogen extraction by degassing from the molten steel are better. Equation (2) makes it possible to calculate the condition of steel vacuum degassing in units of RH type.

Reduction in intensity of hydrogen extraction from the steel at its rapid cooling is explained by increase in metal viscosity, and, as a consequence, in deterioration of hydrogen diffusion from molten metal into gas phase. The obtained regularities have a good correlation with results of industrial tests of Valster and Maas for revealing the nature of changing [H] in the RH type unit [9]. The effect of temperature of structural steels at the beginning of vacuum degassing on the amount of evolved hydrogen Δ[H] was also studied. The most significant effect of metal temperature on the amount of evolved hydrogen is manifested in the 1570–1630 °C interval when the coefficient of hydrogen mass transfer and rate of its removal from metal is changed greatly:

$$-\frac{d[H]}{d\tau} = \beta_H \{ [H] - [H]_{int} \} \frac{F}{V}, \qquad (3)$$

where β_H is the coefficient of hydrogen mass transfer, m / s; F is the area of metal–gas interface, m^3; V is the metal volume, m^3; $\{[H] - [H]_{int}\}$ is the gradient of initial and equilibrium concentrations of hydrogen at metal–gas phase interface, ppm.

With a growth in metal temperature the coefficient of hydrogen mass transfer is increased by decrease in the metal viscosity. However, at definite temperatures (higher than 1630 °C) its growth does not influence the metal viscosity and the coefficient of mass transfer, that stipulates its low effect on the amount of hydrogen extracted (Figure 9).

The equation of a pair correlation was obtained on the basis of experimental data:

$$\Delta[H] = -8.9312 + 0.0063T, \quad r = 0.9276, \qquad (4)$$

where T is the steel temperature at the beginning of vacuum degassing, °C.

The degree of nitrogen and oxygen extraction from steel of 12KhN3MFA grade steel is much lower than that of hydrogen and equals, respectively, to 6.0–14.1 and 7.6–18.5 %. The results obtained have a good correlation with data of work [5].

CONCLUSIONS

1. To reduce the concentration of gases in initial electric arc steel it is necessary to decrease the duration of charging and melting periods; to have high concentration of carbon in melting with a simultaneous providing the rate of carbon oxidation of not less than 0.5 % C / h; to decrease to minimum the contact of bare metal with electric arcs, i.e. to provide a well-organized slag condition in the period of finishing and minimum its duration.

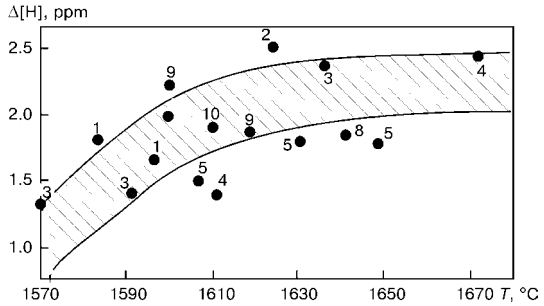

Figure 9. Effect of temperature of vacuum degassed steel on the amount of hydrogen extracted

2. The equation was obtained, combining the effect of intensity of carbon oxidation and duration of reduction period on hydrogen content in steel.

3. It was established as a result of mathematical processing of experimental data of steel vacuum degassing in the RN type unit that with increase in duration of vacuum degassing from 5 up to 25 min the hydrogen content is decreased, on average, from 4 down to 2 ppm; increase in metal temperature (1570–1670 °C) contributes to the hydrogen extraction; degree of hydrogen removal depends linearly on the rate of metal cooling in the process of vacuum degassing. Two equations of pair and multiple correlation are derived, binding the vacuum degassing technological parameters studied.

Ackhowledgement. *Authors express thanks to L.V. Rebrov, A.V. Zbyshevsky and A.P. Varchich for their contribution to this work.*

1. Bodyaev, Yu.A., Burmistrova, E.V., Ovsyannikov, V.G. et al. (2003) Degassing of steel by RH process at Magnitogorsk metallurgical works. In: *Bull. Chermetinform. Institute on Fessous Metallurgy*. Issue 11(**1247**), 48–52.
2. Takhautdinov, R.S., Hosov, A.D., Sarychev, A.F. et al. (2003) Development and mastering of technology of super low-carbon steel production for automotive industry. *Stal*, **4**, 20–23.
3. Belitchenko, A.K., Chernovol, A.V., Derevyanchenko, I.V. et al. (2003) Mastering of steel degassing technology at Moldavian metallurgical works. In: *Bull. Chermetinform. Institute on Fessous Metallurgy*. Issue 9(**1245**), 29–32.
4. Kukushkin, O.N., Bejtsun, S.V., Mikhajlovsky, N.V. et al. (2003) Mathematical model of variation of metal level in ladle degassing. *Teoriya i Praktika Metallurgii*, 33(**1**), 27–32.
5. Shulga, V.O., Korol, L.N., Knokhin, V.G. (2003) Mastering of technology of 10Kh13G12BS2N2D2 steel production. *Stal*, **8**, 28–31.
6. Shcherbina, V.N., Pilchuk, R.N., Kasian, G.I. et al. (2003) Current technology of electric steel production. In: *Bull. Chermetinform. Institute on Fessous Metallurgy*. Issue 10(**1246**), 47–49.
7. Mylnikov, R.I., Gavrilenko, Yu.V. (1980) Production of steel with carbon and nitrogen content of not less than 0.01 %. *Stal*, **8**, 84–86.
8. Zinchenko, S.D., Lamukhin, A.M., Ordin, V.G. et al. (2003) Development and mastering of production of pure steels. In: *Bull. Chermetinform. Institute on Fessous Metallurgy*. Issue 4(**1240**), 17–19.
9. Morozov, A.N., Strekalovsky, M.M., Chernov, G.I. et al. (1975) *Ladle degassing of steel*. Moscow: Metallurgiya.

SPECIFICS OF METALS REDUCTION BY CARBON FROM OXIDE MATERIALS IN LIQUID-PHASE REDUCTION MELTING

V.N. KOSTYAKOV[1], **V.L. NAJDEK**[1], **E.B. POLETAEV**[1], **G.M. GRIGORENKO**[2], **Yu.A. BYSTROV**[3] and **S.N. MEDVED**[3]
[1]Physical-Technological Institute for Metals and Alloys, NASU, Kiev, Ukraine
[2]E.O. Paton Electric Welding Institute, NASU, Kiev, Ukraine
[3]Dneprodzerzhinsk Steelmaking Plant, Dneprodzerzhinsk, Ukraine

Behavior of carbon in the process of liquid-phase reduction melting of iron-ore concentrate in DC arc furnace was investigated. It is shown that the high degree of iron reduction and decreased carbon losses are provided in adding of a reducing agent to the briquettes together with oxide-containing materials.

Keywords: *oxides, arc, slag, carbon, charge, reduction of metals*

At present the intensive works are carried out for the development of technology of producing alloys from oxide materials using a method of liquid-phase reduction of metals and there are convincing data that confirm the effectiveness of this trend [1–8]. The oxide-containing materials include slags of steelmaking industry, slimes of steelmaking, blast furnace and galvanic industries, used catalysts, dust of arc furnaces and others.

In metallurgy the large amount of metal-containing waste in the form of fine-dispersed dust and slimes is formed in manufacture of metal products. Thus, for example, the specific yield of slime at the metallurgical enterprises of Russia is 60–80 kg / t of steel, while in West Europe this value is equal to 30 kg / t [9]. Therefore, the problem of utilization of these waste materials is very actual. This is stipulated, from the one hand, by large amounts of this kind of the secondary raw material, and, from the other hand, by the scientific developments appeared over the recent years in the field of technology of waste utilization. The annual output of fine-dispersed iron-containing waste of ferrous metallurgy enterprises at the territory of CIS countries is about 15 mln t, among them 3 mln t are slimes of agglomeration, 3 mln t of blast furnace and 1.3 mln t of steelmaking industries [9]. Only 80 % of the total volume of these waste materials are utilized, and the rest amount of slimes and dust are thrown into pits and slime-storages, thus having at present more than 200 mln t of iron-containing waste.

In Ukraine the composition of waste materials of metallurgical production of an integrated cycle is distributed, on average, as follows: slags ---- 57–63 %; mineral waste (scrap of refractories, components) ---- 4–6 %; metal scrap (own) ---- 15–17 %; dust, slime, scale ---- 9–13 %; other ---- 2–4 % [10]. As is seen, the share of metallurgical slimes in the formation of waste is very large. However, due to physical-chemical composition their main application is not connected with a metallurgical conversion. Dust and slime of metallurgical conversion contain 33–74 % of iron and, consequently, can be used again in the production of metal products. In agglomaration and steelmaking industries the above-mentioned waste materials amount to 2–4 % or 20–50 kg / t of products.

The modern conception of waste utilization at the metallurgical enterprises supposes the multiple utilization of secondary resources-valuable materials for own needs of the enterprise or beyond it at the condition of their processing.

It is known that oxides of metals can be subjected to reduction by carbon [11]. This method is one of the main methods used in metallurgy for producing metals, alloys and ferroalloys. At carbon interaction with metal oxides the important role belongs to the process of their transition into vaporous condition and transfer of vapours to the reducing agent surface. In this case the main reducing element is carbon, on which surface the reactions of reduction of oxides are proceeding. This mechanism was revealed both at low-temperature and also high-temperature reduction of metal oxides by carbon [12]. The proceeding of reactions of carbide formation, which are developed usually at high-temperatures, are typical of carbon-thermal processes. During the process of carbide formation the intermediate oxide-carbide solutions are appeared, representing the phases of variable composition with a wide area of homogeneity. It is very difficult to make analysis of real stages of the reduction process as the thermodynamic characteristics of most oxide-carbide phases have not been yet studied. In work [13] some generalized data are given about the thermodynamics of phases of a variable composition and a rational classification of phase equilibriums of complex oxide solutions is offered.

It was above-noted that the reduction of metal oxides by a solid carbon can proceed by a mechanism

No. of melt	Composition of charge, %	Ratio of amount of added carbon to stoichiometrically necessary amount	Degree of iron reduction, %	Carbon consumption for proceeding the processes of melting, %		
				Reduction	Carburization	Oxidation
1	Cast iron — 50, iron-ore concentrate — 50	1.0	86.0	89.6	7.5	2.9
2	Cast iron — 70, iron-ore concentrate — 30	1.0	91.3	93.3	4.8	1.9
3	Cast iron — 50, iron-ore concentrate — 50	--	85.0	--	--	--
4	Cast iron — 70, iron-ore concentrate — 30	--	87.1	--	--	--
5	Cast iron — 50, iron-ore concentrate — 50	1.3	92.8	64.2	6.9	28.9
6	Cast iron — 70, iron-ore concentrate — 30	1.4	94.2	61.2	4.45	34.35
7	Cast iron — 47, iron-ore concentrate — 53	1.4	95.7	69.5	15.8	14.7
8	Cast iron — 66, iron-ore concentrate — 34	1.5	95.4	65.3	16.3	18.4

of transfer of oxide vapours to the reducing agent. The mechanism of reduction with a participation of carbon monoxide and its regeneration by $CO_2 + C = 2CO$ reaction is also probable for some oxides of metals under definite temperature conditions (above 800–900 °C). Therefore, it is possible to study the processes of interaction by applying the adsorption-catalytic and diffusion-kinetic schemes under the appropriate conditions. Thermodynamic aspect of these mechanisms was described comprehensively enough in works [14–16].

It is known that the thermodynamic strength of oxide compounds is not similar as the metals are differed by their affinity with oxygen. For example, aluminium, zirconium, titanium, niobium, chromium and others form the thermodynamically strong compounds, while oxides of molybdenum, tungsten, copper, nickel and others have a relatively not high thermodynamic strength. The growth of thermodynamic strength with temperature rise is typical of carbon monoxide. It means that at sufficiently high temperatures any oxide of metal can be reduced by the carbon monoxide.

The intensive works are carried out over the recent years at the Physical-Technological Institute for Metals and Alloys of the NAS of Ukraine to study the specifics of a liquid-phase reduction melting and creation of technology for producing alloys from oxide-containing materials in electric furnaces with arc and plasma heating.

The aim of the present work is to study the carbon behavior at different methods of its adding in the process of melting. Experimental melts were performed in 30 kg capacity DC arc furnace with an acid lining. Reference alloy of the following composition was used as charge materials, wt.%: 3.95C; 1.90Si; 0.86Mn; 0.09Ca; 0.18Al; 0.16Cu; 0.66S; 0.067P. The charge was also composed of iron-ore concentrate of Inguletsk mining-dressing plant, the concentrate composition was as follows, wt.%: 58.9Fe_2O_3; 28.6FeO; 9.8SiO_2; 0.3CaO; 0.7MgO; 0.02MnO; 0.6Al_2O_3; 0.22S; 0.02P; 0.08N_2O; 0.07K_2O; PPP — 1.1. Broken electrode served as a reducing agent.

Technology of melting envisaged the melting of the reference cast iron with a subsequent adding of pelletized iron-ore concentrate into the molten pool. Table gives the composition of charge, ratio of added carbon to stoichiometrically necessary amount, degree of iron reduction and carbon consumption for proceeding melting processes.

In melts Nos. 1 and 2 the amount of carbon added to the charge corresponded to stoichiometrically necessary amount for the complete reduction of iron from its oxides. In the next series of experimental melts (Nos. 3 and 4) the iron-ore concentrate was loaded into the furnace pool without a reducing agent with allowance for iron reduction by carbon dissolved in cast iron. In melts Nos. 5 and 6 the carbon in stoichiometrically necessary amount was added to the molten pool together with concentrate and fed additionally to the slag surface at the end of melting. And finally, in melts Nos. 7 and 8 the amount of carbon added together with a pelletized iron-ore concentrated exceeded the stoichiometrically necessary amount.

Analysis of given data shows that in all the melts, except melts Nos. 3 and 4, the carbon is consumed for iron reduction, metal carburization and oxidation of furnace atmosphere by oxygen. When adding carbon in the stoichiometrically necessary amount, 89.6–93.3 % C is consumed for iron reduction, and only 2.9–6.7 % is used for oxidation. Another situation is observed in melts Nos. 3 and 4, where carbon was not

added to the charge. In these melts the iron was reduced by carbon and silicon of cast iron, that is proved by decrease in their content in the melted alloy. Thus, 73.2 % C and 80.5 % Si, dissolved in cast iron, was consumed for iron reduction in melt No.3. With increase in cast iron content in the charge up to 70 % the consumption of carbon and silicon of cast iron for iron reduction was lower and amounted to 68.3 and 75.7 %, respectively.

Slag deoxidation by carbon, which is fed to the melt surface at the end of melting (melts Nos. 5 and 6), leads to the increased its oxidation by oxygen of the furnace atmosphere. In this case the carbon losses in melts Nos. 5 and 6 were 28.90 and 34.35 %, respectively. In melting of the pelletized iron-ore concentrate, containing carbon above the stoichiometrically necessary amount, the carbon losses for fumes are decreased, and its consumption for carburization of the metal pool is increased.

The interesting regularity is observed in study of effect of the method of carbon adding on the degree of iron reduction. Thus, carbon, added to the charge in the amount, corresponding to the stoichiometrically necessary amount, is consumed mainly for iron reduction. Degree of iron reduction in melts Nos. 1 and 2 is 86.0 and 91.3 %, respectively. Iron reduction by carbon, dissolved in cast iron, decreases the degree of iron reduction. This is explained by a slow proceeding of diffusion processes in molten metal. The additional feeding of carbon to the pool surface at the end of melting increases the degree of iron reduction (melts Nos. 5 and 6). However, the large part of carbon is oxidized by the furnace atmosphere.

In melting of pelletized iron-ore concentrate, containing the excessive amount of carbon, the highest degree of iron reduction is observed, because the charge is melted under the layer of a foaming slag at intensive its stirring by the formed monoxide of carbon and gas exchange in the zone of arc burning. As a result of this, the coefficient of heat exchange between the solid charge and slag melt is significantly increased that accelerates greatly the proceeding of mass- and heat exchange processes. This is correlated with data of investigations of melting the iron-ore raw material [16, 17].

Results of investigations showed that the method of carbon adding to the molten pool influences greatly the nature of interaction of phases in the processes of liquid-phase melting. The most favourable conditions for proceeding reduction processes are attained in adding carbon to the pelletized iron-ore concentrate in the amount exceeding the stoichiometrically necessary amount for the complete reduction of iron.

1. Romenets, V.A., Vechman, E.R., Soskir, N.F. (1993) Process of liquid-phase reduction. *Izvestiya Vuzov. Chyorn. Metallurgiya*, **7**, 9–19.
2. Kostelov, O.A. (1998) Mechanisms of reduction of metal oxides by carbon. *Teoriya i Praktika Metallurgii*, **2**, 15–17.
3. Lapukhov, G.A. (1998) Recycling of electric steel dust by use of the liquid-phase reduction. *Elektrometallurgiya*, **5 / 6**, 55–56.
4. Kostyakov, V.N., Poletaev, E.B., Grigorenko, G.M. et al. (2000) Carbon-thermal reduction of metals from electrolytic slime in plasma furnace. *Problemy Spets. Elektrometallurgii*, **1**, 32–37.
5. Shalimov, A.G. (2000) Corex process for production of high quality steels in mini-works. *Metallurg*, **1**, 52–53.
6. Kostyakov, V.N., Najdek, V.L., Poletaev, E.B. et al. (2002) Specifics of technology of melting alloys from used nickel-containing catalysts. *Metallurgiya Mashinostroeniya*, **5**, 2–4.
7. Smith, R.B., Boom, R., Sexton, M.G. (2000) The future for DR and SR: European prospective. In: *Proc. of 4th European Coke and Ironmaking Congr.*, Paris, June 19–21, 2000. Vol. 2.
8. Utkin, Yu.V. (1994) Secondary resources — important reserve of ferrous metallurgy. *Stal*, **3**, 2–6.
9. Konenko, G.M., Noskov, V.A., Makogon, V.F. (2001) State-of-the-art of recycling of iron-containing waste in Ukrainian metallurgical production. *Metallurgich. i Gornorudnaya Promyshlennost*, **4**, 98–100.
10. Elyutin, V.N., Pavlov, Yu.A., Polyakov, V.P. et al. (1976) *Interaction of metal oxides with carbon*. Moscow: Metallurgiya.
11. Sazhin, N.P., Kolchin, O.P., Sumarokova, N.V. (1961) About the processes of reduction of niobium oxides. *Izvestiya AN SSSR. OTN. Metallurgiya i Toplivo*, **6**, 8–24.
12. Chufarov, G.I., Men, A.N., Balakirev, V.F. et al. (1970) *Thermodynamics of reduction of metal oxides*. Moscow: Metallurgiya.
13. Esin, O.A., Geld, P.V. (1962) *Physical chemistry of pyrometallurgical processes*. Part 1. Sverdlovsk: Metallurgizdat.
14. Filippov, S.I. (1967) *Theory of metallurgical processes*. Moscow: Metallurgiya.
15. Men, A.N., Vorobiov, Yu.P., Chufarov, G.I. (1973) *Physico-chemical properties of nonstochiometric oxides*. Leningrad: Khimiya.
16. Rovnushkin, V.A., Bokovikov, B.A., Bratchikov, S.G. et al. (1988) *Coke-free processing of titanium-magnetite ores*. Moscow: Metallurgiya.
17. Trakhimovich, V.I., Shalimov, A.G. (1982) *Application of iron of direct reduction in melting of steel*. Moscow: Metallurgiya.

SPECIFICS OF THERMOANTHRACITE HEATING IN AC ELECTRIC FIELD

V.I. LAKOMSKY and **G.M. GRIGORENKO**
E.O. Paton Electric Welding Institute, NASU, Kiev, Ukraine

Model of furnace-calcinator of anthracite was created allowing visualization of the process of electric contact heating of coal. Specifics of thermoanthracite grains heating was studied preliminary.

Keywords: *anthracite, annealing, furnace-calcinator, electric contact heating, visualization of heating process*

The present article is the continuation of works on study of processes of electric annealing of anthracite in large-capacity shaft furnaces [1–3]. In all the works made by many researchers and manufacturers over the recent years [4–7], the authors proceeded from speculative models of electric heating. Some of them [4, 5] considered that anthracite heating occurs as a result of evolution of energy of electric contact heating of coal, while the others [6, 7] explained the occurrence of high temperatures in axial zone of the furnace, especially under the lower edge of upper electrode, by the effect of multiple electric microarcs generated between the neighboring grains of coal. Unfortunately, the authors of the mentioned works did not observe directly the process of coal heating. At the same time, to have a clear idea about the object studied, it is necessary, in our opinion, to see it. There are many examples in science when the keen scientists discovered new phenomena, not using any equipment. Let us take as an example Chernov Dmitrij Konstantinovich, the famous Russian metallurgist, who was the first to discover the existence of several points of allothropic transformations in iron by only the thorough observation of the process of cast steel cooling in the mould.

This way of research at the present time can seem anachronism. Now, on the contrary, we have an era of computer research, when the comprehensive works are carried out even not seeing the «alive» industrial unit, explaining this by reduction in time of investigations and money saving. Moreover, the authors of such works pass over in silence the validity of data obtained [7]. They do not compare them with results of real experiments. In our opinion, the invasion of computer investigations during recently is only a tribute of respect to modern fashion of computers.

We are supporters of another approach to the study of unknown phenomena and, therefore, consider it necessary to visualize the process of coal heating in electric furnace, i.e. to look inside the furnace.

It is problematic to visualize the process of coal heating in industrial furnace-electric calcinator IET-10-UKhL-4 of 1600 kV·A (Figure 1) because of its large sizes and high material costs. In this connection, we have created a furnace model of 1:35 scale, in which a quartz pipe of 57 mm internal diameter was used as a transparent wall (Figures 2 and 3). The upper and lower electrodes of the model were manufactured from carbon steel, as we were not going to heat coal up to temperatures attained in a real furnace. Unique part of the table-mounted model is a tube representing an alundum 20 mm diameter pipe. A transparent sapphire plane-parallel window of the same diameter as the pipe was brazed to the inner end of the tube.

Window of tube, through which it is possible to observe the behavior of thermoanthracite grains at their heating by electric current, is arranged in horizontal at the distance of 5–6 mm from the model axis, while in vertical —– almost in the middle of interelectrode gap, but closer to the upper electrode.

The model was tested by connecting electrodes to the AC source for electric arc welding with falling volt-ampere characteristic. Internal space of the model was filled with thermoanthracite of 4–6 mm fractions without any packing. Open-circuit voltage of the power source was 92 V, current value could be changed in the ranges from 20 up to 100 A.

Electric resistance of anthracite column in the model in cold state varied from 20 to 10 Ohm in different experiments. With heating of thermoanthracite its electric resistance was decreased gradually to 0.7 Ohm. Here, the current value was changed spontaneously from 20 up to 60 A.

It should be noted here that all the experiments were performed under the condition of a stationary behavior of the coal charge, i.e. thermoanthracite grains were not moving with respect to each other. The process in the industrial furnace is going on in the same way, as the loading of portions of «raw» anthracite into furnace and unloading of a ready thermoanthracite are made discretely.

The coal behavior, observed outside the model and through the tube, was recorded by a digital photo-

camera to analyze further the data obtained and to study the dynamics of heating process in the computer.

Figure 4 shows the state of thermoanthracite grains, heated by electric current, observed through the tube. Six positions of the object under observation were recorded each 45–50 s.

Process of coal heating occurred as follows. It could be seen through the model transparent body after power supply that fine electric sparks appeared and quickly extinguished at the periphery of the coal charge. It is characteristic that sparks were observed firstly in the entire height of the model, and then they were mainly in that its part which was located in the interelectrode spacing. The sparks were also observed through the tube, but their amount was much smaller due to a smaller area of observation. In this case the coal was poorly heated, that can be seen by the temperature of a quartz wall of the model.

After some period of time, when, in our opinion, the coal charge was heated sufficiently to have significant heat losses through a quartz wall, a definite temperature gradient occurred, probably, in a transverse section of the charge. Coal in the axial part of charge had somewhat higher temperature than in the periphery areas of the model. This has led to the redistribution of current density, the current rushed to a central zone of charge as the thermoanthracite has a negative temperature coefficient of resistance [8]. The higher the temperature of coal in the central zone, the higher current passes in the axial part of the coal charge, thus leading in its turn to the higher heating.

It is well seen through the tube how rapid is the heating of separate grains. Two-three dark red points appear on the dark background (Figure 4, *a*).

In next Figure 4, *b*, which has records of state of the central part of coal charge after 45 s, these points were growing in sizes and became brighter and two more points appeared.

After 50 s (Figure 4, *c*) the points, visible at the beginning, acquired configurations of thermoanthracite grains, and their brightness increased to light-crimson color.

The next photos (Figure 4, *d–f*) show the growth of new heated grains of thermoanthracite and brightness of the first heated grains which have already reached white (glowing) heat (their hotspots are seen on the tube walls).

The last pattern is as follows: at the very sapphire window the poorly heated grains and, therefore, rather dark thermoanthracite grains, are located. Their background is the well-heated and incandescent grains located at the model axis.

So, the thermoanthracite grains in the central zone of model were heated almost for 5 min from the state shown in Figure 4, *a* to white heat. During this period the external layers of thermoanthracite near the quartz walls, as is well-seen on all six photos, have no time to be heated and, therefore, they remained dark. And only after 8–10 min the coal grains near quartz wall of model begin to be slightly red. It is clear that it is a result of heat flow spreading from central part of charge to external layers of the coal column.

The process of heating very fine fractions of coal, which are the grains of 4–6 mm size, is proceeding very rapidly at intensive increase in temperature of separate grains. This, unfortunately, does not give us opportunity to distinguish visually the sequence of heating with time, firstly, of small volumes of thermoanthracite grain near contact spots between neighboring grains, and then the heating of the whole grain. The latter phenomenon was observed by us when two grains, coarser than those charged into model were heated by electric current. The pattern is especially clear expressed if one grain has a flat shape, and the second grain has a conical shape. Apex of cone, contacting plane, is heated very fast up to white heat.

The procedure of heating coal charge was repeated under conditions of mechanical load applying. For this purpose, the charge column was loaded through electrically-insulated washer to provide uniform distribution of pressure with small stubs of tungsten electrodes of 230 and 590 g total mass that corresponded to specific pressure 0.73 and 1.88 kPa in upper layers of charge, respectively. Other differences consisted in the fact that current in load applying increased spontaneously up to 65 A due to drop of electric resistance of coal charge. In spite of such high current for the model, we did not see even after 5–7 min any reddenings of coal grains in the central part of charge through the model tube. At the same time the coal charge was intensively heated all over the volume.

Only on the basis of these first observations it is possible to make several preliminary conclusions. Firstly, we did not observe electric microarcs between grains of thermoanthracite at various heating conditions. Consequently, it can be supposed that either they are absent at all both in the model and also in industrial furnaces or, if they appear in large furnaces-calcinators, then they are irregular. Secondly, the scheme of thermoanthracite heating gives an idea about changing both design of furnace and also conditions of its operation. Really, the process of coal heating shows that electric currents, once selecting the definite way of passing at the very beginning, does not change it spontaneously during all further heating of charge. Therefore, the chains of thermoanthracite grains, along which the current started its passing, continue to be heated up to white heat, whereas neighboring chains remain currentless and are heated only by indirect heat from hot «neighbors». This behavior of «clusters» of grains is explained by negative value of temperature coefficient of electric

resistance and tendency of current to select the easiest way. However, this behavior of current increases greatly the non-uniformity of coal heating. Hence, the conclusion can be made about a forced mixing of coal and about pulsed power supply to the furnace.

There is an impression that designers of the furnace, we mean the staff of companies ELKEM and also SIBELEKTROTERM, designed the industrial furnaces, followed another considerations in the development of designs and technology of annealing, but not electric contact heating of layer of thick crushed coal.

In our opinion, the existing design of furnace and accepted technology of anthracite annealing can be radically improved.

1. Lakomsky, V.I. (2003) Mathematical model of calculation of specific electrical resistance of grained thermoanthracite depending on its fractional composition. *Advances in Electrometallurgy*, **3**, 44–47.
2. Lakomsky, V.I., Bykovets, V.V. (2004) On problem of contact heating of thermoanthracite in electric calcinator. *Tsvetnye Metally*, **1**, 52–54.
3. Bykovets, V.V., Lakomsky, V.I., Kirilenko, V.P. (2004) Specific electric resistance of lumpy thermoanthracite in thin layer. *Advances in Electrometallurgy*, **1**, 44–45.
4. Soldatov, A.I. (1991) *Electro-calcinated anthracite. Peculiarities of its production and application*. Syn. of Thesis for Cand. of Techn. Sci. Degree. Kharkov. Coal-Chemical Institute.
5. Arnold, J.J., Arifinn, V. *Method and calcining furnace for electrical calcination of hydrogen-containing material*. Pat. 2167377 C1 RU. Publ. 22.10.98.
6. Bernard, J.C., Brassart, J.L., Lacroix, S. (1987) Electrical calcination anthracite: A new technology. In: *Proc. of Session 116 AIME Annual Meeting.*
7. Rui, R.T., Hachette, R., Simard, G. et al. (1999) Computer simulation of the anthracite calcining furnace. *Ibid*.
8. Bykovets, V.V., Lakomsky, V.I. (2003) Specific electric resistance of thermal anthracite. *Advances of Electrometallurgy*, **4**, 46.

JUBILEE OF INTERNATIONAL CENTER OF ELECTRON BEAM TECHNOLOGIES OF THE E.O. PATON ELECTRIC WELDING INSTITUTE OF THE NAS OF UKRAINE

In June, 2004, 10 years have passed since the establishment of the International Center of Electron Beam Technologies (IC EBT) of the E.O. Paton Electric Welding Institute of the NAS of Ukraine. This center was founded on the base of PWI Department.

The ten-year intensive work of this academic self-supporting organization, which had no budget financing in principle, is an interesting experiment at the National Academy of Sciences of Ukraine. All these years the IC EBT was proving by hard work its competitiveness, justifying its name, dictated by life, and fulfilling mainly the research contracts by the order of foreign companies and universities.

During 10 passed years the IC EBT under the supervision of Prof. B.A. Movchan, its founder, has won the international recognition both in the field of studies of structure and properties of new inorganic materials (amorphous, nanocrystalline, dispersion-strengthened, microlayer, microporous) and coatings (gradient thermal barrier, damping, erosion-resistant), deposited from a vapour phase in vacuum, and also in realization of developed technological processes and creation of electron beam equipment of the next generation and its successful commercializing.

The visiting-card of the IC EBT is the new technologies of producing functional gradient materials and coatings by electron beam evaporation and condensation in vacuum, and also the development and manufacture of different-purpose electron beam installations (laboratory, experimental-industrial and industrial).

The new generation of electron beam installations, developed and manufactured at the IC EBT over the recent years, provides the realization of almost all existing technological processes and also the feasibility for implementation of challenging technologies of deposition of functional gradient materials and coatings with a nano- and micro-dimensional structure.

Scientific and technological developments of the IC EBT are protected by patents of the USA, Europe, Russia, China and numerous Ukrainian patents. Such well-known US companies as General Electric, Pratt & Whitney, Chromalloy were and remain to be the main customers during all these years. At the present time the research project with Canadian company Cametoid is under the realization, the joint Ukrainian-Indian Research Laboratory has been created and starts its work in the scope of the Intergovernmental Agreement. Contracts for manufacture of electron beam units for US and Chinese customers are at the stage of realization. Over the recent years the cooperation with Design Office «Progress» (Zaporozhie, Ukraine) has been started, by the order of which the IC EBT performs the deposition of gradient protective coatings on blades of advanced gas turbine engines. The works are continuing with NPO «Saturn» (Russia), directed to the modification of equipment and implementation of electron beam technology of deposition of gradient coatings.

During the past decade the potential of staff, working in the IC EBT, 55 persons in total, among which 3 Dr. of Techn. Sci. and 9 Cand. of Techn.

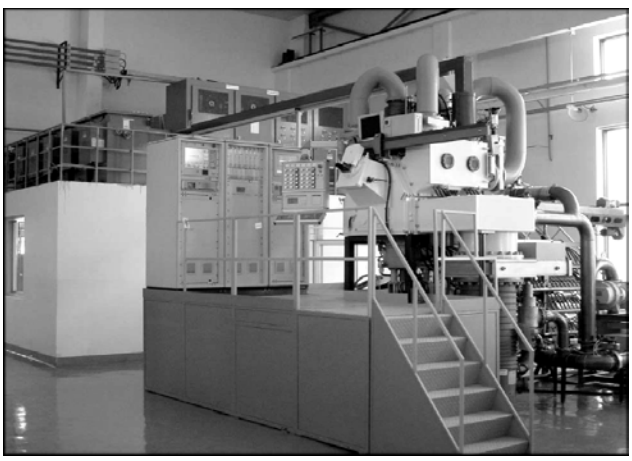

Experimental-industrial electron beam installation

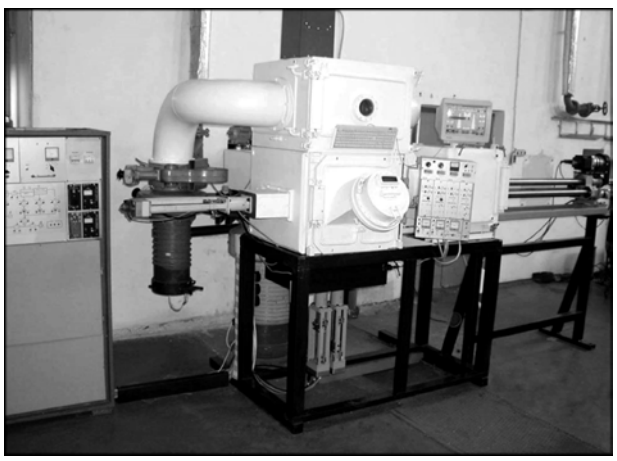

Laboratory electron beam installation

Sci., has been preserved and strengthened. Laboratory-research base of the Center has been widened. It consists now of 8 laboratory and experimental-industrial electron beam installations, fluorescent X-ray microanalyzer of chemical composition of samples and parts, transmission and scanning electron microscopes, units for examination of porosity of materials and coatings, optical microscopes, microhardness meters, high-temperature vacuum furnaces, units for conductance of furnace thermocyclic tests of coatings, investigation of kinetics of high-temperature oxidation of materials, investigation of mechanical characteristics of samples (strength, creep, fatigue, damping ability).

The ten-year experience of practical cooperation with numerous foreign partners and customers, having own developments and ideas, the use of close mutually-profitable relations with subdivisions and structures of the E.O. Paton Electric Welding Institute, other organizations and institutes of the National Academy of Sciences of Ukraine, the growing contacts with domestic industry allowed the staff of the IC EBT to look to the future with optimism.

Administration of the IC EBT